

ลักษณะเฉพาะของกรรมวิธีทางความร้อนของเหล็กหล่อโครเมียมสูงเพื่อความต้านทานต่อการกัดสี



นาย สุตสาคร อินธิเดช

สถาบันวิทยบริการ

จุฬาลงกรณ์มหาวิทยาลัย

วิทยานิพนธ์นี้เป็นส่วนหนึ่งของการศึกษาตามหลักสูตรปริญญาวิศวกรรมศาสตรมหาบัณฑิต

สาขาวิชาวิศวกรรมโลหการ ภาควิชาวิศวกรรมโลหการ

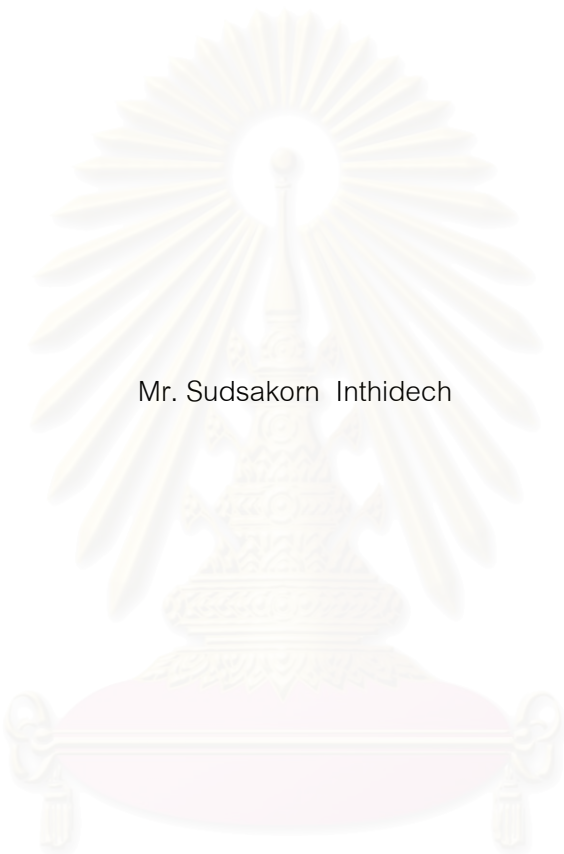
คณะวิศวกรรมศาสตร์ จุฬาลงกรณ์มหาวิทยาลัย

ปีการศึกษา 2545

ISBN 974-171-088-7

ลิขสิทธิ์ของจุฬาลงกรณ์มหาวิทยาลัย

HEAT TREATMENT CHARACTERISTICS OF HIGH CHROMIUM CAST IRON FOR ABRASION WEAR  
RESISTANCE



Mr. Sudsakorn Inthidech

สถาบันวิทยบริการ  
จุฬาลงกรณ์มหาวิทยาลัย

A Thesis Submitted in Partial Fulfillment of the Requirements  
for the Degree of Master of Engineering in Metallurgical Engineering

Department of Metallurgical Engineering

Faculty of Engineering

Chulalongkorn University

Academic Year 2002

ISBN 974-171-088-7

Thesis Title                                   HEAT TREATMENT CHARACTERISTICS OF HIGH CHROMIUM  
CAST IRON FOR ABRASION WEAR RESISTANCE

By   Mr. Sudsakorn Inthidech

Field of Study                                 Metallurgical Engineering

Thesis Advisor                               Associate Professor Prasonk Sricharoenchai, D.Eng.

Thesis Co-advisor                           Professor Yasuhiro Matsubara, D.Eng.

---

Accepted by the Faculty of Engineering, Chulalongkorn University in Partial  
Fulfillment of the Requirements for the Master 's Degree

..... Dean of Faculty of Engineering  
(Professor Somsak Panyakeow, D.Eng.)

THESIS COMMITTEE

..... Chairman  
(Sawai Danchaiwijit, Ph.D.)

..... Thesis Advisor  
(Associate Professor Prasonk Sricharoenchai, D.Eng.)

..... Thesis Co-advisor  
(Professor Yasuhiro Matsubara, D.Eng.)

..... Member  
(Suwanchai Pongsukitwat, M.Eng.)

สุดสาคร อินธิเดช : ลักษณะเฉพาะของกรรมวิธีทางความร้อนของเหล็กหล่อโครเมียมสูง เพื่อความต้านทานต่อการขัดสี (HEAT TREATMENT CHARACTERISTICS OF HIGH CHROMIUM CAST IRON FOR ABRASION WEAR RESISTANCE) อ. ที่ปรึกษา : รองศาสตราจารย์ ดร. ประสงค์ ศรีเจริญชัย, อ. ที่ปรึกษาร่วม : Professor Yasuhiro Matsubara ; 95 หน้า. ISBN 974-171-088-7.

เพื่อศึกษาลักษณะเฉพาะของกรรมวิธีทางความร้อนของเหล็กหล่อโครเมียมสูง ได้เตรียมเหล็กหล่อโครเมียมสูงสองชนิดคือ ยูเทคติกและไฮโปยูเทคติก ซึ่งมีปริมาณส่วนผสมโดยประมาณของโครเมียมร้อยละ 16 และ 26 โดยมวล ในสภาวะหลังชุบแข็งความแข็งเปลี่ยนแปลงเล็กน้อย แต่สัดส่วนเชิงปริมาตรของออสเทนไนต์เหลือค้าง (V<sub>V</sub>) มีการแปรเปลี่ยนอย่างมากขึ้นกับปริมาณของคาร์บอนที่ระดับปริมาณโครเมียมเท่ากัน สัดส่วนเชิงปริมาตรของออสเทนไนต์เหลือค้างมีค่าสูงในเหล็กที่ชุบแข็งจากอุณหภูมิที่ทำให้เป็นออสเทนไนต์สูงกว่า และค่อยๆลดลงเมื่อค่าสัดส่วนโครเมียมต่อคาร์บอนเพิ่มขึ้น กราฟของความแข็งขึ้นงานในสภาพอบคืนตัวแสดง Secondary Hardening แต่ระดับของการแข็งขึ้นน้อยกว่าเหล็กหล่อขาวธาตุผสมหลายธาตุ ความแข็งเนื่องจากการตกตะกอนของคาร์ไบด์ (precipitation hardening) มีค่าสูงกว่าในเหล็กที่ชุบแข็งจากอุณหภูมิของการทำให้เป็นออสเทนไนต์ที่สูงกว่า หรืออีกความหมายหนึ่งคือในเหล็กที่มีสัดส่วนเชิงปริมาตรของออสเทนไนต์สูงกว่า ค่าความแข็งสูงสุดภายหลังจากการอบคืนตัว (H<sub>Tmax</sub>) เกิดขึ้นที่อุณหภูมิของการอบคืนตัวสูงขึ้นเมื่ออุณหภูมิของการทำให้เป็นออสเทนไนต์เพิ่มขึ้น ค่าความแข็งภายหลังการอบคืนตัวสูงสุดมีความสัมพันธ์กับสัดส่วนเชิงปริมาตรของออสเทนไนต์เหลือค้างเหมือนกัน โดยไม่ขึ้นกับอุณหภูมิการทำให้เป็นออสเทนไนต์ และมีค่าเพิ่มขึ้นเมื่อค่าของสัดส่วนเชิงปริมาตรของออสเทนไนต์เหลือค้างสูงขึ้น โดยมีค่าสูงสุดที่ระดับความแข็ง 800 HV<sub>30</sub> ที่ปริมาณของออสเทนไนต์เหลือค้างมีค่าเท่ากับร้อยละ 30 และมีค่าคงที่เมื่อปริมาณออสเทนไนต์เหลือค้างเพิ่มขึ้นแม้ว่าจะมีค่ามากกว่าร้อยละ 30 ความแตกต่างของความแข็งมหภาคของเหล็กหล่อที่มีปริมาณของโครเมียม ร้อยละ 16 และ 26 เกิดจากความแตกต่างของรูปร่างยูเทคติกคาร์ไบด์ที่มีอัตราส่วนยูเทคติกที่เท่ากัน คือมีลักษณะหนาหรือใหญ่กว่า และมีการเชื่อมต่อกันระหว่างยูเทคติกคาร์ไบด์มากกว่าในเหล็กหล่อโครเมียมร้อยละ 16 กับมีลักษณะที่บางกว่าและมีการเชื่อมต่อกันของยูเทคติกคาร์ไบด์น้อยกว่าในเหล็กหล่อโครเมียมร้อยละ 26

ภาควิชา.....วิศวกรรมโลหการ.....ลายมือชื่อนิสิต.....  
 สาขาวิชา.....วิศวกรรมโลหการ.....ลายมือชื่ออาจารย์ที่ปรึกษา.....  
 ปีการศึกษา.....2545.....ลายมือชื่ออาจารย์ที่ปรึกษาร่วม.....

## 4370566821 : MAJOR METALLURGICAL ENGINEERING

KEYWORD : HEAT TREATMENT, HIGH CHROMIUM CAST IRON, RETAINED AUSTENITE, Cr/C  
VALUE

SUDSAKORN INTHIDECH: HEAT TREATMENT CHARACTERISTICS OF HIGH CHROMIUM CAST IRON FOR ABRASION WEAR RESISTANCE. THESIS ADVISOR : ASSOCIATE PROFESSOR PRASONK SRICHAROENCHAI, THESIS CO-ADVISOR : PROFESSOR YASUHIRO MATSUBARA, 95 pp. ISBN 974-171-088-7.

Eutectic and hypoeutectic cast irons containing 16% and 26%Cr were prepared in order to investigate their heat treatment characteristics. In as-hardened state, hardness does not change much but volume fraction of retained austenite ( $V\gamma$ ) varies greatly depending on carbon content at the same chromium level. The  $V\gamma$  is high in the iron hardened from higher austenitizing temperature. It gradually decreases with an increase in Cr/C value of iron. In tempered state, curve of tempered hardness shows a secondary hardening but the degree is smaller compared with multi-component white cast iron. The precipitation hardening is greater in the iron hardened from higher austenitizing temperature, in other words, in the iron with more  $V\gamma$ . The tempering temperature to obtain the maximum hardness ( $H_{T_{max}}$ ) shifts to the long time side when the austenitizing temperature rises. The  $H_{T_{max}}$  is uniformly related to the  $V\gamma$  value in as-hardened state irrespective of austenitizing temperature and it increases gradually up to the highest value of around 800 HV30 at 30%  $V\gamma$ , and the  $H_{T_{max}}$  is settled even if the  $V\gamma$  increases over 30%. The difference in macro-hardness between 16%Cr and 26%Cr cast irons is due to the difference in morphology of eutectic carbide at the same eutectic ratio, thick or large massed and more interconnected eutectic carbides in 16%Cr cast irons, and thin and less interconnected ones in 26%Cr cast irons.

Department.....Metallurgical Engineering.....Student's signature .....

Field of study...Metallurgical Engineering.....Advisor's signature .....

Academic year.....2002.....Co-advisor's signature .....

## Acknowledgement

This research for the Master's thesis on Heat Treatment Characteristics of High Chromium Cast Irons for Abrasion Wear Resistance was carried out at Professor Y. Matsubara's Laboratory in Kurume National College of Technology (KNCT). I wish to thank Professor Matsubara for his continual and patient guidance and also Professor N. Sasaguri for his indirect suggestions for my experiments. In addition, I appreciate Mr. K Nanjo, technician, for his lessons on the directions for the use of experimental equipment and Miss Wanaporn for her heartfelt guidance of Japanese daily life.

My acknowledgement and appreciation should be also conveyed to the faculty members of the Department of Materials Science and Metallurgical Engineering, KNCT, for their encouraging me. Besides, I wish to express my appreciation to KAWARA STEEL WORKS Co., Ltd. for the production of high chromium cast iron specimens for my experiment.

Again, I would like to thank Professor Matsubara for the financial support for my staying expenses from his research fund, President N. Enomoto, ENOMOTO Co., Ltd. and President T. Watanabe, TAIYO MACHINERY Co., Ltd. for aiding me with their scholarship.

Finally, I thank Associate Professor P. Sricharoenchai for his thoughtful suggestion to study abroad and have this wonderful opportunity.

สถาบันวิทยบริการ  
จุฬาลงกรณ์มหาวิทยาลัย

## Contents

	Page
<b>Abstract (In Thai)</b> .....	iv
<b>Abstract (In English)</b> .....	v
<b>Acknowledgements</b> .....	vi
<b>Content</b> .....	vii
<b>List of Tables</b> .....	xi
<b>List of Figures</b> .....	xii
<b>Chapter 1</b>	
<b>Introduction</b>	
1.1 Background.....	1
1.2 Objective of Research.....	4
1.3 Advantages of Research.....	4
<b>Chapter 2</b>	
<b>Literature Survey</b> .....	6
<b>Chapter 3</b>	
<b>Experimental Procedure</b>	
3.1 Preparation of Specimens.....	26
3.1.1 Mold Design and Test Piece.....	26
3.1.2 Production of Specimens.....	27
3.2 Heat Treatment Procedure.....	27
3.2.1 Annealing.....	27
3.2.2 Hardening.....	29
3.2.3 Tempering.....	29

## Contents (continued)

	Page
3.3 Observation of Microstructure.....	29
3.1.1 Optical Microscopy.....	29
3.1.2 Scanning Electron Microscopy.....	32
3.4 Hardness Measurement.....	32
3.5 Measurement of Volume fraction of Retained Austenite.....	35
3.5.1 Theory for Measurement of Retained Austenite by X-Ray Diffraction Method.....	35
3.5.2 Equipment and Measureing Condition.....	35
3.5.3 Calculation of the Volume Fraction of Retained Austenite.....	35
<b>Chapter 4</b>	
<b>Experimental Result</b>	
4.1 Microstructure of Test Alloys.....	41
4.1.1 As-cast State.....	41
4.1.2 As-hardened State.....	43
4.2 Influence of Heat Treatment Condition on Macro-hardness and Volume Fraction of Retained Austenite.....	43
4.2.1 As-cast State.....	43
4.2.2 As-hardened State.....	45
4.2.3 Tempered State.....	47
4.3 Relationship between Micro-hardness of Matrix and Tempering Temperature.....	58
<b>Chapter 5</b>	
<b>Discussion</b>	
5.1 Relationship between $V_{\gamma}$ and Cr/C Value.....	65
5.2 Relationship between Macro-hardness and Cr/C Value in As-hardened State.....	67



## Contents (continued)

	Page
5.3 Relationship between Macro-hardness and Volume Fraction of Retained Austenite in Tempered State.....	70
5.4 Relationship between Maximum Tempered Hardness( $H_{Tmax}$ ) and Cr/C Value.....	73
5.5 Relationship between Maximum Tempered Hardness ( $H_{Tmax}$ ) and $V_{\gamma}$ .....	74
5.6 Observation of Transformed Matrix by SEM.....	77
<b>Chapter 6</b>	
<b>Conclusions</b> .....	83
<b>References</b> .....	86
<b>Appendix</b> .....	88
<b>Biography</b> .....	95

สถาบันวิทยบริการ  
จุฬาลงกรณ์มหาวิทยาลัย

## List of Tables

Table	Page
3-1 Chemical composition of raw materials.....	28
3-2 Chemical composition, eutectic ratio, Cr/C value and carbide type of test specimens.....	28
3-3 Heat treatment conditions.....	30
3-4 List of etchants.....	32
3-5 Condition of X-Ray diffraction to measure the volume fraction of retained austenite.....	36
4-1 Volume fraction of retained austenite( $V_{\gamma}$ ) and hardness in as-cast state.....	45
4-2 Volume fraction of retained austenite( $V_{\gamma}$ ) and macro-hardness of as-hardened specimens.....	47

## List of Figures

Figure	Page
2-1 Liquidus surface phase diagram for Fe-Cr-system.....	7
2-2 As-cast micrographs of hypoeutectic, eutectic and hypereutectic high chromium cast irons.....	9
2-3 Effect of chromium content on colony diameter.....	10
2-4 Effect of destabilization heat treatment on IT diagram of high chromium white cast iron.....	14
2-5 Influence of chromium on the optimum hardening temperature in high chromium cast irons. ....	17
2-6 Effect of volume fraction of carbide on the overall hardness of white cast iron with different matrix structures.....	20
2-7 Effect of volume fraction of carbide on the abrasion rate of high chromium cast irons.....	20
2-8 Relationship between abrasion resistance and hardness of the two high chromium cast irons.....	21
2-9 Relationship between mean jaw-plate weight loss (g) and retained austenite content.....	21
2-10 Relationship between jaw-plate weight loss and hardness.....	22
2-11 Relationship between mean high-stress abrasion pin weight loss(mg) and austenitizing temperature( $^{\circ}$ C) of 27%Cr cast iron..	22
2-12 Relationship between mean high-stress abrasion pin weight loss (mg) and tempering temperature( $^{\circ}$ C) of 27%Cr cast iron.....	24
2-13 Relationship between pin weight loss and hardness.....	24
2-14 The relationship between wear rate (Rw) and volume fraction of retained austenite.....	25
2-15 The relationship between wear rate (Rw) and macro-hardness...	25
3-1 Schematic drawing of CO <sub>2</sub> mold.....	26

## List of Figures(continued)

Figure	Page
3-2 Heat treatment cycle for annealing, hardening and tempering.....	31
3-3 Photograph of special sample stage for retained austenite measurement by X-ray diffraction.....	37
3-4 Effect of sample stage condition on diffraction pattern (A), and volume fraction of retained austenite( $V_\gamma$ ) (B) calculated from the profiles in (A). (Specimen No.6 in as-cast state).....	38
3-5 X-Ray diffraction patterns of specimens with different volume fraction of retained austenite( $V_\gamma$ ). $V_\gamma$ : (a) 14.8%, (b) 20.8%, c) 41.0%.....	40
4-1 Microphotographs of as-cast with 16% and 26%Cr cast irons.....	42
4-2 SEM microphotographs of as-hardened 16% and 26%Cr cast irons.....	44
4-3 Relationship between macro-hardness, volume fraction of retained austenite( $V_\gamma$ ) and tempering temperature. (Specimen No.1) .....	49
4-4 Relationship between macro-hardness, volume fraction of retained austenite( $V_\gamma$ ) and tempering temperature. (Specimen No.2) .....	51
4-5 Relationship between macro-hardness, volume fraction of retained austenite( $V_\gamma$ ) and tempering temperature. (Specimen No.3) .....	53
4-6 Relationship between macro-hardness, volume fraction of retained austenite( $V_\gamma$ ) and tempering temperature. (Specimen No.4) .....	54
4-7 Relationship between macro-hardness, volume fraction of retained austenite( $V_\gamma$ ) and tempering temperature. (Specimen No.5) .....	56

## List of Figures(continued)

Figure	Page
4-8 Relationship between macro-hardness, volume fraction of retained austenite( $V_\gamma$ ) and tempering temperature. (Specimen No.6) .....	57
4-9 Comparison of micro-hardness of matrix with macro-hardness. (Specimen No.1) .....	59
4-10 Comparison of micro-hardness of matrix with macro-hardness. (Specimen No.2) .....	60
4-11 Comparison of micro-hardness of matrix with macro-hardness. (Specimen No.3) .....	61
4-12 Comparison of micro-hardness of matrix with macro-hardness. (Specimen No.5) .....	63
4-13 Comparison of micro-hardness of matrix with macro-hardness. (Specimen No.6) .....	64
5-1 Relationship between volume fraction of retained austenite( $V_\gamma$ ) and Cr/C value of as-hardened specimens.....	66
5-2 Relationship between macro-hardness and Cr/C value of as-hardened specimens.....	68
5-3 Influence of volume fraction of retained austenite( $V_\gamma$ ).....	69
5-4 Relationship between macro-hardness and volume fraction of retained austenite ( $V_\gamma$ ) of tempered specimens. (Austenitized at 1273 K) .....	71
5-5 Relationship between macro-hardness and volume fraction of retained austenite ( $V_\gamma$ ) of tempered specimens. (Austenitized at 1323 K) .....	72
5-6 Relationship between maximum tempered macro-hardness ( $H_{Tmax}$ ) and Cr/C value.....	75
5-7 Influence of volume fraction of retained austenite( $V_\gamma$ ) in	

## List of Figures(continued)

Figure	Page
as-hardened state on maximum tempered hardness( $H_{Tmax}$ ) .....	76
5-8 SEM micrographs of 16%Cr cast iron (No.2) hardened from 1323 K and then tempered at four different temperature.....	78
5-9 SEM micrographs of 26%Cr cast iron (No.5) hardened from 1323 K and then tempered at four different temperature.....	80
5-10 SEM microphotographs of eutectic chromium carbides. (a) 16%Cr and (b) 26%Cr cast irons.....	82


  
 สถาบันวิทยบริการ  
 จุฬาลงกรณ์มหาวิทยาลัย

# Chapter1

## Introduction

### 1.1 Background

Alloyed white cast irons have been developed for a long time for many applications mainly as abrasion wear resistant materials. The developments of them have been carried out to improve higher wear resistance and higher toughness at an acceptable cost. For the last half century past, the abrasion wear resistant materials changed from low-alloy cast iron through Ni-hard iron to high chromium white cast iron. The high chromium cast iron was discovered by Frederick Becket in 1915. The low-alloy white cast iron was replaced by the high-alloyed white cast irons with better wear resistance and a little more toughness. The representative alloy is high chromium cast iron.

Particularly high chromium cast iron which contains chromium from 12 to 30 mass % (hereafter shown by %) has found wide applications as raw materials of the parts and components in the various fields of industries because of the superiority above-mentioned. The industries such as cement, mining, steel-making and thermal power plant have been main users. For pulverizing mills in cement industry, it is known that balls and liners made by high chromium cast iron shows better performance than Ni-hard iron in all type of cement mills.

In general, pearlite phase in matrix is considered to deteriorate the wear resistance and to reduce the service life. To overcome this problem, the alloying elements such as Ni, Cu, Mo and V are added to improve the hardenability.

Chromium is a strong carbide forming element and it is well known that chromium combines with carbon to form chromium

carbide of  $(\text{FeCr})_7\text{C}_3$  or  $\text{M}_7\text{C}_3$  type as eutectic when cast iron contains higher level of chromium. The  $\text{M}_7\text{C}_3$  carbide is harder and has discontinuous morphology[1] in comparison with the carbide of  $(\text{FeCr})_3\text{C}$  or  $\text{M}_3\text{C}$  type that forms in cast iron with low chromium content. The eutectic of high chromium cast iron grows with cellular interface and solidifies as colony structure, and the eutectic structure varies depending on the combination of contents of carbon, chromium and other alloying elements. The size of eutectic colony and the coarseness of eutectic carbides can be controlled by solidification rate or cooling rate[2]. On the other side, the matrix structure can be controlled by the condition of heat treatment. Therefore it can be said that not only abrasion wear resistance but also mechanical properties should be determined by both the carbide and matrix structure. With respect to the matrix structure, there are reports indicating that high chromium cast iron with some volume fraction of retained austenite shows higher abrasion wear resistance under the certain wear conditions [3,4].

Ni-hard iron, which is represented in low chromium white cast irons and contains eutectic  $\text{M}_3\text{C}$  carbide in ledeburitic or continuous morphology, was afterward replaced by tougher high chromium cast iron with eutectic carbide of  $\text{M}_7\text{C}_3$  type in discontinuous morphology. Once high chromium cast iron solidifies, it is very hard to modify the shape of carbide crystallized from the liquid as primary and/or eutectic without using the plastic deformation techniques like rolling, forging and pressing. Therefore, heat treatment, which is usually given at the final stage and can widely control the matrix structure, becomes an only means for the improvement of wear resistance and mechanical properties. It is considered that main factors affecting the abrasion wear resistance could be hardness of the iron. When the carbide structure is similar, the hardness depends mostly on the volume fraction of austenite in the matrix. Quantitative measurement of the retained austenite for the



high chromium cast iron is performed successfully by X-ray diffraction method. Then it is possible to connect the wear resistance and other properties to the amount of retained austenite.

In the practical application of high chromium cast iron, adequate heat treatment should be given to get the optimal combination of the hardness and the quantity of retained austenite. The usual heat treatments are homogenizing or annealing, hardening and tempering. These heat treatments for cast iron seem to be same as those for general steels, but in high chromium cast irons, there occurs a peculiar phenomena that are the precipitation of carbide during austenitizing (so-called as destabilization of austenite) and during cooling after austenitizing. The precipitation of secondary carbides in matrix during heat treatment must be also related to the wear resistance and somewhat to the mechanical properties[4 ].

Recently, most of hot work rolls made of high chromium cast iron were replaced by very expensive rolls made of newly developed multi-component white cast iron because of much higher performance. The applications of the new type alloy are increasing gradually in other fields[5]. In the severe recession, however, employment of relatively cheaper high chromium cast iron has been eyed with fresh interest in place of high class alloy like a multi-component white cast iron. In these circumstances, further betterment of conventional high chromium cast iron has been demanded. It is considered for this purpose that more researches on the improvement of solidification structure and matrix structure are necessary. Many research papers have been published for solidification of high chromium cast iron[6-10] but systematic researches on its heat treatment are a few[11].

From the viewpoint above-mentioned, it is found that the heat treatment characteristics of high chromium cast irons with free or less alloy must be studied systematically and more in detail.

## 1.2 Objective of Research

The objective of this research for thesis is to clarify the heat treatment behavior of matrix in high chromium cast iron with different chromium and carbon contents. The employed specimens are 16%Cr irons for main materials of hot work roll and 26%Cr irons as abrasive wear resistant materials of the parts for pulverizing mill. Particularly the investigations are focused on the variation of hardness and the volume fraction of retained austenite and their correlation associated with heat treatment conditions.

The experiments were carried out as follows:

- (1) Heat treatments of annealing, hardening and tempering are given to high chromium cast irons.
- (2) To measure the macro-hardness and micro-hardness in as-cast and heat-treated states.
- (3) To measure the volume fraction of retained austenite in as-cast and heat-treated states.
- (4) To investigate the microstructure of the specimens by using an optical microscope (OM) and scanning electron microscope (SEM) to discuss the experimental results.
- (5) To clarify the correlation among hardness, volume fraction of retained austenite and condition of heat treatment.

## 1.3 Advantages of Research

- (1) This research reveals the quantitative and systematic data that are macro- and micro-hardness in as-hardened and tempered states of high chromium cast iron.
- (2) This research also reveals the quantitative and systematic data of retained austenite connected with the condition of heat treatment.
- (3) These data are keenly helpful for the practical heat treatment

to improve the properties such as strength, toughness and wear resistance of high chromium cast iron.



สถาบันวิทยบริการ  
จุฬาลงกรณ์มหาวิทยาลัย

## Chapter 2

### Literature Survey

#### I Solidification and Microstructure of High Chromium Cast Iron

High chromium cast iron is basically an Fe-Cr-C ternary alloy of which solidification structure consists of carbides precipitated from liquid and matrix. According to the liquidus surface phase diagram of Fe-Cr-C system shown in Fig.2-1 which was constructed by Thorpe and Chicco[12], the primary phases in the region of high chromium cast iron with 12 to 30%Cr are austenite( $\gamma$ ) in hypoeutectic and  $M_7C_3$  carbide in hypereutectic compositions, respectively. In addition, Thong[13] proposed the convenient equations (2.1 and 2.2). From these equations, the liquidus or primary and eutectic temperatures at various combinations of carbon and chromium contents in hypoeutectic cast irons can be forecast.

$$T_{\text{liquidus}} = 1554.5 - 89.2xC\% - 0.77xCr\% \quad (2.1)$$

$$T_{\text{Eutectic}} = 1201.7 - 20.3xC\% + 5.97xCr\% \quad (2.2)$$

The paper describes that these formulas are appropriate for industrially used cast irons having the chromium content from 12 and 30%. In the alloy with hypoeutectic composition which is widely and commercially produced,  $\gamma$  solidifies first from the melt and followed by ( $\gamma+M_7C_3$ ) binary eutectic solidification. In the alloy with hypereutectic composition,  $M_7C_3$  carbide precipitates first from the melt and solidification of ( $\gamma+M_7C_3$ ) is followed. In the case of alloy with low chromium content (less than 10%Cr),  $(Fe,Cr)_3C$  or  $M_3C$  carbide precipitates as a eutectic, whereas in the alloy with chromium contents over about 15%[2], only  $(Fe,Cr)_7C_3$  or  $M_7C_3$  carbide crystallizes as a eutectic. The  $M_7C_3$  carbide is

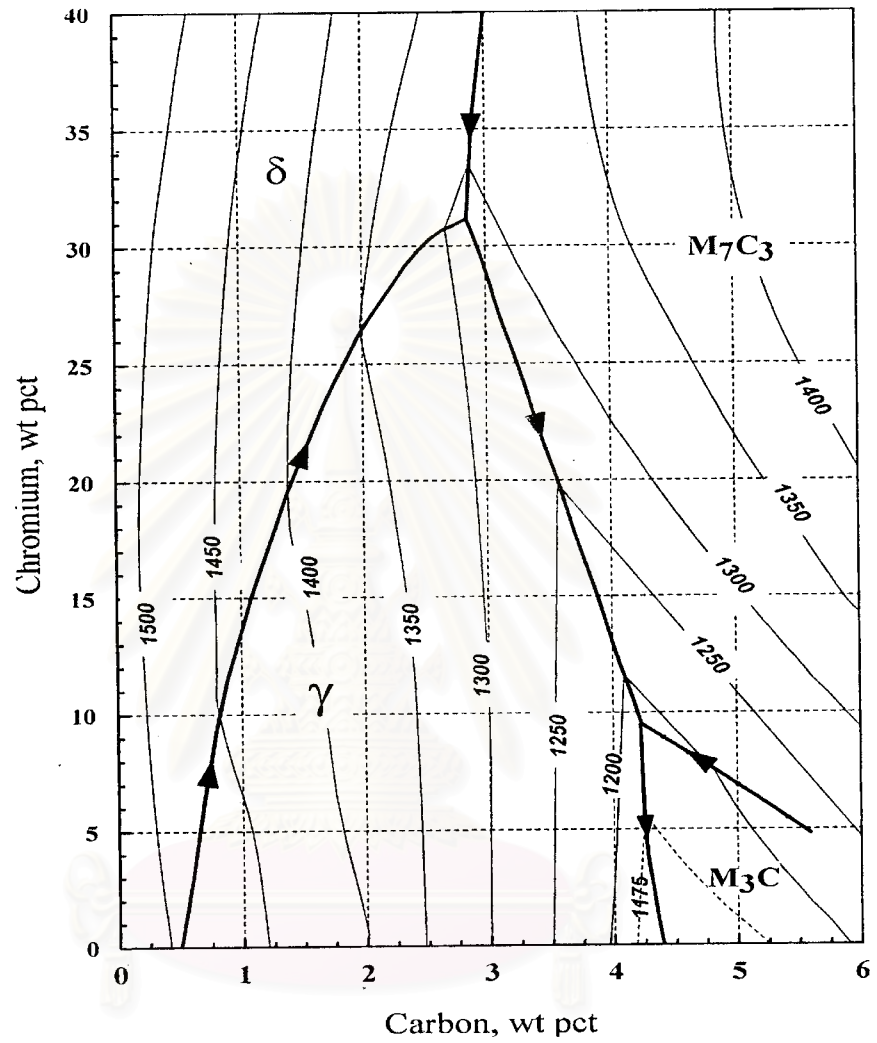


Fig. 2-1 Liquidus surface phase diagram of Fe-Cr-C system[12].

quite different in morphology from  $M_3C$  carbide precipitated in low chromium cast iron like Ni-hard iron. The crystal lattice of  $M_7C_3$  carbide is hexagonal, while the  $M_3C$  carbide is orthorhombic.

The hardness of  $M_7C_3$  carbide is 1400-1800 HV and it is much harder than that of  $M_3C$  carbide with 800-1100 HV. Powell[1] observed the carbide morphology of white cast iron by SEM using deep-etched specimen. It is noted that the hexagonal  $M_7C_3$  carbides in the white cast iron with chromium content more than 9% were in rod- and blade-like morphology and they were not completely discontinuous. Matsubara[2] worked widely on the eutectic solidification of high chromium cast iron. The three-dimensional configuration of ( $\gamma+M_7C_3$ ) eutectic colony in high chromium cast iron containing chromium 15% to 20% were illustrated by optical microphotographs and it was pointed out that the eutectic carbides were interconnected and that the interconnectivity decreased with an increase in chromium content. With respect to the relationship between microstructure and solidification rate, high solidification rate leads a tendency to promote the selective crystallization of  $M_3C$  carbide. Irrespective of the solidification rate, the eutectic carbide of only  $M_7C_3$  type precipitates when the chromium content is more than 15%. The as-cast microstructures are shown in Fig.2-2. The eutectic colony is clearly revealed and the size of colony is found to change depending on chemical compositions, carbon and chromium contents. The colony size decreases as the carbon content increases from hypoeutectic to hypereutectic composition when the chromium content is same. It is also changed by chromium content when compared with almost the same eutectic ratio. As is shown in Fig.2-3 graphically [2], the colony size is smallest in the iron with 30% Cr. Ogi and Matsubara[7] investigated the growth mechanism of the eutectic cell. The eutectic cell takes a shape of lanky bell and the length of the eutectic cellular projection become larger with an increase in the temperature range of eutectic freezing ( $\Delta T_E$ ).

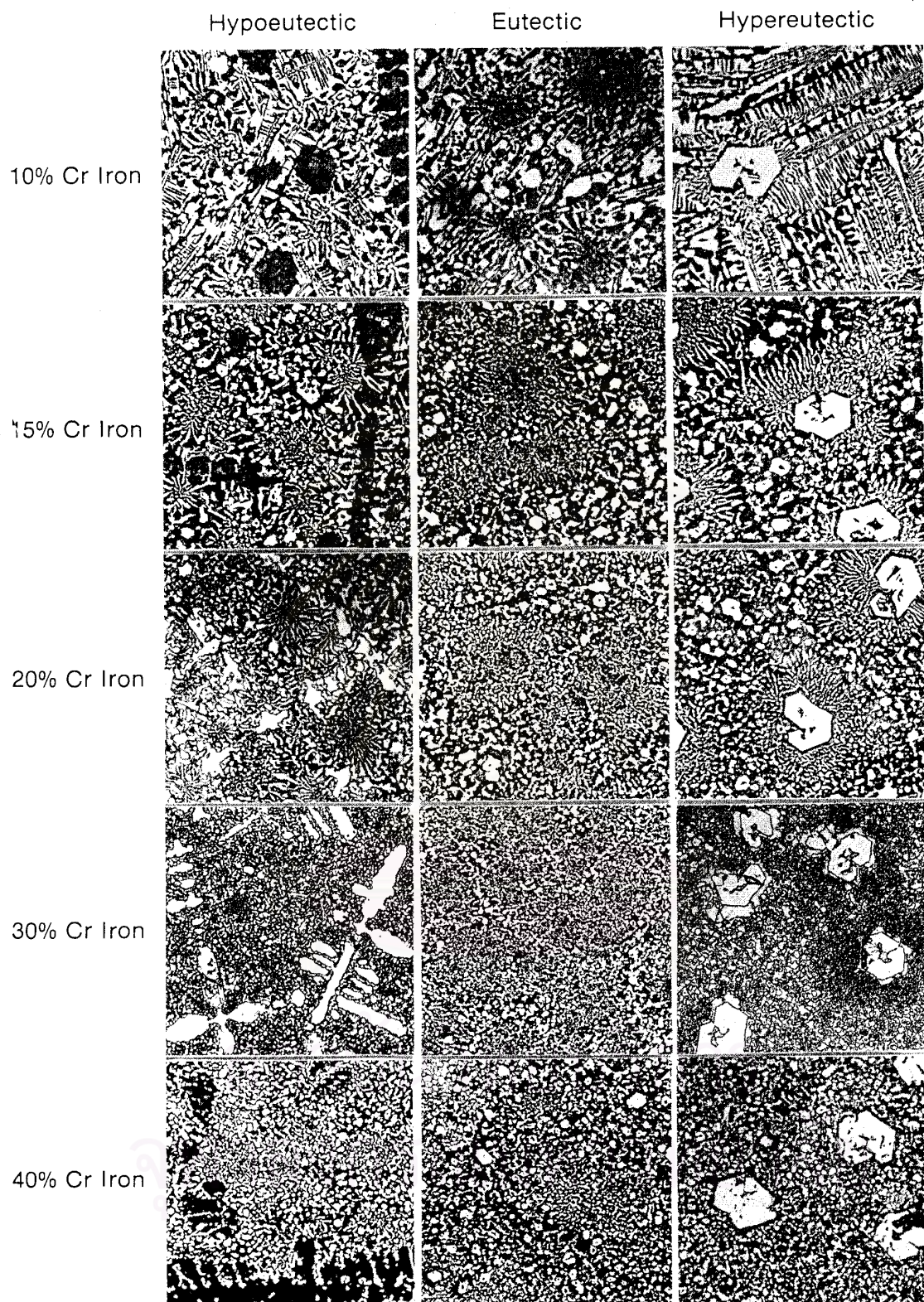


Fig2-2 Microphotographs of as-cast hypoeutectic, eutectic and hypereutectic high chromium cast irons[2].

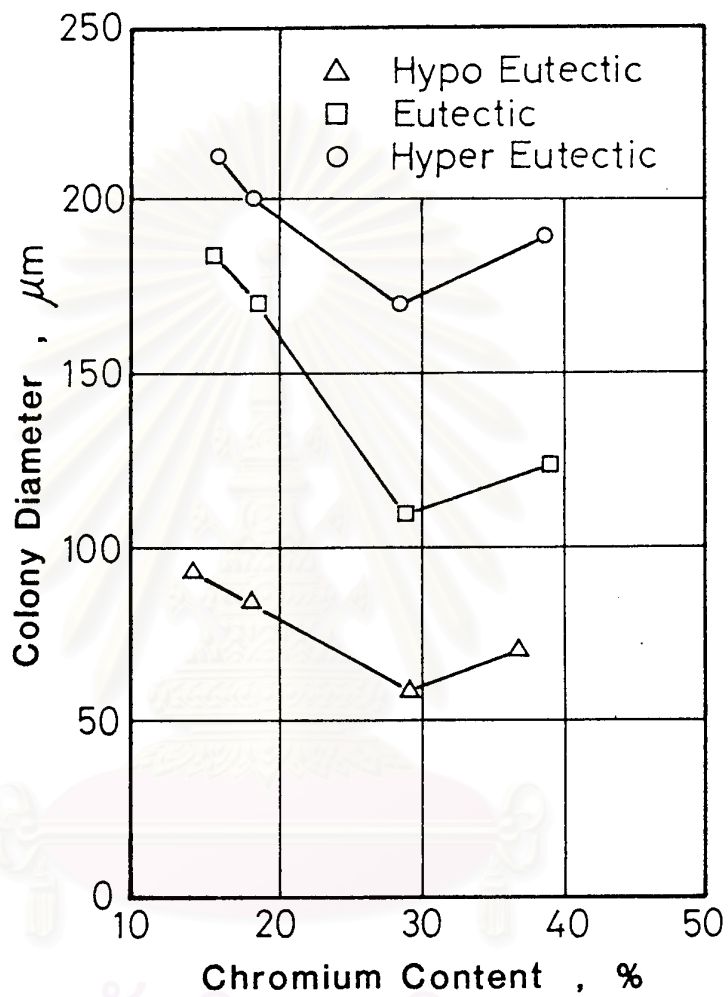


Fig. 2-3 Effect of chromium content on colony diameter at RE(Eutectic solidification rate)= 0.5cm/min[2].



On the other hand, the eutectic colony size can be also connected to the  $\Delta T_E$ , and it increases with an increase in the  $\Delta T_E$ . The rate of radial growth of eutectic cell is closely related to the size of eutectic carbide particles, that is, carbide spacing; particularly in the outside region of the colony. Base on thermodynamic principle, alloying elements are distributed to both phases, austenite dendrite and eutectic carbide during solidification. Therefore, the microstructure of high chromium cast iron is greatly influenced by the addition of alloying elements. The volume fraction of carbide ( $V_C$ ) can be estimated from the initial chemical composition of the iron. Maratray[14] demonstrated a following equation that the amount of carbides( $V_C$ ) increases in proportion to the carbon and chromium contents.

$$\% V_C = 12.33(\%C) + 0.55(\%Cr) - 15.2 \quad (2.3)$$

High chromium cast irons are sometimes used in as-cast state where some quantity of  $\gamma$  retains in the matrix. It is said that the hardness is very important factors affecting the abrasive wear resistance and that the wear resistance increases with an increase in the hardness. The hardness of cast iron is determined by the microstructure consisting of volume fraction of carbide, morphology of carbide and matrix structure.

In as-cast condition, the matrix of high chromium cast iron often contains some austenite. It is because supersaturation of chromium and carbon in matrix occurs during solidification. The carbon content has more effect on the amount of austenite, the more the carbon content, the more the retained austenite. The influence of chromium on the transformation of austenite in as-cast state was investigated by G. Laird II[15]. Chromium retards the transformation from austenite to pearlite and it lowers  $M_s$  temperature. Resultantly, a large amount of austenite exists usually in as-cast matrix of high chromium cast iron. The as-cast matrix is composed of plural constituents such as pearlite, bainite, martensite and retained austenite. Some martensite appears in the matrix

due to the depletion of chromium and carbon around the eutectic carbides. When hardened, the destabilized austenite during austenitization transforms partially into martensite, mixing with retained austenite.

In order to improve the mechanical properties, the trails to control or to modify the  $M_7C_3$  eutectic carbide were done by inoculation. Rickard[16] studied the effect of Ti inoculation on ferritic high chromium iron with 1.5%C and 30%Cr. The results showed that TiC carbides precipitated first and followed by delta ferrite( $\delta$ ) in the solidification process and resultantly finer grained microstructure was obtained. This suggests that TiC particles act probably as nucleation sites for the primary  $\delta$  ferrite during solidification. He also showed the tensile test data indicating that the grain refinement increased the tensile strength from 45 MPa to 54 MPa. The effect of rare earth on the morphology of eutectic carbide was reported by Liang et al.[9]. The mischmetal was added into the low and high chromium cast irons (3.7%Cr and 18%Cr, respectively), and considerable modification of eutectic carbide was seen in the low chromium cast iron but little change was in high chromium cast iron because eutectic  $M_7C_3$  carbide precipitated in the chromium cast iron grew fast forming the characteristic morphology like laths or rods. However, they suggested that the carbide morphology might be changed by adding some elements which could hinder the growth of eutectic during solidification. The other way to control the size of eutectic is to make the melt cool fast by using chill mold or permanent mold. Matsubara et al. [17] investigated the influence of alloying element on the eutectic structure of high chromium cast iron and clarified that the size of eutectic colony and carbide particle could be controlled by the addition of the third alloying elements which vary the temperature range of eutectic solidification, being extended by Mo, Al and shortened by V. The former case enlarges both the eutectic colony and carbide particle and the later case refines them. The addition of Ti refined the eutectic structure, the sizes of colony and carbide particle, because of its inoculation effect.

## II Heat treatment

It is known that as-cast high chromium white cast iron has usually some volume fraction of austenite which decreases the hardness. High hardness, good abrasion resistance and resistance to spalling are said to be obtained in martensitic matrix. Generally, as-cast state does not display the maximum hardness. However, the high chromium white iron is seldom used in as-cast condition with some retained austenite, because the austenite can transform into martensite under a certain wear condition and it results in an increase of the abrasion wear resistance. Under the certain wear circumstances, therefore, the martensitic matrix is requested for superior wear performance. In order to obtain more martensite, the cast iron should be hardened by heat treatment. The important thing in the heat treatment of alloys is that the transformation behaviors of the alloy have been clarified and understood. It tells us the behavior of alloying elements in the matrix involving the formation of secondary carbide. As an example, the destabilization treatment of austenite is introduced. In as-cast state, the matrix is austenitic due to supersaturation of carbon and chromium. During austenitizing, the carbon and chromium in matrix are reduced by the precipitation of secondary carbides. This so-called destabilization is taken at 1273 – 1323 K for the as-cast high chromium cast iron with considerable amount of austenite. The types of secondary carbides are  $M_7C_3$  and  $M_{23}C_6$ . The effect of destabilization on IT diagram has been explained using a schematic diagram shown in Fig. 2-4[22]. On the way when high chromium cast iron cools after solidification or from extremely high temperature, consider the case (a) that cast iron cools directly below subcritical temperature, the case (b) that iron is stopped cooling at about 1000 °C and held there for a certain time and the case (c) that iron is held at the because more alloy dissolved in austenite stabilizes the  $\gamma$ . In the cases of (b) and (c), the cooling of  $\gamma$  is interrupted in the austenitic region at high temperature. When irons are

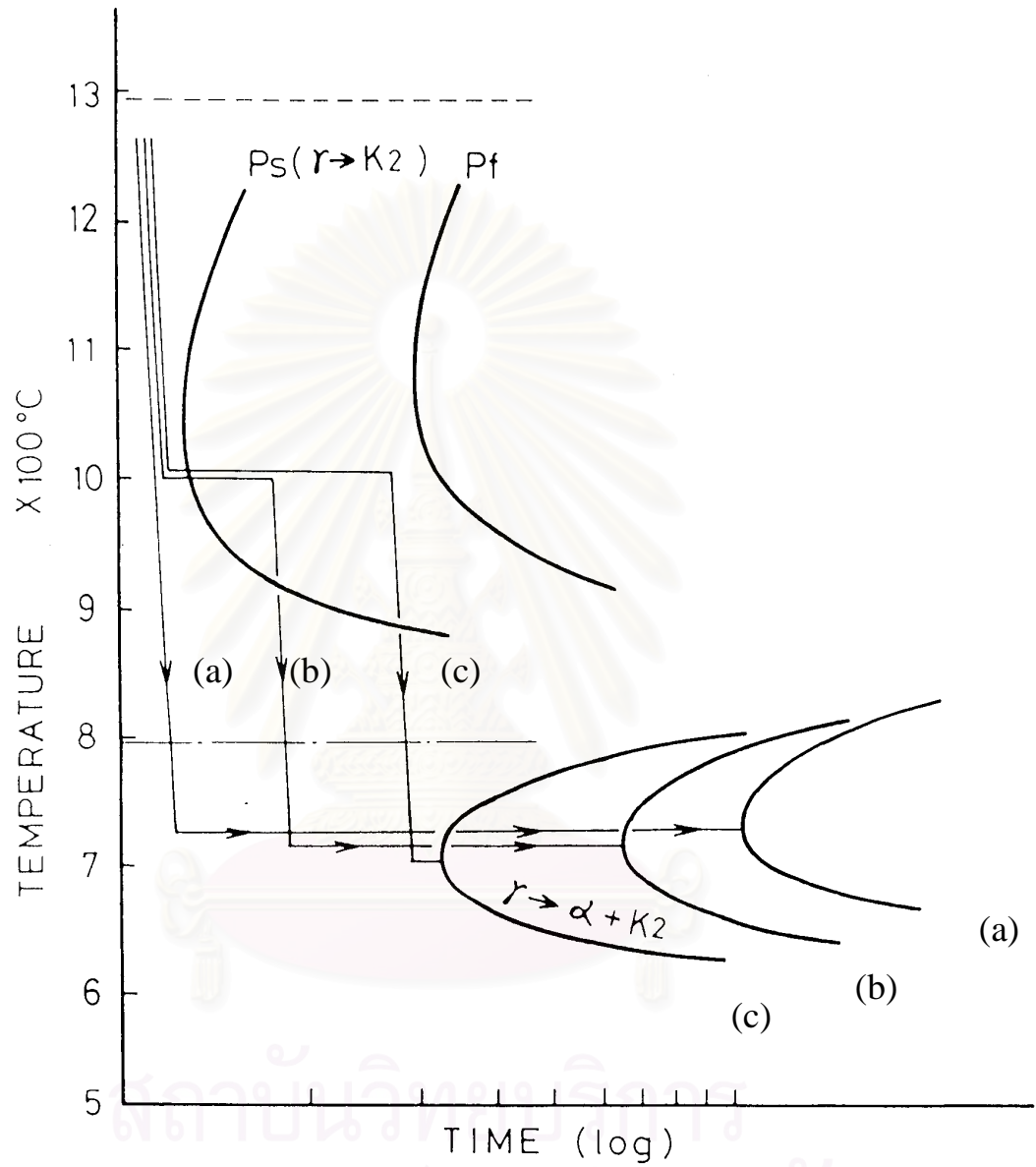


Fig.2-4 Effect of destabilization heat treatment on IT diagram of high chromium white cast iron[22].

kept isothermally, they proceed toward the area of precipitation of carbide which is shown by the curves of Ps (precipitation start) and Pf (precipitation finish), the more the iron proceeds (c), the more the precipitation of carbide occurs. In this process, unstable austenite is destabilized but it is not fully destabilized because the holding does not reach the Pf. When the  $\gamma$  cooled rapidly after holding and held it again in the region of subcritical temperature, the general pearlite transformation takes place. Since alloy concentration in austenite decreases as the holding time between the curves of Ps and Pf gets longer, resultant pearlite transformation begins earlier. Therefore the start of pearlite transformation in the case of (b) takes place earlier than that of (a), and much earlier in (c) than in (b). Maratray [14] has reported that, at lower austenitizing temperature, the longer holding time is required to reach equilibrium. When austenitized at 1273 to 1323K, two hours have to be taken whereas eight hours is needed for the austenitizing temperature of 1200 K. The initially pearlitic matrix reaches an equilibrium carbon content very rapidly relatively to austenitic matrix. He also noted that if the casting is segregated heavily or very high temperature is used for annealing, longer holding time is required for destabilization.

Due to the precipitation of carbides during destabilization, the alloy concentration in  $\gamma$  reduces and therefore Ms temperature of matrix goes up over room temperature, in other word, martensite transformation appears. With an increase in the austenitizing temperature, the hardness in as-hardened state may increase but the hardness falls down conversely due to an increase in retained austenite when the austenitizing temperature increases too much.

As for high chromium cast iron, it can be said that the one goal of heat treatment is to increase the hardness for the wear resistance. Maratray [18] reported that the highest hardness is obtained when the matrix contains 20% retained austenite in as-hardened state. The influence of chromium content on the relationship between hardening temperature and macro-hardness of high chromium cast irons is shown in

Fig.2-5. Since chromium is a strong-carbide forming element, the volume fraction of carbide increases as the carbon content rises. Resultantly chromium concentration in matrix is decreased if carbon content is same. Therefore, a parameter of Cr/C value has been introduced to understand the effect of both the chromium and carbon in the cast iron. The alloying elements such as Mo, Ni and Cu are usually added to high chromium cast iron in order to improve the hardenability.

As described previously, martensite formation in high chromium cast iron usually occurs at low temperature and then the matrix contains high quantity of retained austenite in as-hardened state. In this case, the subzero treatment must be given to obtain more or full martensitic matrix structure. According to the effect of alloying elements on the Ms temperature of steel, carbon has a greatest effect followed by the other of Mn, Ni, Cr and Mo. A following equation has been proposed experimentally[19]:

$$\begin{aligned} M_s(^{\circ}C) = & 539 - 423(\%C) - 30.4(\%Mn) - 12.1(\%Cr) \\ & - 17.7(\%Ni) - 7.5(\%Mo) \end{aligned} \quad (2.4)$$

During cooling from austenitizing temperature to 973K (700 °C), precipitation of carbides occurs due to the decrease of solubility of carbon in the matrix and the ratio of precipitation is varied by the cooling rate, the more the cooling rate, the less the precipitation.

Some papers reported that the spalling resistance decreased when the matrix transformed fully into martensite. This could be due to too high hardness. To overcome this weakness, the tempering or subcritical heat treatment is given. The tempering temperature must be carefully chosen so that the martensite must not be over-tempered, or in other words, so that the tempered martensite can remain greatly in the matrix. Over-tempering leads to a decrease in hardness and resultantly strength of the matrix. Maratray[19] reported that in the range of tempering

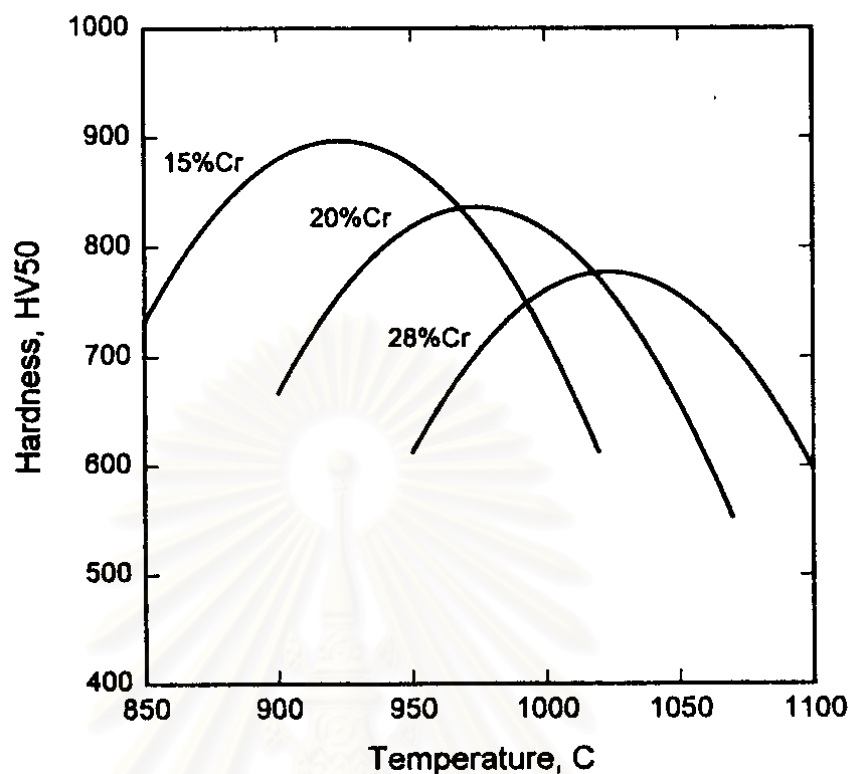


Fig.2-5 Influence of Cr content on the optimum hardening temperature in high chromium cast irons[14].

temperature from 753 K to 923 K (480 to 650 °C),  $M_{23}C_6$  carbide is more stable than  $M_7C_3$  carbide. Biss[20] showed that the tempering at 923 K (625 °C) produced  $M_{23}C_6$  carbide and he also found that some martensite was still in the matrix. I.R. SARE et al.[21] reported that in a kind of alloy white cast iron, the hardness does not change until the tempering temperature was risen to 723 K (450 °C) but over 723 K (500 °C), it gradually decreases as the tempering temperature increases.

### III Wear resistance

In the field of mining, iron and steel, electric power plant and cement industries, various kinds of machines are used for digging, crushing or milling and rolling. Abrasive wear usually occurs in these parts. Abrasive wear can be classified into three types,

- (1) Gouging abrasion which arises when the surface of machine is scooped out by the large mass of abrasives such as ores or stones with heavy impact load.
- (2) Grinding or high-stress abrasion which takes place when mineral or cement clinker is pulverized between two moving metals like rolls.
- (3) Scratching abrasion or low-stress abrasion which occurs when the small abrasives are touching on the surface of working parts and when low stress is sufficient to crush or grind the abrasives.

Generally, the combination wear of two or three types occurs on the surface of parts during service. As we know, wear resistance of high chromium cast iron is related to the microstructure, that is, morphology and amount of carbide and the matrix structure, which are factors to determine the macro-hardness of cast iron. These factors may also determine mechanical properties, particularly toughness of the cast iron. Since the eutectic carbide change little in both the quantity and morphology after solidification, the matrix structure becomes an important factor to improve the wear property. Many researches reported that the large volume fraction of retained austenite was preferable to the abrasive wear resistance against the heavy abrasive load or high stress abrasive condition, whereas in light abrasive condition, martensitic matrix is preferred. Even to an impact abrasive load, a certain amount of retained austenite is considered to be effective. It is known that the retained austenite may often lead to cracking when it is used, because of the great expansion by the stress-induced martensite transformation. This



phenomenon is solved by using heat treatment which decomposes the retained austenite to a low level. I.R. Sare[4,21] reported that the level of retained austenite which gives the optimum wear resistance is, for example, 10% for repetitive-impact condition and 30-40% for gouging abrasive condition, respectively.

Abrasion wear resistance of 15% and 26% Cr cast iron in as-cast condition was investigated by O.N. Dogan[10] and it was discussed by connecting it to the volume fraction of carbide ( $V_C$ ). In this paper, an equation (2.5) of  $V_C$  vs. carbon and chromium content which had proposed by maratray[14] was used for calculation of the  $V_C$ .

$$\%V_C = 14.05(\%C) + 0.43(\%Cr) - 0.22 \quad (2.5)$$

The relationship between hardness and volume fraction of eutectic carbide is shown in Fig.2-6. At the same chromium content, the hardness increases with an increase in carbon content, and higher hardness is obtained in high chromium content. The relation between volume fraction of carbide and wear rate is shown in Fig. 2-7. The wear rate decreases as the volume fraction of carbide increases and the decreasing rate is larger in 15%Cr iron, but the wear rate of 15% Cr is three times as much as 26%Cr cast iron. As shown in Fig. 2-8, the wear rate decreases roughly in proportion to the hardness. From above reviews, it can be concluded that the abrasive wear resistance of 26%Cr cast iron, which has more austenitic matrix and high volume fraction of carbide, is greater than that of 15%Cr cast iron with bainitic and pearlitic matrix and lower volume fraction of carbide. The effect of heat treatment on the gouging abrasion resistance or the high stress-abrasion resistance of alloy white cast iron was investigated by I.R. Sare and B.K. Arnold[4,21] using a jaw crusher. They found that lowest wear loss is obtained at the intermediate level of retained austenite like 30-40%, as shown in Fig.2-9. The relationship between hardness and weight loss is shown in Fig.2-10. Though the data are scattered, it is found that the weight loss decreases as the hardness.

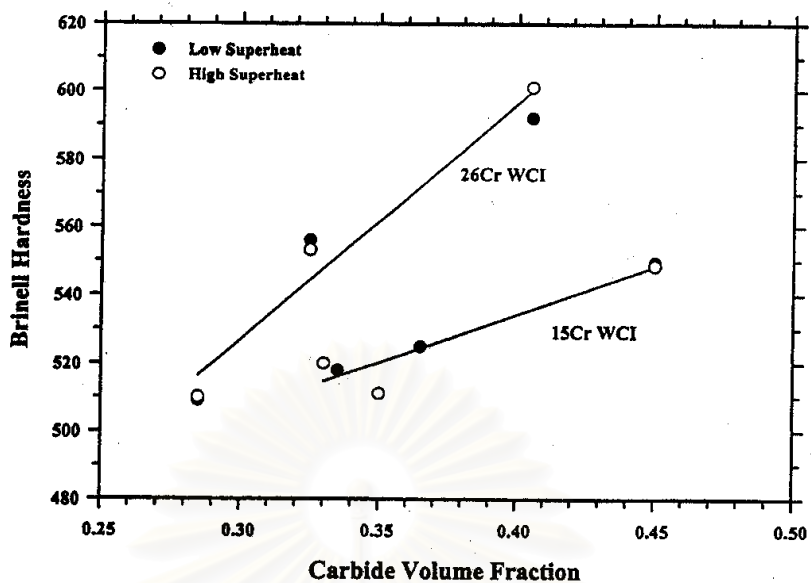


Fig. 2-6 Effect of volume fraction of carbide on the overall hardness of white cast irons with different matrix structures[10].

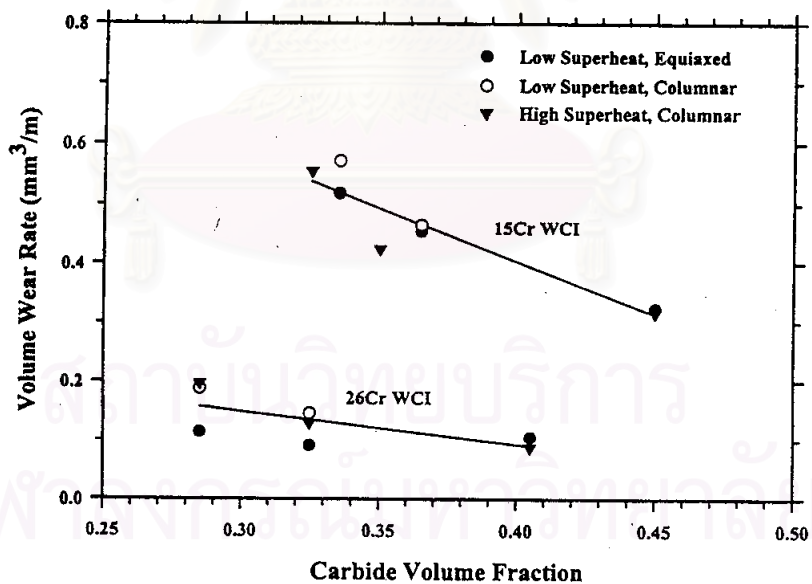


Fig 2-7 Effect of volume fraction of carbide on the abrasion rate of high chromium cast irons[10].

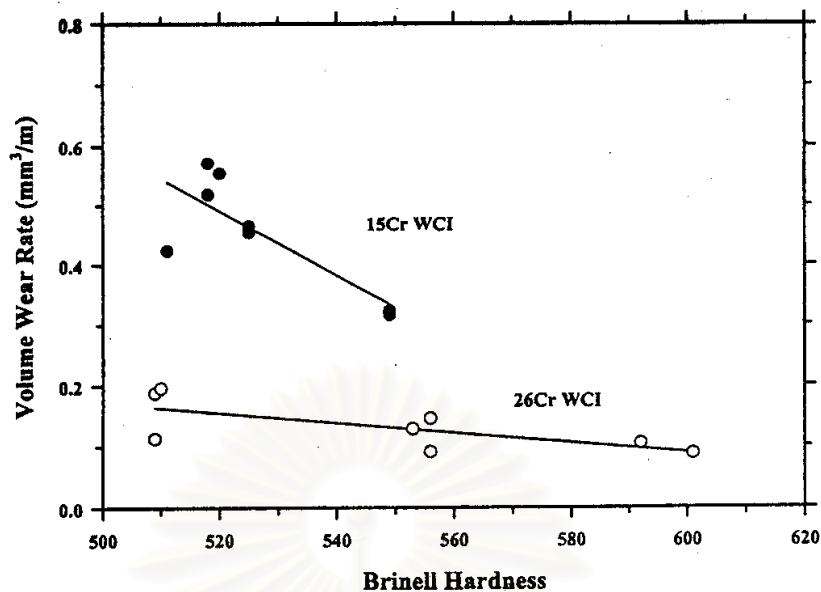


Fig. 2-8 Relationship between abrasion resistance and hardness of the two high chromium white cast irons[10].

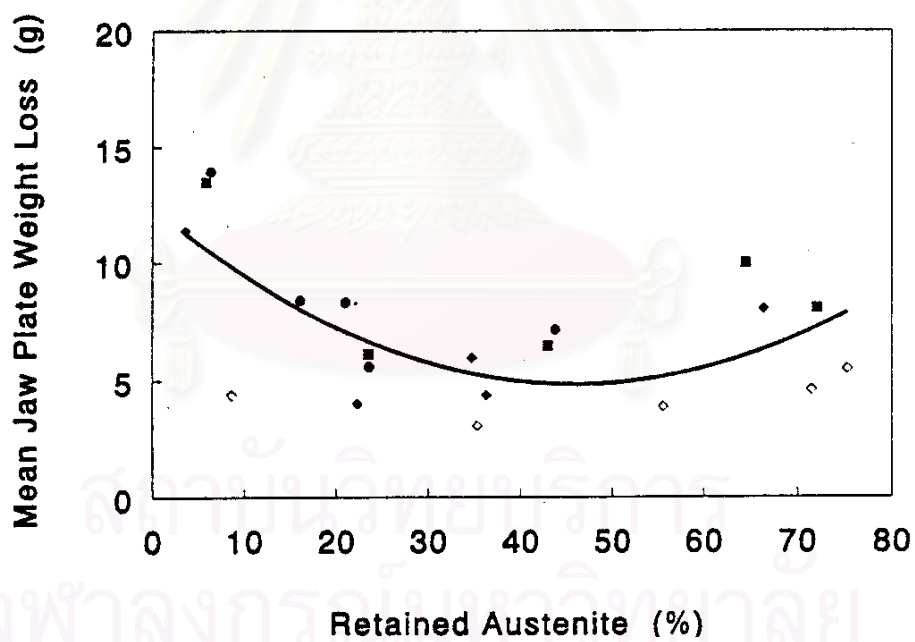


Fig. 2-9 Relationship between mean jaw-plate weight loss(g) and volume fraction of retained austenite[4].

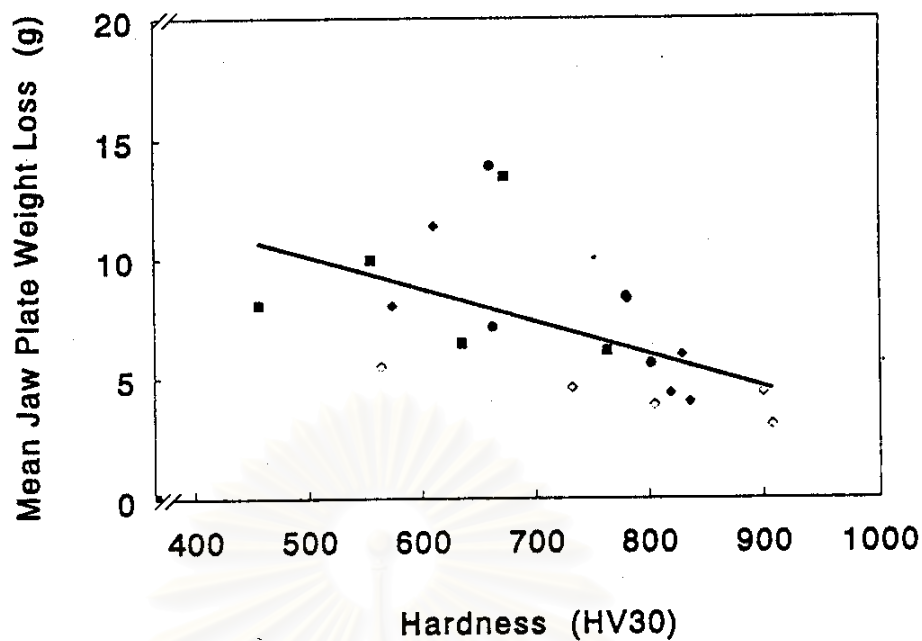


Fig. 2-10 Relationship between Jaw-plate weight loss and hardness[21].

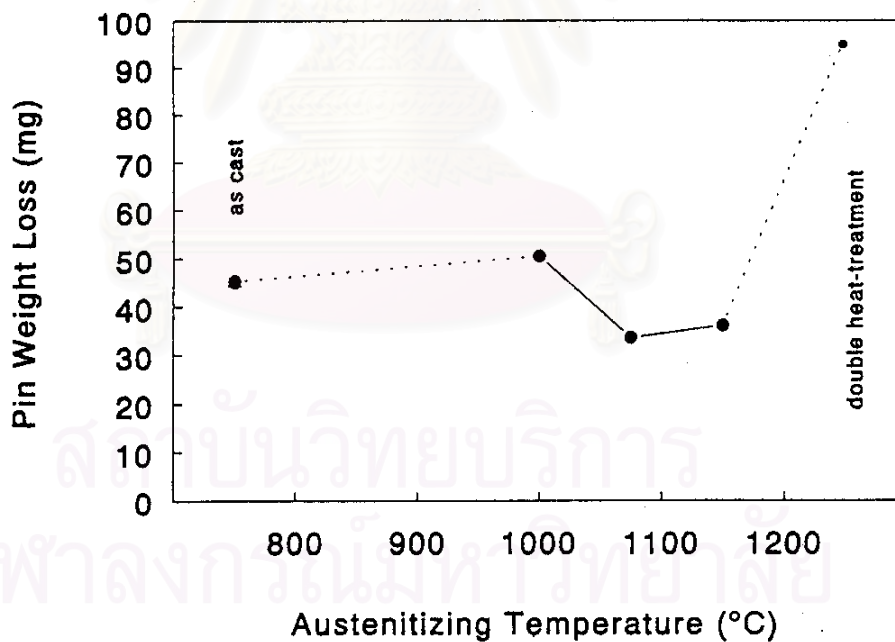


Fig. 2-11 Relationship between mean high-stress abrasion pin weight loss (mg) and austenitizing temperature(°C) of 27%Cr cast iron[21]. Data are also shown in the as-cast and as-tempered condition.

In high-stress abrasive condition, the effects of austenitizing temperature on the wear losses in as-hardened and tempered states are shown in Fig.2-11. It is usually said that the abrasion resistance after tempering is reduced and the highest abrasion resistance is obtained in as hardened-state. In tempered state, Fig.2-12, the wear loss decrease gradually as the tempering temperature rises to 723 K (500 °C). This can explain that over the 798 K (525°C), carbides formed by tempering starts to aggregate and to be coarsened. Result of pin disks wear test is shown in Fig.2-13. It is clear that the wear resistance in tempered state is in good accordance with the macro-hardness and it decreases as the hardness increases. To obtain high hardness, the tempering temperature must be chosen by considering the amount of retained austenite in the matrix. Wanaporn et al.[23] has clarified those relations in multi-component white cast irons that the higher tempering temperature should be adopted as volume fraction of retained austenite is become higher.

S.K. Yu et al.[3] investigated the effect of volume fraction of retained austenite( $V_\gamma$ ) on the rate of abrasion wear ( $R_w$ ) in hypoeutectic high chromium white cast iron. As shown in Fig.2-14, the  $R_w$  decreases with increasing the  $V_\gamma$  and also as shown in Fig.2-15, the  $R_w$  increases with an increase in macro-hardness because of the transformation of retained austenite to martensite during abrasion test.

สถาบันวิทยบริการ  
จุฬาลงกรณ์มหาวิทยาลัย

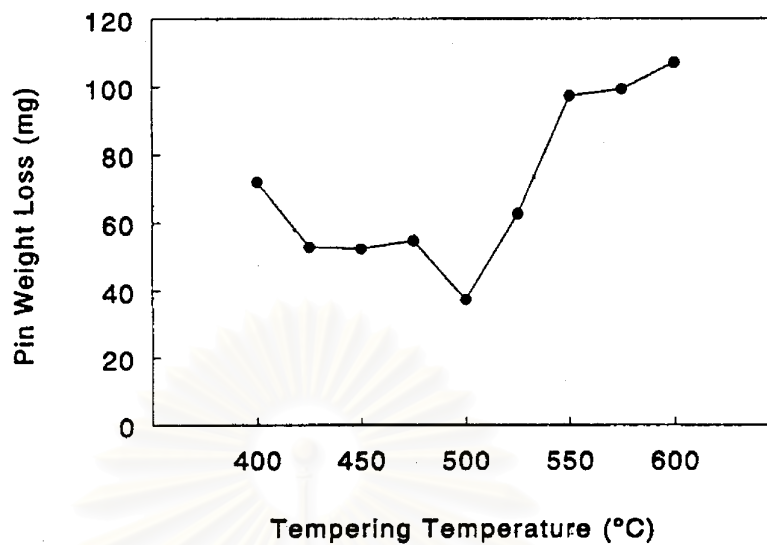


Fig 2-12 Relationship between mean high-stress abrasion pin weight loss(mg) and tempering temperature(°C) of 27%Cr cast iron[21].

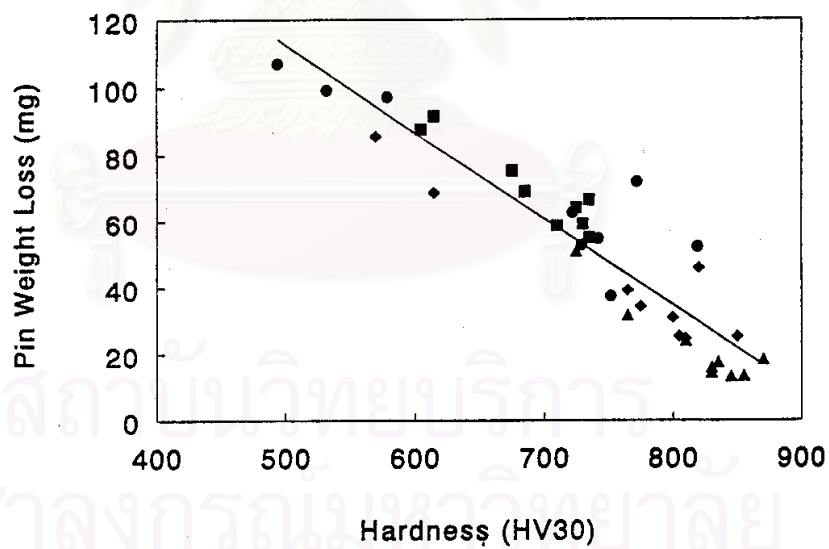


Fig. 2-13 Relationship between pin weight loss and hardness[21].

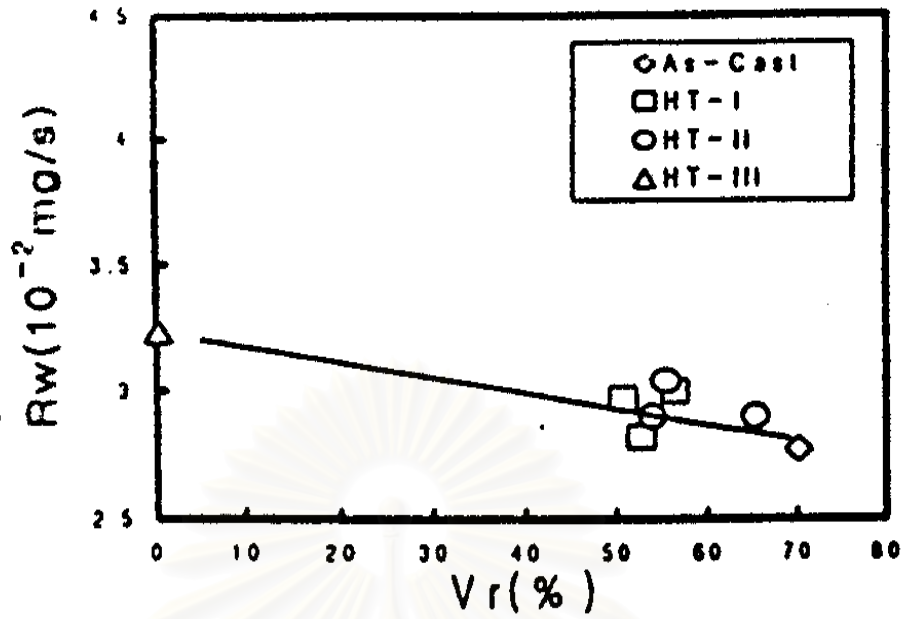


Fig.2-14 The relationship between wear rate and volume fraction of retained austenite( $V_r$ )[3].

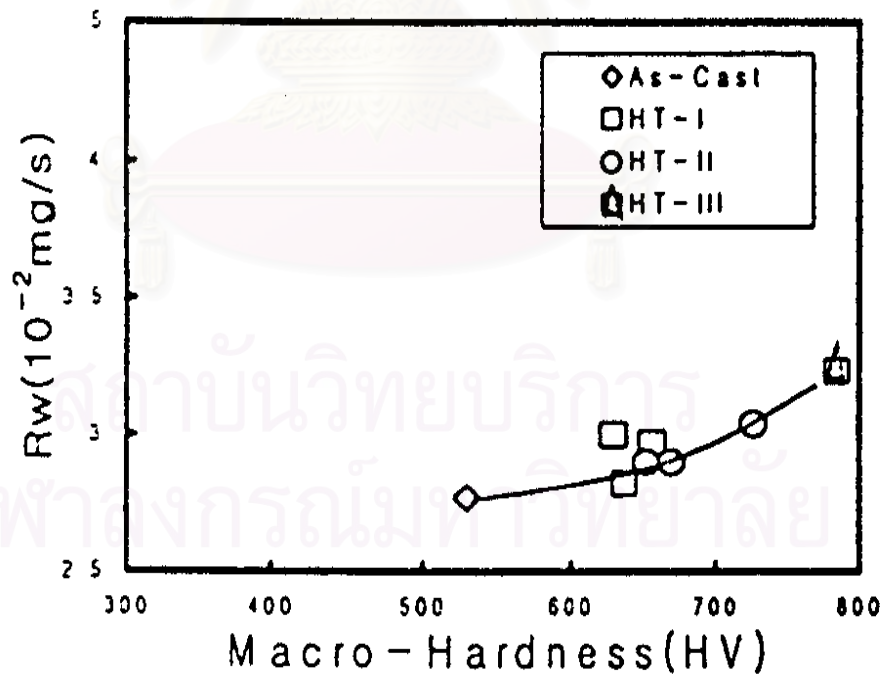


Fig.2-15 The relationship between wear rate ( $R_w$ ) and macro-hardness [3].

## Chapter 3

### Experimental Procedure

#### 3.1 Preparation of Specimens

##### 3.1.1 Mold Design and Test Piece

The shape and dimension of the CO<sub>2</sub> mold is shown in Fig. 3-1. The wood pattern or cavity consists of a portion (25 mm x 65 mm) for test piece and the riser on it. The cast specimen was sliced by a wire-cut EDM (Electric Discharge Machine) to obtain the disk-shaped test piece with 7 mm in thickness.

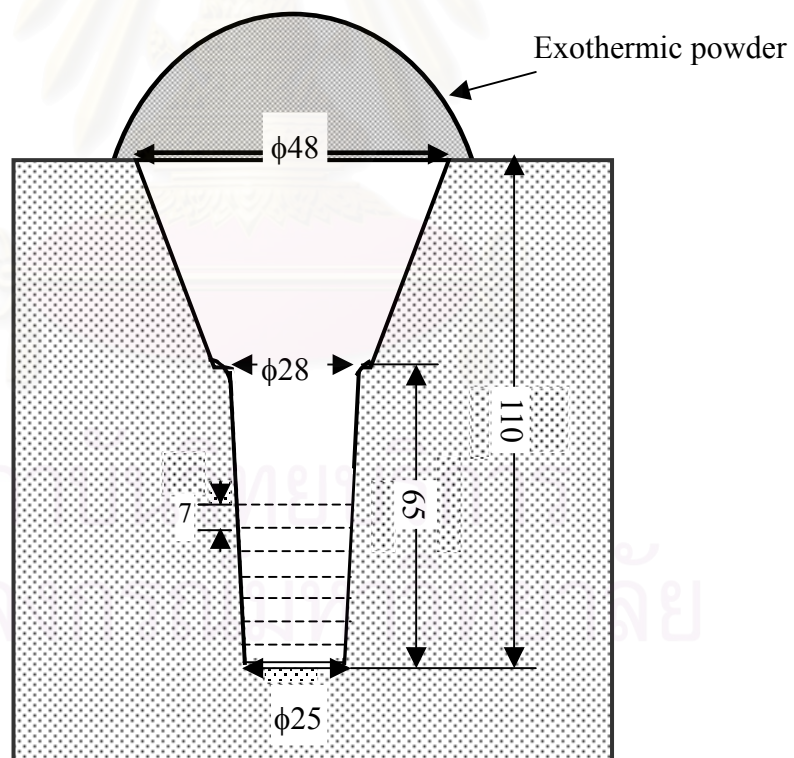


Fig. 3-1 Schematic drawings of CO<sub>2</sub> mold. Unit: mm



### 3.1.2 Production of Specimens

The charge calculations were carried out for the target chemical compositions of eutectic and hypo-eutectic cast irons. As raw materials, mild steel scrap, pig iron, ferroalloys such as Fe-Cr with low carbon and high carbon, Fe-Mn and Fe-Si, pure metals were used. The chemical compositions of raw materials are shown in Table 3-1. The total weight of 10 kg was melted down in 10 kg-capacity high frequency induction furnace with alumina ( $\text{Al}_2\text{O}_3$ ) lining and superheated at 1853 K (1580 °C). After holding the melt, it was cast from the pouring temperature of 1773-1793 K (1500-1520 °C) into the preheated  $\text{CO}_2$  mold shown in Fig.3-1. The melt was immediately covered with dry exothermic powder to hold the temperature of riser high. The chemical compositions, eutectic ratio, ratio of chromium and carbon (Cr/C) and type of eutectic carbide of the test specimens are summarized in Table 3-2. Two series of cast iron with 16%Cr and 26%Cr were made. In each chromium series, the carbon content was varied so that the eutectic ratio could range widely from 100%.

### 3.2 Heat Treatment Procedure

For the investigation of heat treatment characteristics, the conditions of heat treatment listed in Table 3-3 were introduced. Each heat treatment cycle are illustrated in Fig. 3-2.

#### 3.2.1 Annealing

In order to remove the micro-segregation produced during solidification, the test piece (hereafter expressed by specimen) was coated with an anti-oxidation liniment to prevent the decarburization.

Table 3-1 Chemical composition of raw materials

Materials	Element (mass%)						
	C	Cr	Si	Mn	P	S	Fe
Mild steel scrap	0.05	-	0.02	0.28	0.011	0.011	bal
Pig iron	4.44	-	1.14	0.19	0.08	0.019	bal
Fe-Cr (HC)	8.42	62.02	1.02	-	0.025	0.036	bal
Fe-Cr (LC)	0.02	69.24	0.25	-	0.030	0.005	bal
Fe-Mn(L)	0.96	-	0.24	75.3	0.144	0.012	bal
Fe-Si	0.047	-	75.00	-	0.016	-	bal

Table 3-2 Chemical composition, eutectic ratio, Cr/C value and carbide type of test specimens

Specimen	Element (mass.%)				Eutectic ratio	Cr/C	Type of carbide
	C	Cr	Si	Mn			
No.1	3.45	16.01	0.39	0.67	96.3	4.64	M <sub>7</sub> C <sub>3</sub>
No.2	3.01	16.48	0.62	0.78	78.0	5.48	
No.3	2.62	15.93	0.41	0.69	45.2	6.08	
No.4	2.99	26.76	0.51	0.54	100	8.96	
No.5	2.65	25.56	0.37	0.51	74.0	9.65	
No.6	2.32	25.53	0.37	0.54	62.3	11.0	

Specimens were cold-charged in an electric furnace and heated up by heating rate of 0.1 K/s. At 1173 K (900 °C), the specimens were held for 18 ks (3 hours) and cooled in the furnace (FC) down to the room temperature.

### **3.2.2 Hardening**

Two austenitizing temperatures were introduced for hardening. Specimens homogenized by annealing were heated up at 1273 K (1000 °C) and 1323 K (1050 °C) for austenitization. After holding for 5.4 ks (1.5 hours) at the austenitizing temperatures, the specimens were hardened by fan air cooling (FAC).

### **3.2.3 Tempering**

The hardened specimens were arranged on the alumina boat and held in the furnace at several temperatures from 573 K to 873 K for 7.2 ks (2 hours). The tempering temperatures were changed at intervals of 50 K. After the tempering finished, they were cooled to the room temperature in the still air (AC).

## **3.3 Observation of Microstructure**

### **3.3.1 Optical Microscopy**

To observe the microstructure of specimen by means of an optical microscope (OM), it was polished using emery papers in the order of #180, 320, 400 and 600 and finished by a buff cloth with extremely fine alumina powder of 0.3  $\mu\text{m}$  in diameter. The microstructure was revealed using the etchants shown in Table 3-4.

Table 3-3 Heat treatment conditions

Heat Treatment Process	Annealing	Hardening	Tempering
Temperature (K)	1173	1273 1323	573 623 673 723 773 823 873
Holding Time (ks)	18.0	5.4	7.2
Cooling Conditon	FC	FAC	AC

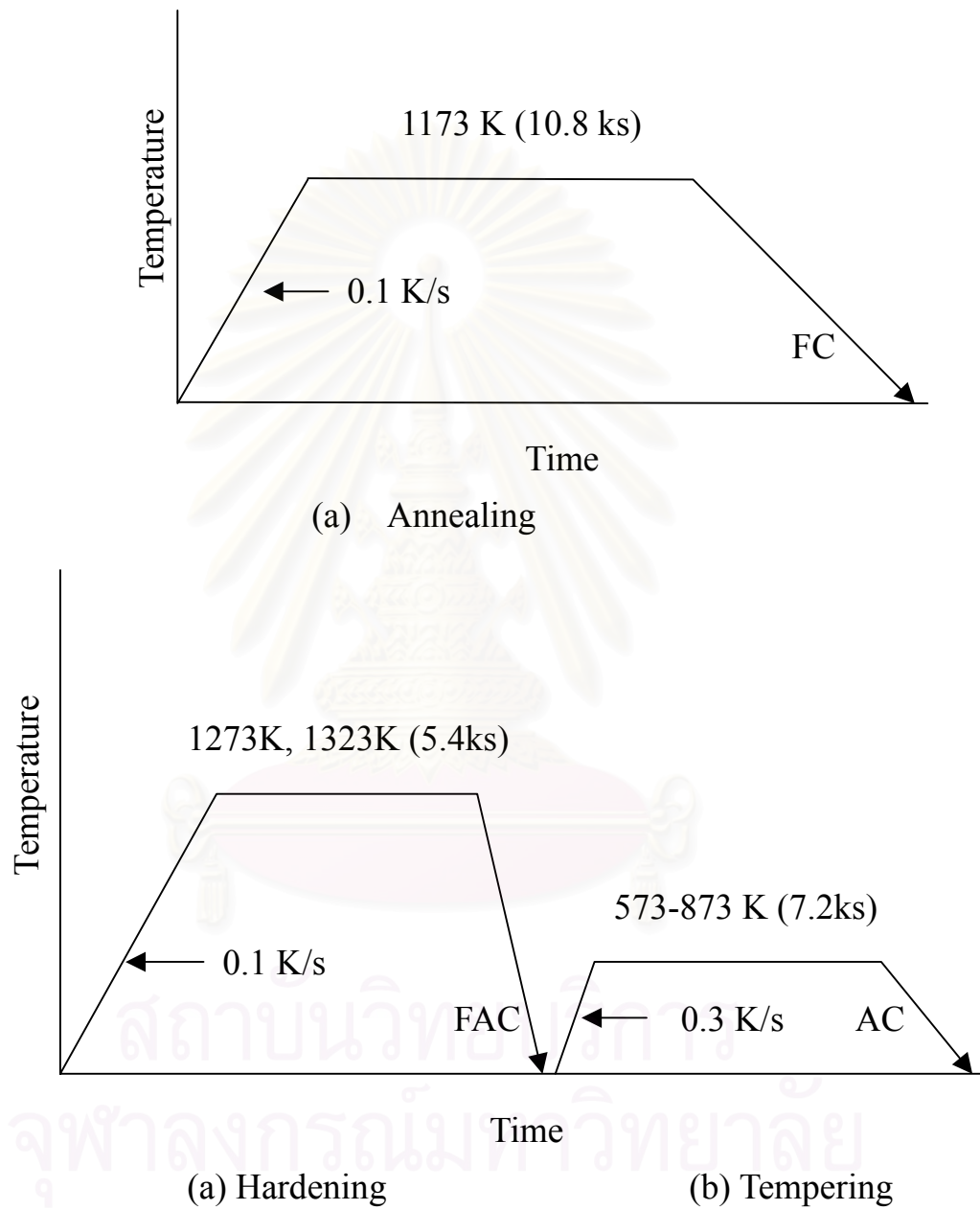


Fig.3.2 Heat treatment cycle for annealing, hardening and tempering.

Table 3-4 List of etchants

Type	Etchant	Etching method	Attack
A	Picric acid 1 g HCl 5 cc Ethanol 100 cc	Immersion at room temperature	Carbide and matrix
B	Nital reagent HNO <sub>3</sub> 5 cc Ethanol 95 cc	Immersion at room temperature	Matrix

### 3.3.2 Scanning Electron Microscopy

For more discussions, the microstructure involving secondarily precipitated carbides was observed in detail using a Scanning Electron Microscope (SEM) of Hitachi Model S2380 N. A polished specimen was lightly etched using the B etchant to reveal the microstructure. The microphotographs mainly focusing on carbide morphology in matrix were taken by high magnifications,(2500X).

### 3.4 Hardness Measurement

Macro-hardness of specimen was measured by means of vickers hardness tester (Akashi Model AVK) applying the load of 297 N (30 kgf). Five indentations were taken at random and the average value was adopted. On the other hand, micro-hardness of matrix was measured also five times by micro-vickers hardness tester (Akashi Model MVK-G1) applying the load of 1 N (100 gf) and the measured values were averaged.

### 3.5 Measurement of Volume Fraction of Austenite

#### 3.5.1 Theory for Measurement of Retained Austenite by X-ray Diffraction Method

Quantitative measurement of austenite in matrix is not so easy because the bulk test specimen with strong orientation of dendrite must be used. In the methods to measure the volume fraction of austenite, X-ray diffraction method is convenient when the texture is cancelled as if the powder sample is used.

The basic equation of diffraction intensity of a phase is expressed as

$$I_{hkl} = K(FF^*)(LPF)me^{-2M}A(\theta)V_i/v_i^2 \quad (3.1)$$

where,

K	=	proportional constant
FF*	=	structure factor of the unit cell of the interest phase, equal to $4f^2$ and $16f^2$ for diffraction lines of $\alpha$ (martensite/ferrite) and $\gamma$ (austenite), respectively, where f is the atomic scattering factor of the atom species which make up the unit cell : f relates to $(\sin \theta)/\lambda$
LPF	=	Lorenz Polarization Factor, $(1+\cos^2 2\theta)/\sin^2 \theta \cos \theta$
M	=	multiplicity factor, the number of {hkl} planes in a unit cell
$e^{-2M}$	=	Debye –Waller temperature factor where
M	=	$(B\sin^2 \theta) / \lambda^2$ : B is a material constant
A( $\theta$ )	=	absorption factor, independent of $\theta$ if sample is flat
$V_i$	=	volume fraction of the phase
and		
$v_i$	=	volume of unit cell

Let,

$$K' = K \times A(\theta) \quad (3.2)$$

$$\text{and } R_{hkl} = [FF^*(LPF)me^{-2M}]/v_i^2 \quad (3.3)$$

Here, Debye-Waller temperature factor is negligible. Substitutes  $K'$  and  $R_{hkl}$  in the equation (3.1) to be equation (3.4),

$$I_{hkl} = K' R_{hkl} V_i \quad (3.4)$$

When several peaks in the diffraction pattern participate in the calculation, the above equation is shown by the next equation (3.5),

$$\Sigma I_{hkl} = K' (\Sigma R_{hkl})(V_i) \quad (3.5)$$

Therefore, peaks of ferrite and/or martensite ( $\alpha$ ) and peaks of austenite ( $\gamma$ ) are respectively shown as

$$\Sigma I_{\alpha} = K' (\Sigma R_{\alpha})(V_{\alpha}) \quad (3.6)$$

$$\Sigma I_{\gamma} = K' (\Sigma R_{\gamma})(V_{\gamma}) \quad (3.7)$$

Besides,

$$V_{\alpha} + V_{\gamma} + V_c = 1 \quad (3.8)$$

Where,  $V_c$  is the volume fraction of other phase.

Assume only  $\alpha$  and  $\gamma$  phases exist in the specimen, the equation (3.8) is,

$$V_{\alpha} + V_{\gamma} = 1 \quad (3.9)$$

The relationship between  $V_{\alpha}$  and  $V_{\gamma}$  from the equation (3.6) and (3.7) can be expressed by the next equation,

$$V_{\alpha} = \left[ \frac{\Sigma I_{\alpha} \cdot \Sigma R_{\gamma}}{\Sigma I_{\gamma} \cdot \Sigma R_{\alpha}} \right] \times V_{\gamma} \quad (3.10)$$

Solving the equation (3.9) and the equation (3.10) to obtain the volume fraction of austenite which relates to the diffraction peak intensity and  $R$  values, the following equation is finally given,

$$V_{\gamma} = 1 / [1 + (\alpha \Sigma I_{\alpha} \cdot \Sigma R_{\gamma} / \Sigma I_{\gamma} \cdot \Sigma R_{\alpha})] \quad (3.11)$$

For the determination of the amount of austenite,  $R$  values must be obtained by equation(3.3), and  $I_{\alpha}$  and  $I_{\gamma}$  values by measuring the areas under the diffraction peaks of  $\alpha$  and  $\gamma$ . Resultantly, the volume fraction of austenite ( $V_{\gamma}$ ) is attained numerically.

### 3.5.2 Equipment and Measuring Condition

The measurement of  $V_{\gamma}$  is carried out using X-ray diffraction method which was developed for steel by R.L. Miller and then for high



chromium white iron by C. Kim[24]. The measuring condition is demonstrated in Table 3-5. In this experiment, the simultaneously rotating and swinging sample stage was employed to cancel the influence of preferred orientation or textural configuration of austenite in the cast iron. The sample stage is shown in Fig.3-3. Fig.3-4 is the results of preliminary tests using the this experimental specimen to prove the advantage of use of this sample stage. It is edivalent that the peaks of  $\gamma_{200}$  and  $\gamma_{311}$  are stronger in the specimen with rotating and swinging (a) than those in the both cases of only rotaing (b) and of without rotating and swinging (c). On the other hand, the peaks of  $\alpha_{200}$  and  $\alpha_{220}$  are weaker in a use of state with rotaing and swinging. However, volume fraction of retained austenite calculated from the diffraction pattern measured using the rotating and swinging sample stage is higher than the other cases. It is because the rotaing and swinging could cancle the preferred orientation or texture of austenite. This sample stage has been used in this research. For this investigation, the test specimen was prepared by grinding surface and followed by polishing it in the same way as the specimen for microphotograph was prepared. Mo-K $\alpha$  characteristic line with a wavelength of 0.007 nm (0.711 A $^\circ$ ) was used as a source of X-ray beam.

### 3.5.5 Calculation of Volume Fraction of Austenite

In this investigation, the crystal planes of peaks availed in the calculation are (200), (220) of ferrite or/and martensite and (220), (331) of austenite because these four peaks are independent or not interfering from peaks of other phases like carbides. The diffraction patterns of three specimens with different  $V_\gamma$  are shown for comparison in Fig. 3-5. Reason why the  $\alpha_{211}$  peak in these patterns is not taken into account is that this peak is overlapped with a strong peak of chromium carbide. The integrated areas of these peaks were obtained using an image analyzer (Nireco Model Luzex IIIU). The calculation of  $V_\gamma$  was done by a

Table 3-5 Condition of X-ray diffraction to measure the volume fraction of retained austenite

Target metal	Mo
Tube Voltage · Current	50 kV · 30mA
Slits	Divergence Slit: 1° Receiving Slit: 1.5 mm Scattering Slit: 1°
Filter	Zr
Scanning Range	24-44 deg
Scanning Speed	0.5 deg/min
Step/Sampling	0.01 deg

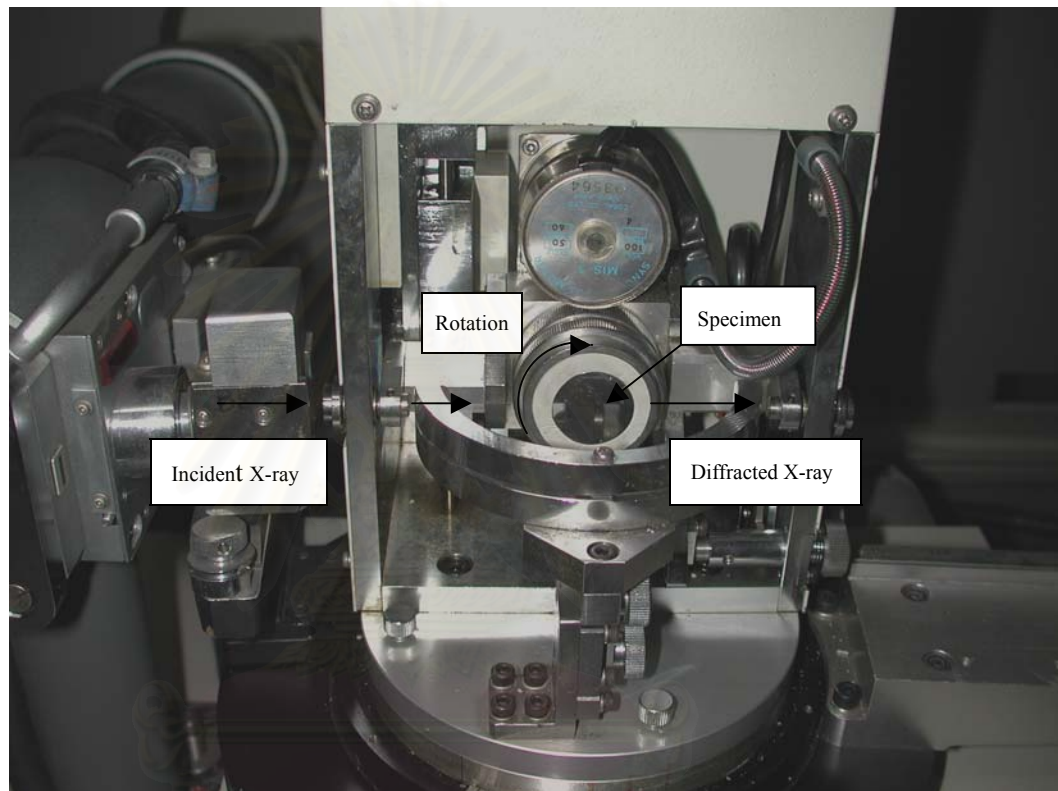
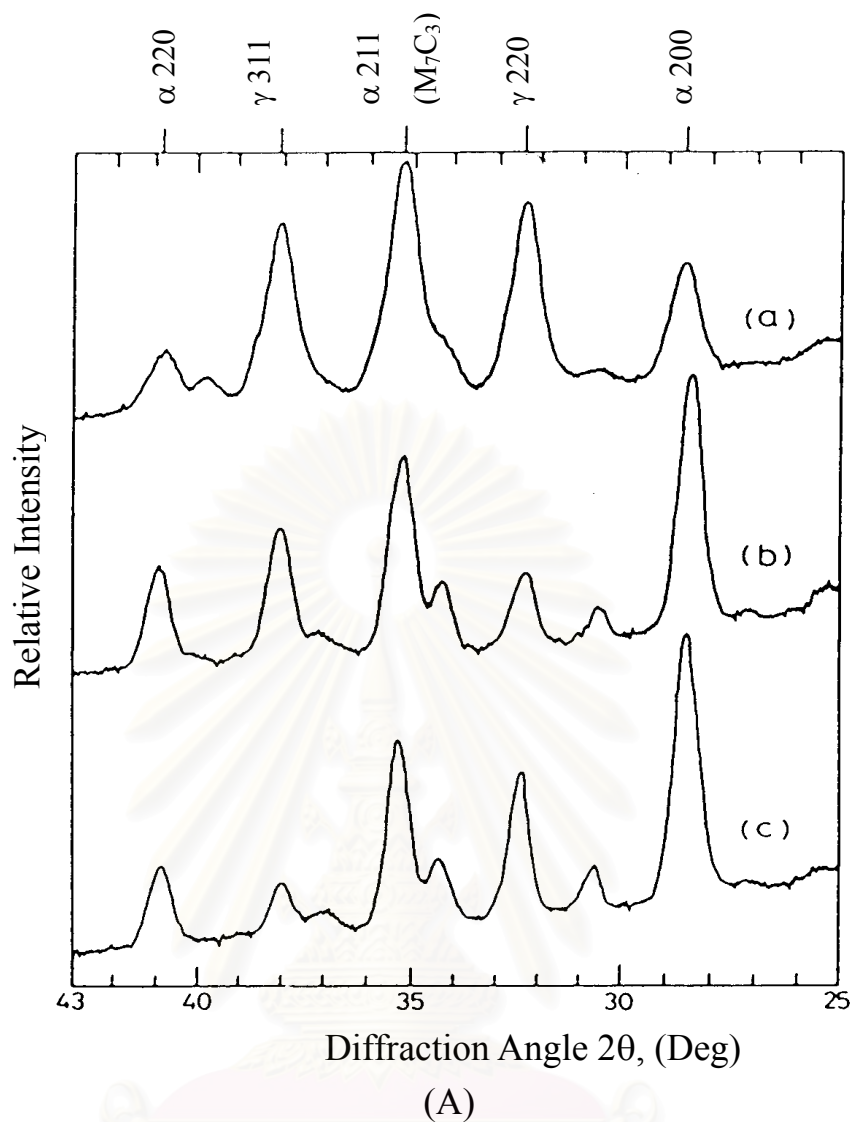


Fig.3-3 Photograph of special sample stage for retained austenite measurement by X-ray diffraction.



Symbol	Condition	$V_{\gamma}(\%)$
(a)	Rotating and swinging	71.3
(b)	Rotating	37.6
(c)	Without (a) and (b)	18.3

(B)

Fig.3-4 Effect of sample stage condition on diffraction pattern(A), and volume fraction of retained austenite( $V_{\gamma}$ ) (B) calculated from the profiles in (A). (Specimen No.6 in as-cast state)

computer for three combination of peaks,  $\alpha_{200} - \gamma_{311}$ ,  $\alpha_{200} - \Sigma\gamma(220,311)$  and  $\Sigma\alpha(200,220) - \gamma_{311}$ . The averages of values calculated from three combinations were used for plotting.



สถาบันวิทยบริการ  
จุฬาลงกรณ์มหาวิทยาลัย

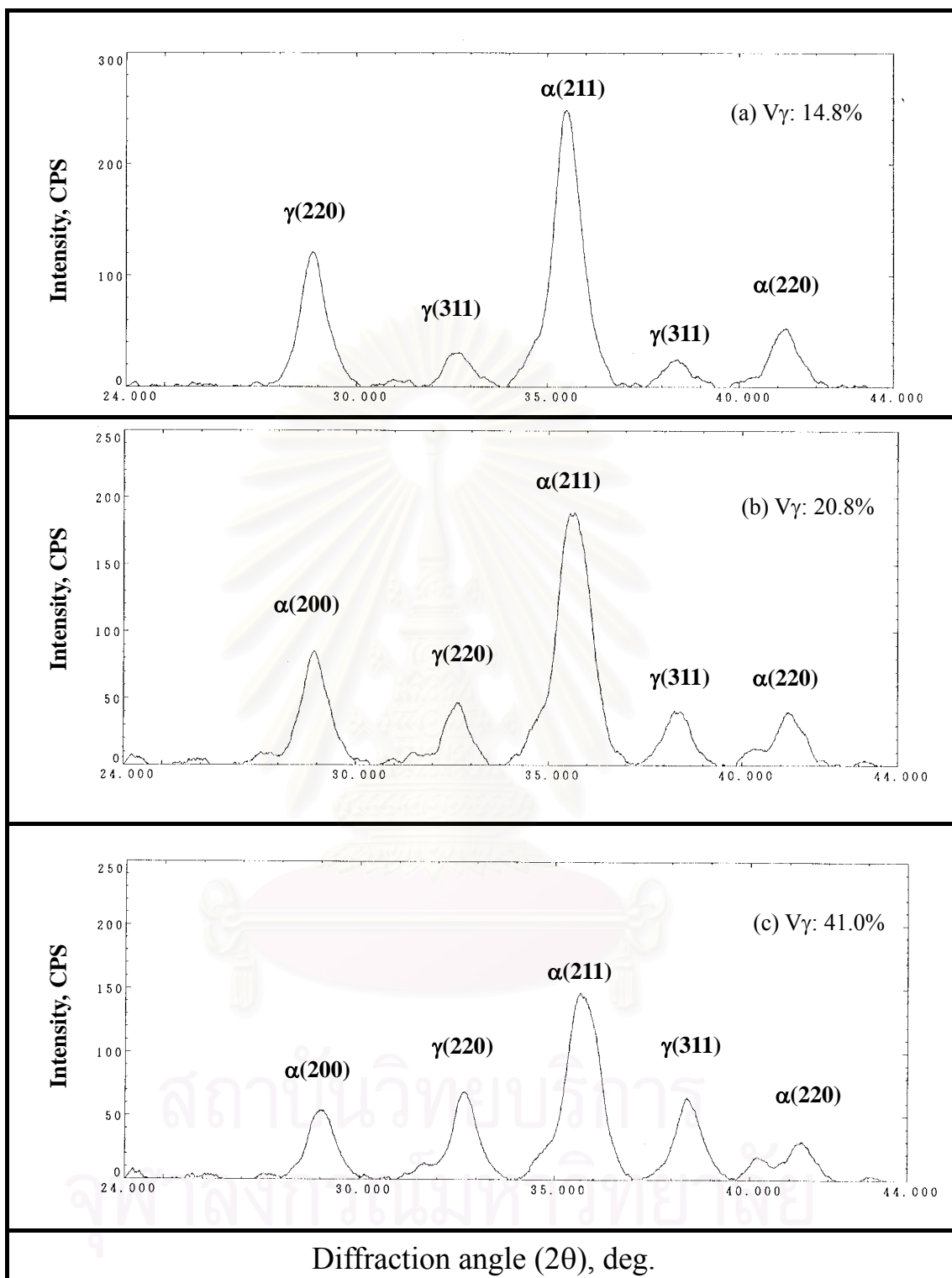


Fig 3.5 X-ray diffraction patterns of specimens with different volume fraction of retained austenite( $V_{\gamma}$ ):(a) 14.8%, (b) 20.8%, (c) 41.0%.

## Chapter 4

### Experimental Results

#### 4.1 Microstructure of Test Alloys

##### 4.1.1 As-cast state

As-cast microstructures of test specimens are shown in Fig.4-1. Specimens No. 1 is roughly eutectic and No.4 is absolutely eutectic cast irons and the others are hypoeutectic cast irons. In 16%Cr irons, the microstructures consist of pearlitic matrix and eutectic carbides embedded in the matrix. On the other side, the microstructures of 26%Cr irons consist of austenitic matrix with some martensite that can not be distinguished by optical microscope and eutectic carbides. According to the work by Matsubara et al.[2], the eutectic carbides are mostly  $M_7C_3$  type and  $M_{23}C_6$  carbides do not precipitate in the range of these chemical composition. As for the morphology of eutectic structure, the eutectic structure shows colony shape because it grows in a cellular interface [7] and it contains fine rod-like  $M_7C_3$  carbides in the center and coarse string-like  $M_7C_3$  carbides growing to the colony boundary. The colony size is affected by chromium content in the cast iron and it is larger in 16%Cr iron and smaller in 26%Cr iron, when compared by the specimens with similar eutectic ratio. By comparing the microstructure at the same chromium level, eutectic colony size decreases with a decrease in carbon content of the iron. With respect to the size of chromium carbides themselves, they are much smaller in 26%Cr iron than in 16%Cr iron. In the 26%Cr cast irons, particularly, the size of carbide particles is very fine in the eutectic cast iron. It is well known that the eutectic carbides in the colony are in rod-like or blade like morphology and three-dimensionally interconnected.

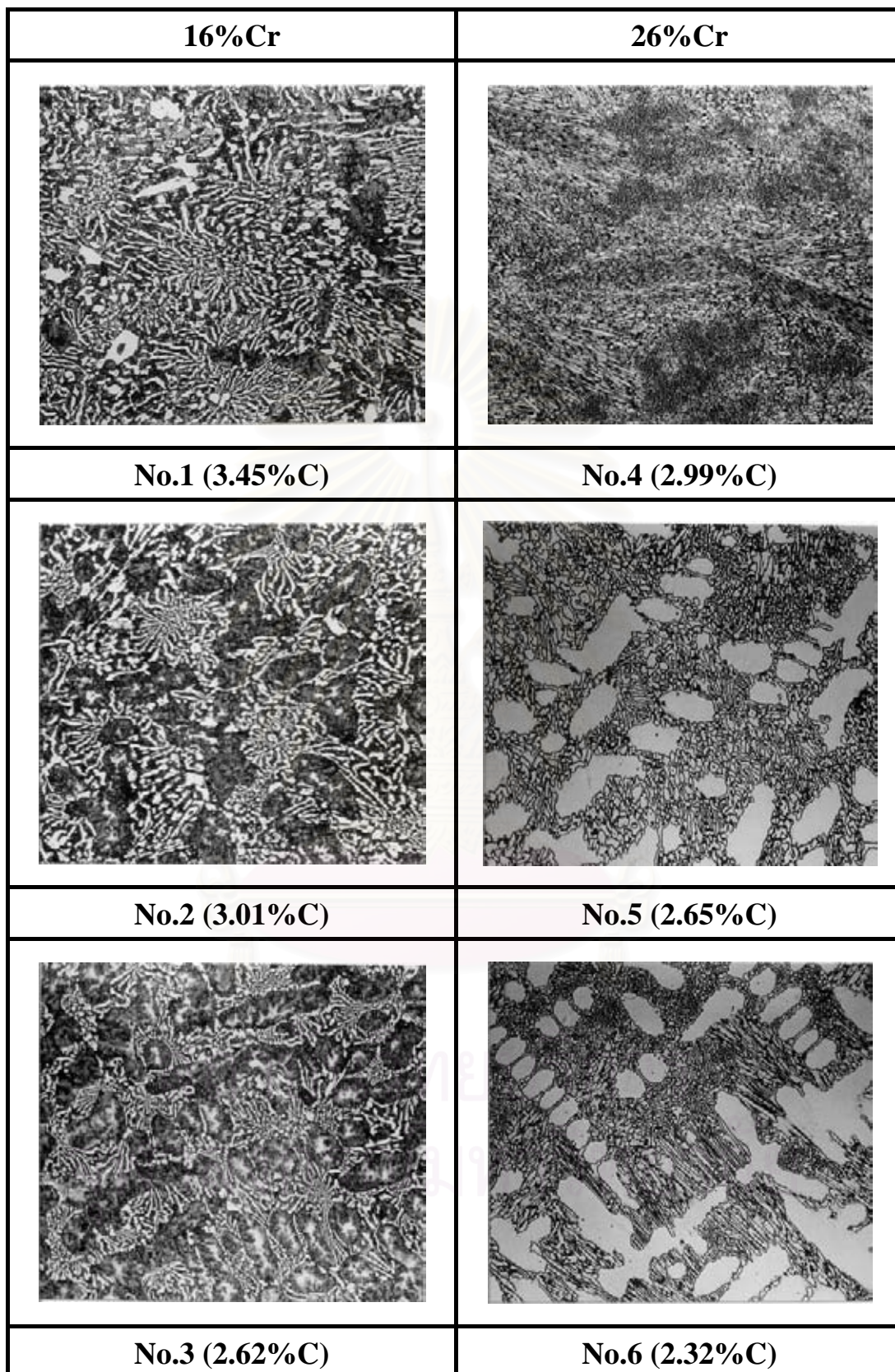


Fig.4-1 Microphotographs of as-cast with 16% and 26%Cr cast irons. morphology and three-dimensionally interconnected.



### 4.1.2 As-hardened State

In order to observe the matrix in detail, the SEM microphotographs of as-hardened specimens were taken at high magnification like 2500 and they are displayed in Fig 4-2. In the case of 16%Cr cast irons, the matrix structure consists of a large number of fine precipitated carbides, martensite and retained austenite. G. Laird II[15] reported in his work that the secondary carbides that precipitate in as-hardened state of high chromium cast irons are mostly  $M_7C_3$  type. The degree of carbide precipitation in hypo-eutectic cast irons is more than that of eutectic cast iron. The microstructures of 26%Cr cast irons also show a same tendency as 16%Cr cast irons. In each series of iron, austenite which existed much more in as-cast state is replaced by fine secondary carbides and martensite. In the eutectic cast irons, the matrix areas among eutectic carbides are very small and therefore the precipitated carbides possibly diffuse to the massed eutectic carbides. In the primary matrix of hypo-eutectic cast irons, it can be seen that there are less or free of precipitated carbides in the region near eutectic carbides. Even if the precipitation of secondary carbides is compared in the specimens with almost the same eutectic ratios (No.2 and No.5). It is hard to discuss the difference in the amount of secondary carbide between 16%Cr and 26%Cr cast irons.

## 4.2 Influence of Heat Treatment Condition on Macro-Hardness and Volume Fraction of Retained Austenite

### 4.2.1 As- cast State

Macro-hardness and volume fraction of retained austenite( $V_\gamma$ ) of as-cast specimens are shown in Table 4-1. Hardness of 16% Cr cast irons does not change according to the carbon content, and that of 26%Cr irons decreases with decreasing the carbon content. O.N. Dogan et al.[10]

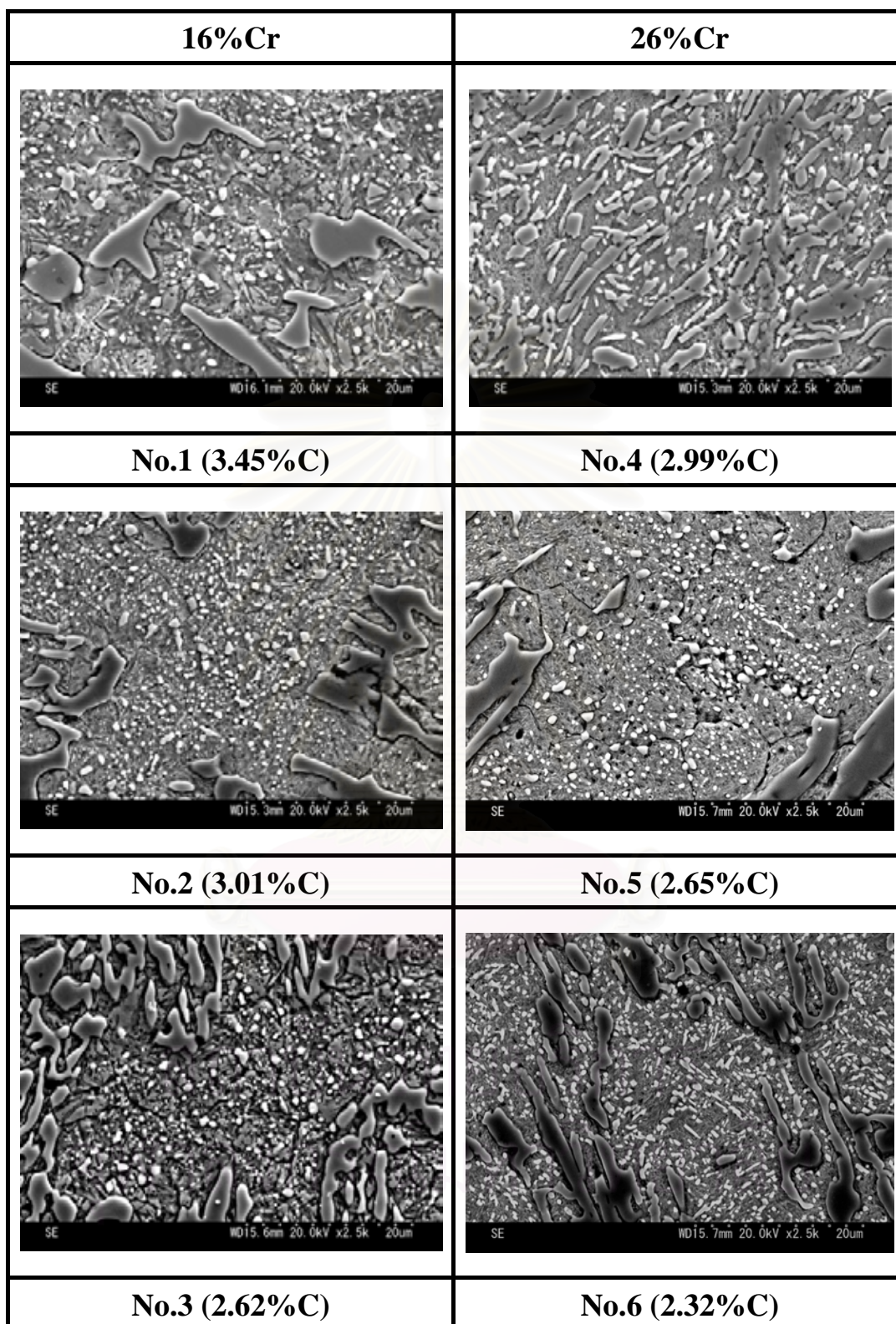


Fig. 4-2 SEM microphotographs of as-hardened 16% and 26%Cr cast irons.

reported that the hardness of as-cast specimen is related to the amount of eutectic carbide in the same chromium content, the more the amount of carbide, the higher the hardness. The  $V_{\gamma}$  of 16%Cr irons are zero regardless of carbon content and this means that most of austenite in 16%Cr irons transformed to pearlite at the cooling condition of this mold. In the case of 26%Cr irons, on the other hand, the  $V_{\gamma}$  is greatly related to the carbon content of the cast iron, that is, the  $V_{\gamma}$  increases with a decrease in carbon content.

Table 4-1 Volume fraction of retained austenite( $V_{\gamma}$ ) and hardness in as-cast state

Specimen	Element (mass%)		HV30	$V_{\gamma}$ , %
	Cr	C		
No.1	16	3.45	564	0
No.2		3.01	537	0
No.3		2.62	564	0
No.4	26	2.99	635	33.7
No.5		2.65	547	67.8
No.6		2.32	514	71.3

#### 4.2.2 As-hardened state

Macro-hardness and  $V_{\gamma}$  are shown in Table 4-2. The hardness is determined by volume fraction of carbides and matrix structure. In particular, the matrix hardness is greatly related to the  $V_{\gamma}$ , the more amount of carbide leads to the increase in macro-hardness and that the more  $V_{\gamma}$  gives the decrease in the hardness. From Table 4-2, the clear relation between macro-hardness and carbon content of the iron is not found. When carbon content reduces, the hardness of 16%Cr iron does not vary so much, even if the austenitizing temperature changes, ranging

from 780 to 763 HV30 and 780 to 775 HV30 at 1273 K and 1323 K austenitization, respectively. In 26%Cr cast iron, the macro-hardness changes a little, ranging 769 to 749 HV30 at austenitization of 1273 K and 796 to 769 HV30 at 1323 K, respectively. On the other hand, the  $V_\gamma$  varies greatly depending on the carbon content at the same chromium level. In case of 1273 K austenitization, however, the variation of  $V_\gamma$  is small, from 29% to 18% in 16% Cr cast iron and from 4 to 3% in 26%Cr iron. In the case of 1323 K austenitization, the  $V_\gamma$  decreases with a decrease in the carbon content, from 41 to 28% in 16%Cr and from 18 to 11% in 26%Cr cast irons, respectively. Comparing the hardness and  $V_\gamma$  by austenitizing temperatures, the hardness are similar in 16%Cr iron and a little higher in 26%Cr iron when the austenitizing temperature rises from 1273 K to 1323 K. However, the  $V_\gamma$  is much higher in the case of 1323 K austenitization. This is because more carbon and chromium dissolve in austenite at higher austenitizing temperature. Maratray[14] reported the similar results in high chromium cast irons containing molybdenum (Mo).

When these results are compared with those of as-cast irons, remarkable difference is observed in the  $V_\gamma$ . The  $V_\gamma$  values are almost zero in as-cast 16% Cr irons, whereas those in as-hardened 16%Cr irons are high. This reason is that carbides precipitated in as-cast state dissolves in austenite and their the precipitation is suppressed by rapid cooling. In 26%Cr irons, on the other side, the  $V_\gamma$  in as-hardened specimens decrease greatly in comparison with that in as-cast state. The reason could be that the austenite in as-cast state where carbon and chromium super-dissolved is destabilized and they precipitate by forming chromium carbides during austenitization. Resultantly, the concentration of carbon and chromium in the austenite is reduced and  $M_s$  temperature rises over room temperature. The decrease of  $V_\gamma$  can be also understood from the fact that the martensite is existing in the matrix.

Table 4-2 Volume fraction of retained austenite ( $V_\gamma$ ) and macro-hardness of as-hardened specimens

Specimen	Austenitizing Temperature (K)			
	1273		1323	
	HV30	$V_\gamma$	HV30	$V_\gamma$
No.1	763	28.8	775	41.0
No.2	775	18.1	780	31.8
No.3	780	18.8	775	27.5
No.4	769	3.8	796	18.1
No.5	763	4.1	777	14.8
No.6	749	3.2	769	11.2

### 4.2.3 Tempered state

Hardness and  $V_\gamma$  also change depending on the tempering condition. To clarify the relationship between the hardness,  $V_\gamma$  and tempering condition, the tempered hardness curve is usually made. The hardness in tempered state should be lower than that in as-hardened state because martensite is tempered and it makes the hardness of martensite itself decreases. On the other side, the  $V_\gamma$  is reduced by its decomposition during tempering, and martensite transformation takes place in the rest of austenite during cooling to room temperature, and which makes the hardness increase. Therefore, the macro-hardness is measured as a sum of both the decrease in hardness of martensite and the increase in hardness due to martensite transformation of retained austenite.

After the specimens were air-hardened from two level of austenitizing temperatures, 1273 K and 1323 K, they were tempered at several temperatures from 573 K to 873 K. Relationship between

macro-hardness,  $V\gamma$  and tempering temperature are shown in Fig.4-3 to Fig.4-5 for 16% Cr and Fig.4-6 to Fig.4-8 for 26%Cr cast irons, respectively. In each diagram, the macro-hardness in as-hardened state are added for comparison. In each specimen, the tempered hardness curve shows more or less a secondary hardening due to the precipitation of carbides. However, the degree of the hardening of high chromium cast iron is less than those of alloyed tool steel and the multi-component white cast iron[25].

### (I) 16%Cr Cast Iron

Fig.4-3 shows the tempering curves of hardness and  $V\gamma$  of specimen No.1 with almost eutectic composition. The hardness of as-hardened specimens are 763 HV30 and 780 HV30 at 1273 K and 1323 K austenitization, respectively. In the range of lower tempering temperatures less than 673 K, the hardness of specimens hardened from 1323 K are lower than those hardened from 1273 K. This is because the more austenite retains in the tempered specimens. When the specimen are tempered at the temperature range over 700 K, the change of hardness takes place conversely, and higher hardness is obtained in the specimens hardened from higher austenitizing temperature, 1323 K. Irrespective of the hardening temperatures, the tempered hardness decreases until 623 K and then it increases as the tempering temperature rises. After the hardness arrives at the peak of tempered hardness curve or the maximum tempered hardness ( $H_{Tmax}$ ), it decreases again because of over tempering in which the condensation of precipitated carbide occurs. The  $H_{Tmax}$  obtained from the specimen hardened by 1273 K austenitization is 780 HV30 at the tempering temperature of 690 K and that obtained from the specimen hardened by 1323 K austenitization is 790 HV30 at 730 K. From these results, it is found that the  $H_{Tmax}$  in the case of 1323 K austenitization is a little higher than that in the case of hardening from 1273 K. The tempering temperature to obtain the  $H_{Tmax}$  is shifted to the

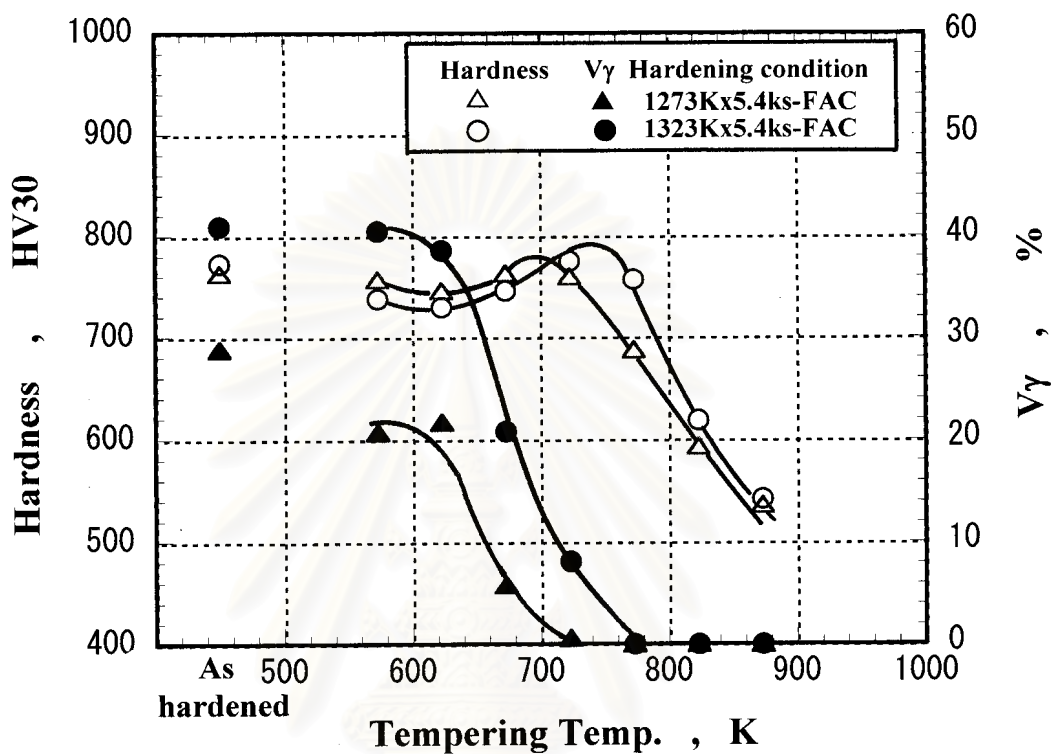


Fig.4-3 Relationship between macro-hardness, volume fraction of retained austenite( $V_{\gamma}$ ) and tempering temperature. (Specimen No.1)

high temperature side by increasing the austenitizing temperature. Regardless of austenitizing condition, the  $V_\gamma$  begins to reduce abruptly over the tempering temperature of 623 K and the tempering temperatures at which  $V_\gamma$  gets to 0% are 723 K and 773 K in the cases of 1273 K and 1323 K austenitization, respectively. The  $V_\gamma$  values at the  $H_{T_{max}}$  are 3% and 5% in the cases of 1273 K and 1323 K austenitization. It is clear even in the specimens with low  $V_\gamma$  that the more the  $V_\gamma$  value, the higher the tempering temperature is necessary for the disappearance of retained austenite.

In the case of specimen No.2 with hypo-eutectic composition shown in Fig.4-4, the hardness in as-hardened state shows little difference even if the austenitizing temperature changes, 775 HV30 at 1273 K and 780 HV30 at 1323 K austenitization, respectively. The tempered hardness curves show similar behavior to those of specimen No.1, and they also show the secondary hardening due to the precipitation of carbides in matrix. The  $H_{T_{max}}$  value of 803 HV30 is obtained in the specimen hardened from 1323 K austenitization and it is larger than that of 783 HV30 obtained in the specimen hardened from 1273 K. The tempering temperature at which the  $H_{T_{max}}$  is obtained is about 50 K higher in the specimens hardened from 1323 K than those hardened from 1273 K austenitization. Both tempered hardness curves gradually decrease as the specimens are tempered over the temperatures at  $H_{T_{max}}$ . The relation of  $V_\gamma$  and tempering temperature shows good correspondence to that of the hardness and tempering temperature. The tempering temperature at which the secondary precipitation hardening starts to occur is 673 K and it is the temperature at which the  $V_\gamma$  value also begins to drop greatly. The 18% and 32 %  $V_\gamma$  in specimens hardened from 1273 K and 1323 K, decrease a little until 673 K but over 673 K they reduce abruptly as the tempering temperature rises. The retained austenite disappears when the specimens were tempered at 730 K for 1273 K and 773 K for 1323 K austenitization. The  $V_\gamma$  that the  $H_{T_{max}}$  values are obtained are 9% and 7% when tempered at 700 K for 1273 K and at 730 K for 1323 K



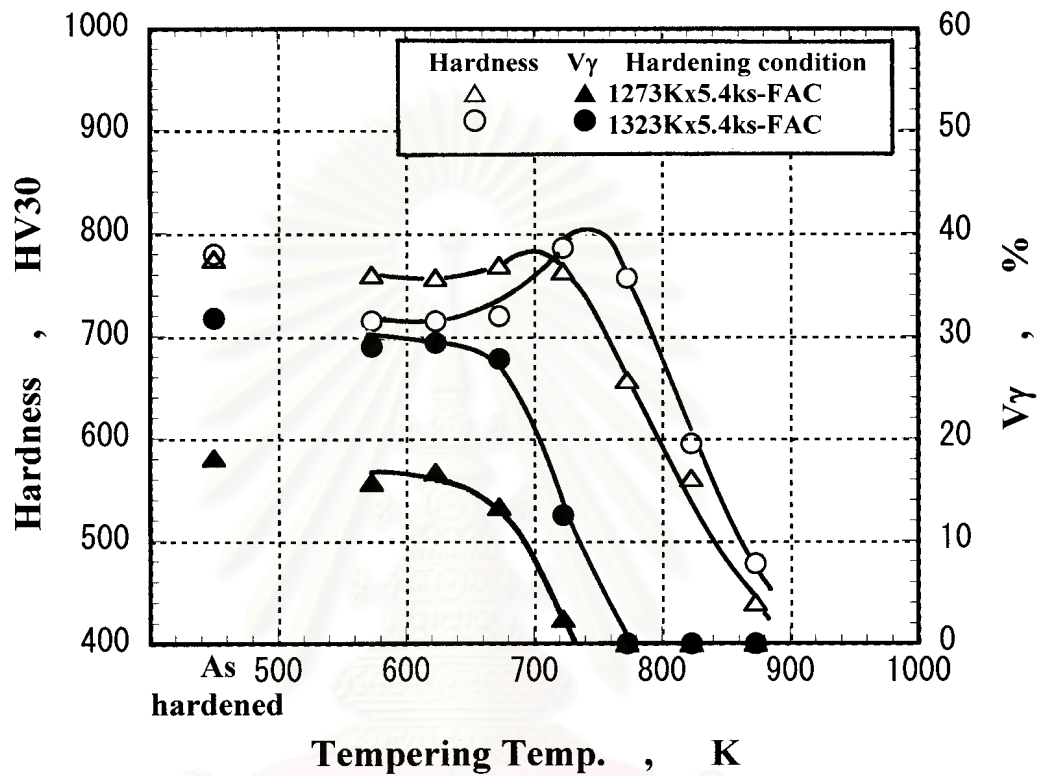


Fig.4-4 Relationship between macro-hardness, volume fraction of retained austenite( $V\gamma$ ) and tempering temperature. (Specimen No.2)

austenitization, respectively.

The relationship between hardness,  $V\gamma$  and tempering temperature of specimen No. 3 with hypo-eutectic composition is shown in Fig.4-5. The hardness in as-hardened specimens are 780 HV30 and 775 HV30 in the case of 1273 K and 1323 K austenitization, respectively. The tempered hardness curves show the similar tendency in a family of 16%Cr cast irons. However, the degree of the secondary precipitation is much larger in the case of higher austenitizing temperature of 1323 K. The  $H_{T_{max}}$  values are respectively 765 HV30 in the case of 1273 K and 780 HV30 in the case of 1323 K austenitization. The  $V\gamma$  values that the hardness shows the maximum value are 4% and 8% in the specimens austenitized at 1273 K and 1323 K. In as-hardened state, the 19% and 27.5%  $V\gamma$  exist in the specimens hardened from 1273 K and 1323 K, respectively. Both gradually reduce in the range of temperature over 623 K and the  $V\gamma$  values reach 0% at the tempering temperatures of 723 K for 1273 K and 773 K for 1323 K austenitization. This suggests that the higher austenitizing temperature requires a higher tempering temperature so that a large quantity of retained austenite can be fully decomposed under the same holding time.

## (II) 26%Cr Cast Iron

The results of specimen No.4 with eutectic composition are shown in Fig.4-6. The hardness of as-hardened specimens are different between the austenitizing temperatures, 769 HV30 and 796 HV30 for 1273K and 1323 K austenitization, whereas the hardness of as-hardened 16%Cr cast irons do not make difference. The higher hardness is obtained in the case of high austenitization. From the tempered hardness curves in Fig.4-6, it is clear that the behavior of tempered hardness curves are different from those of 16%Cr irons and the hardness of specimens hardened from higher austenitizing temperature of 1323 K is overall higher than those hardened from lower temperature of 1273 K. It is similar fact that the

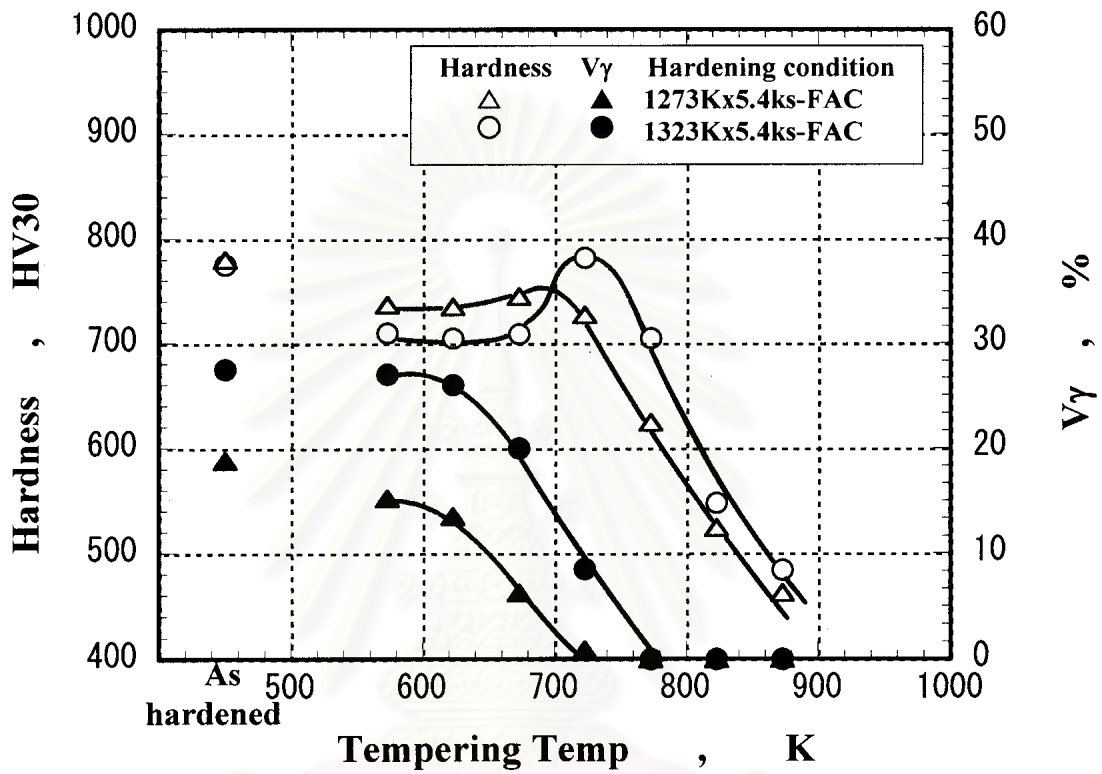


Fig.4-5 Relationship between macro-hardness, volume fraction of retained austenite( $V\gamma$ ) and tempering temperature. (Specimen No.3)

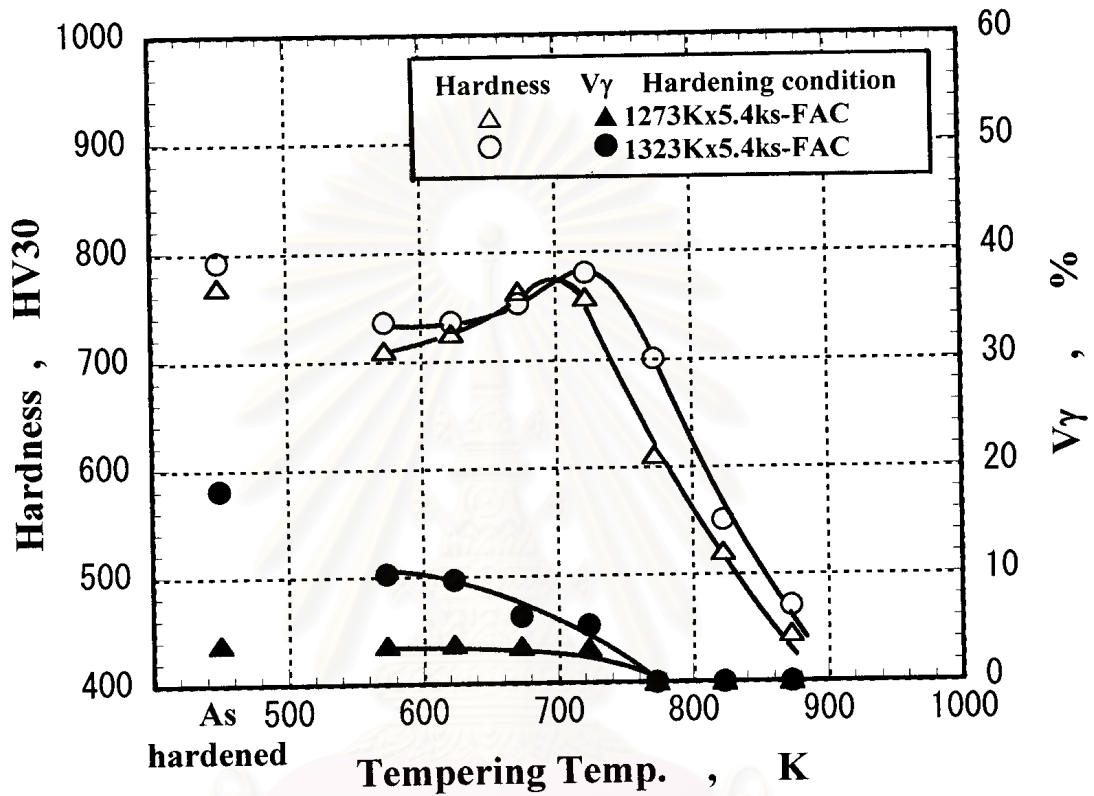


Fig.4-6 Relationship between macro-hardness, volume fraction of retained austenite( $V\gamma$ ) and tempering temperature. (Specimen No.4)

degree of secondary precipitation is more in the case of higher austenitizing temperature and the tempering temperature at which the  $H_{T_{max}}$  is obtained is located in higher temperature. The  $H_{T_{max}}$  value of specimen hardened from 1273 K is 770 HV30 and 780 HV30 in the case of 1323 K austenitization. The  $V_{\gamma}$  values of specimens hardened from 1273 K and 1323 K are 3.8% and 18%, respectively. In the case of 1273 K austenitization, the  $V_{\gamma}$  in the tempered specimens does not change until 723 K and over it, the  $V_{\gamma}$  decreases to 0% at the tempering temperature of 773 K. In the case of 1323 K austenitization, on the other side, the  $V_{\gamma}$  begins to reduce gradually from 623 K to 0% at 773 K. The  $V_{\gamma}$  values at the  $H_{T_{max}}$  are 3% in 1273 K and 5% in 1323 K austenitization.

Fig. 4-7 shows the results of specimen No. 5 with hypo-eutectic compositions. In as-hardened state the hardness in the case of 1323 K austenitization is 777 HV30 which is little higher than 763 HV30 in the case of 1273 K austenitization. The secondary precipitation hardening appears in both of the specimens and the  $H_{T_{max}}$  in the case of 1273 K austenitization is 740 HV30 at 690 K tempering and 780 HV30 in 1323 K austenitization at 723 K tempering. On the other side, the  $V_{\gamma}$  values in as-hardened state are 4 % in 1273 K and 15% in 1323 K austenitization, and the former decreases gradually from 623 K and the latter begins to reduce over the tempering temperature of 673 K and reach 0% at 773 K.

Fig.4-8 shows the results of specimen No.6 with hypo-eutectic composition. In as-hardened state, the hardness in the case of 1273 K austenitization is 750 HV30 and that in 1323 K austenitization is 770 HV30. Both of tempered hardness curves do not show remarkable secondary precipitation hardening, and the  $H_{T_{max}}$  values are 740 HV30 and 780 HV30 in 1273 K and 1323 K austenitization, respectively. The  $V_{\gamma}$  values in as-hardened state are 3% in 1273 K and 11% in 1323 K austenitization. When they are tempered, both the  $V_{\gamma}$  reduce little until 723 K and over 723 K they continuously decrease to 0% at 750 K in 1273 K and 773 K in 1323 K austenitization. The degree of secondary precipitation hardening of this specimen is smallest in the results of other

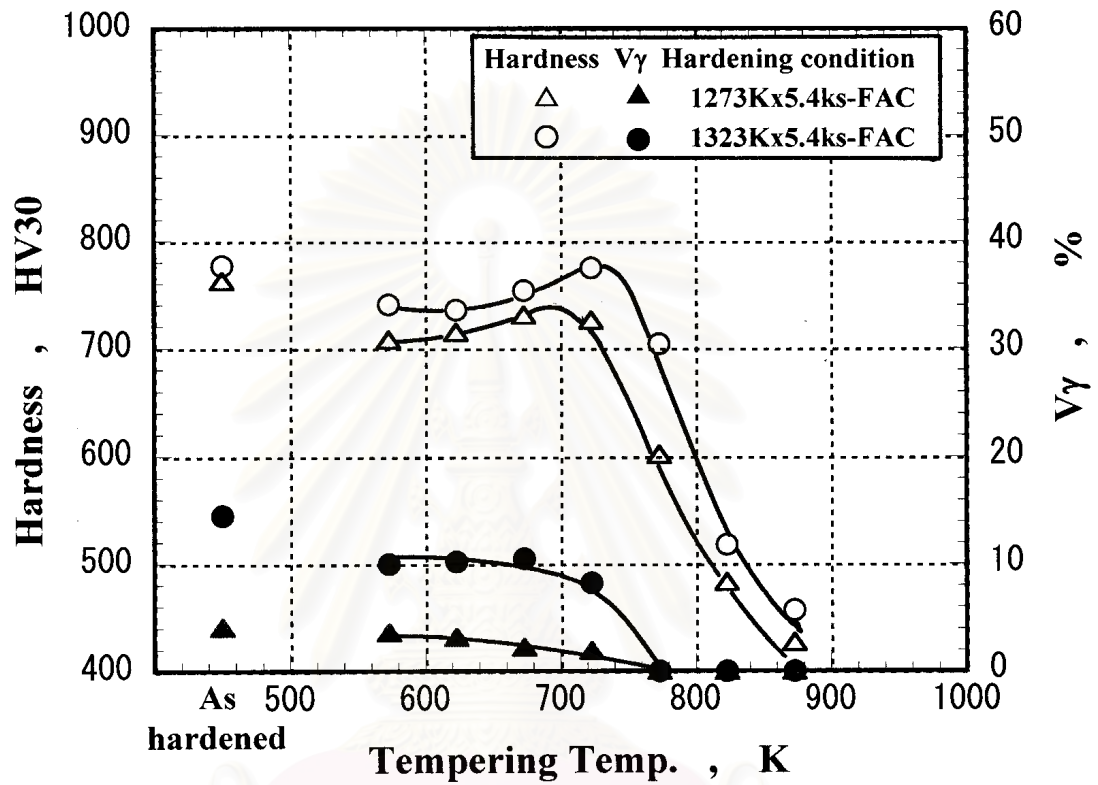


Fig.4-7 Relationship between macro-hardness, volume fraction of retained austenite( $V\gamma$ ) and tempering temperature. (Specimen No.5)

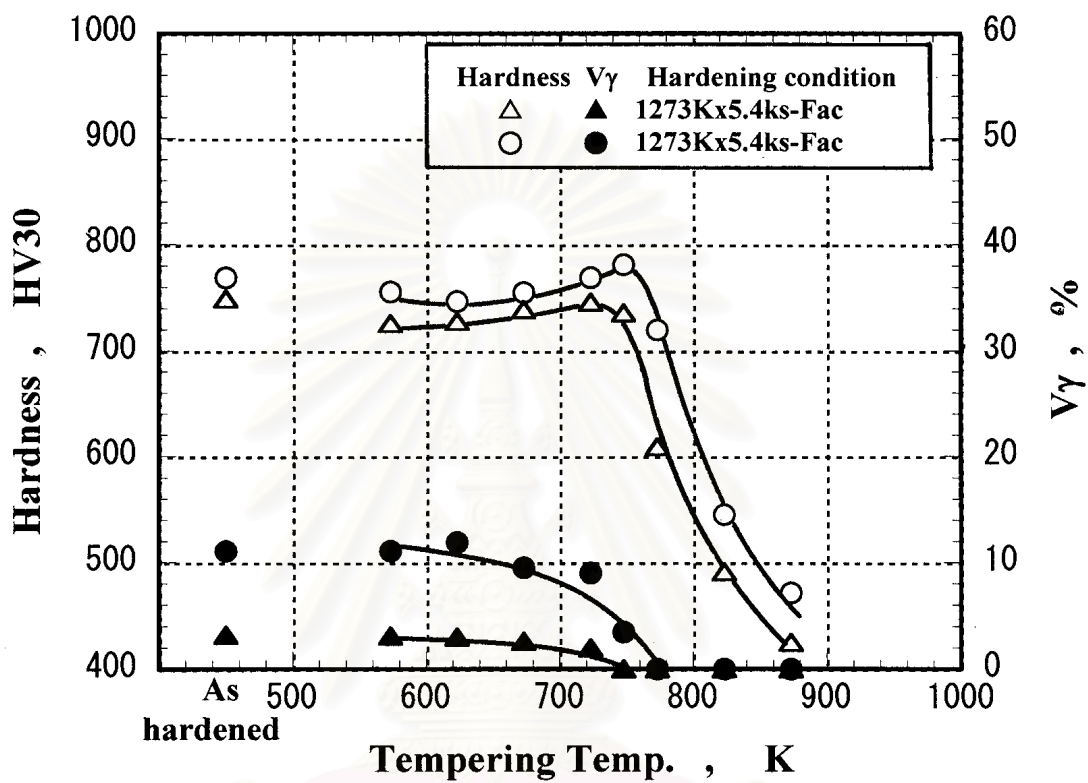


Fig.4-8 Relationship between macro-hardness, volume fraction of retained austenite( $V\gamma$ ) and tempering temperature. (Specimen No.6)

kinds of specimens with 26%Cr. This reason could be due to the low level of retained austenite in as-hardened state.

### **4.3 Relationship between Micro-hardness of Matrix and Tempering Temperature**

As we know well, the strength of matrix can be widely varied by heat treatment. Though it is impossible to measure the strength of matrix itself in cast iron, it is possible to estimate the strength qualitatively from the matrix hardness. Therefore it is worthy to measure the micro-hardness of matrix relating to the condition of heat treatment.

#### **(I) 16%Cr Cast Iron**

The tempered micro-hardness curves of matrix are shown in Fig.4-9 to Fig. 4-11 and, at the same time, macro-hardness curves shown in the figures of Clause 4.2.3 (I) and (II) are displayed in the same diagrams for comparison. The profiles of the micro-hardness curves are very similar to those of tempered macro-hardness curves and the micro-hardness are overall lower than macro-hardness. It is because the micro-hardness expresses only hardness of matrix itself and the macro-hardness is total hardness of both the eutectic carbides and the matrix. In the tempered micro-hardness curves, the secondary precipitation hardening appears in the same manner as macro-hardness, and the peaks of micro-hardness are more in the case of higher austenitization. The tempering temperatures at which micro-hardness curves show the peaks like the  $H_{T_{max}}$  in the case of macro-hardness do not always agree to the temperatures in the case of macro-hardness.



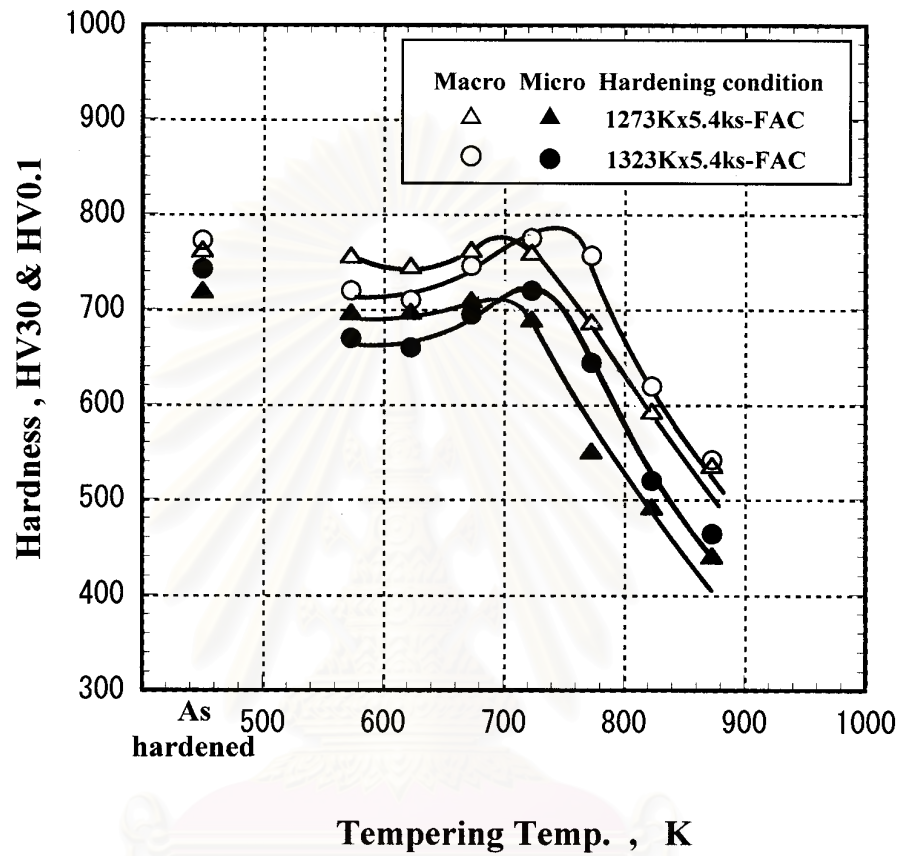


Fig.4-9 Comparison of micro-hardness of matrix with macro-hardness.  
(Specimen No. 1)

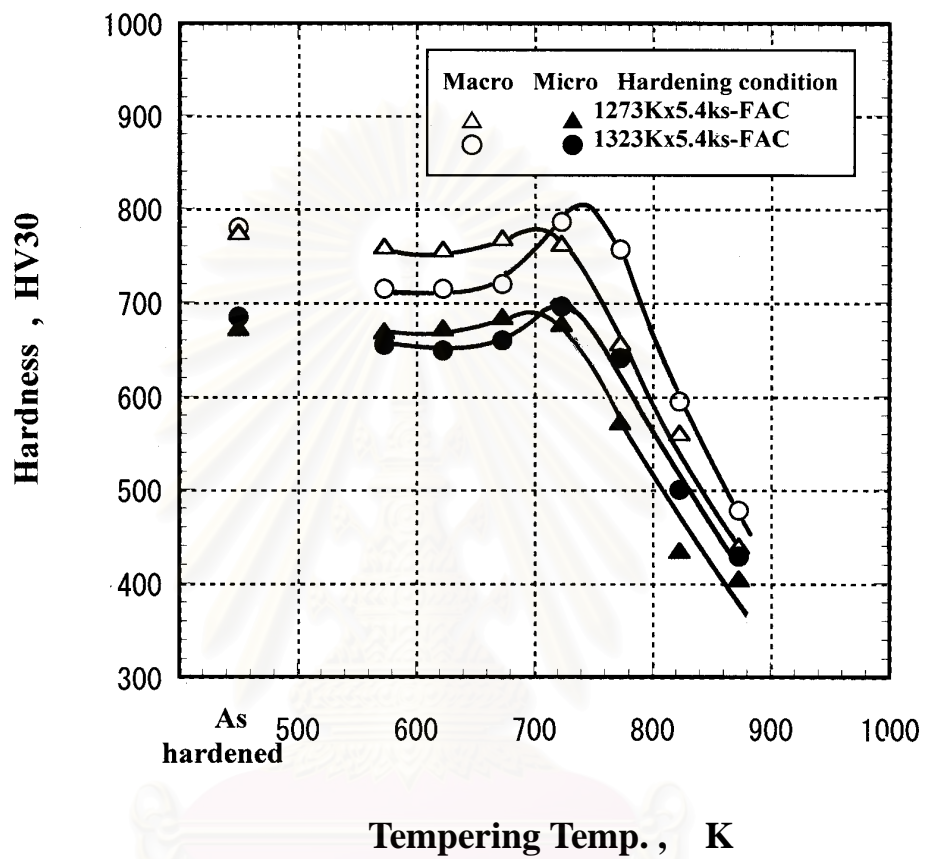


Fig.4-10 Comparison of micro-hardness of matrix with macro-hardness.  
(Specimen No. 2)

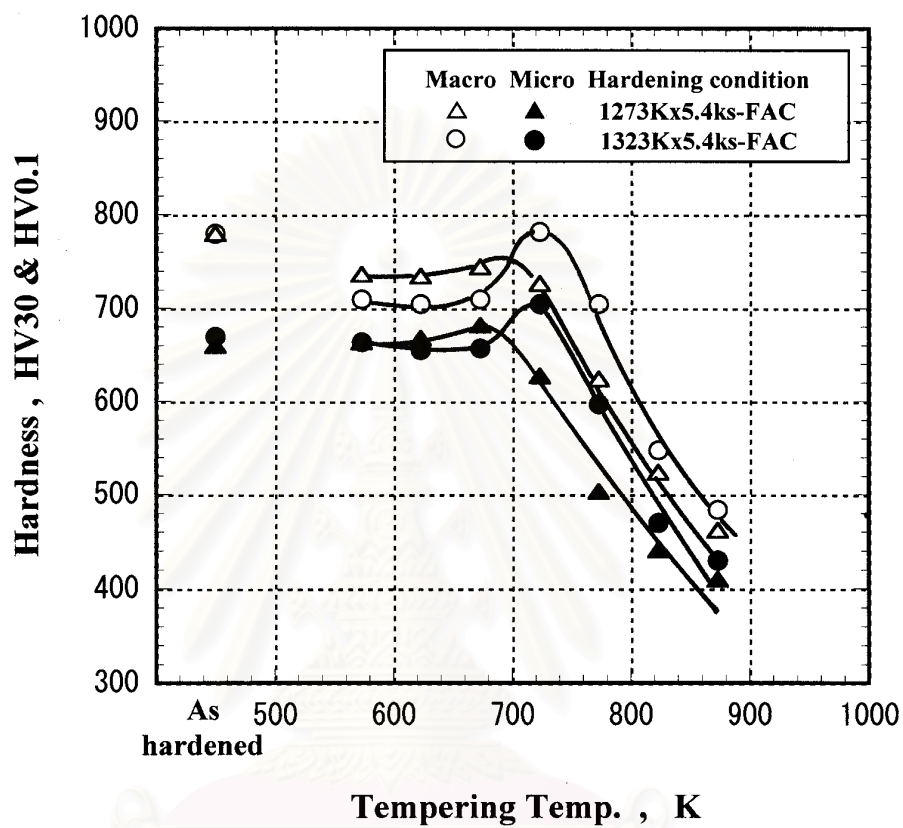


Fig.4-11 Comparison of micro-hardness of matrix with macro-hardness.  
(Specimen No. 3)

The difference between macro-hardness and micro-hardness occurs due to the existence of eutectic carbides that are much harder than the matrix. The differences in the maximum hardness between micro-hardness and macro-hardness in 16%Cr specimens are 50-80 HV30 in 1273 K and 60-110 HV30 in 1323 K austenitization, respectively.

## **(II) 26%Cr Cast Irons**

The comparison between micro-hardness and macro-hardness of 26%Cr cast irons with hypoeutectic composition are shown in Fig. 4-12 and Fig.4-13. Even in 26%Cr cast irons, the behavior of micro-hardness curve is similar to the curve of macro-hardness, and the micro-hardness is overall lower than those of macro-hardness. The maximum hardness obtained from the tempered micro-hardness curves is higher in the case of 1323 K austenitization than those in the case of 1273 K austenitization. From above results, it can be said that the change in micro-hardness affects directly to the change in macro-hardness. The difference between the peak of micro-hardness and macro-hardness is 60 HV30 in 1273 K and 80 HV30 at 1323 K austenitization, respectively.

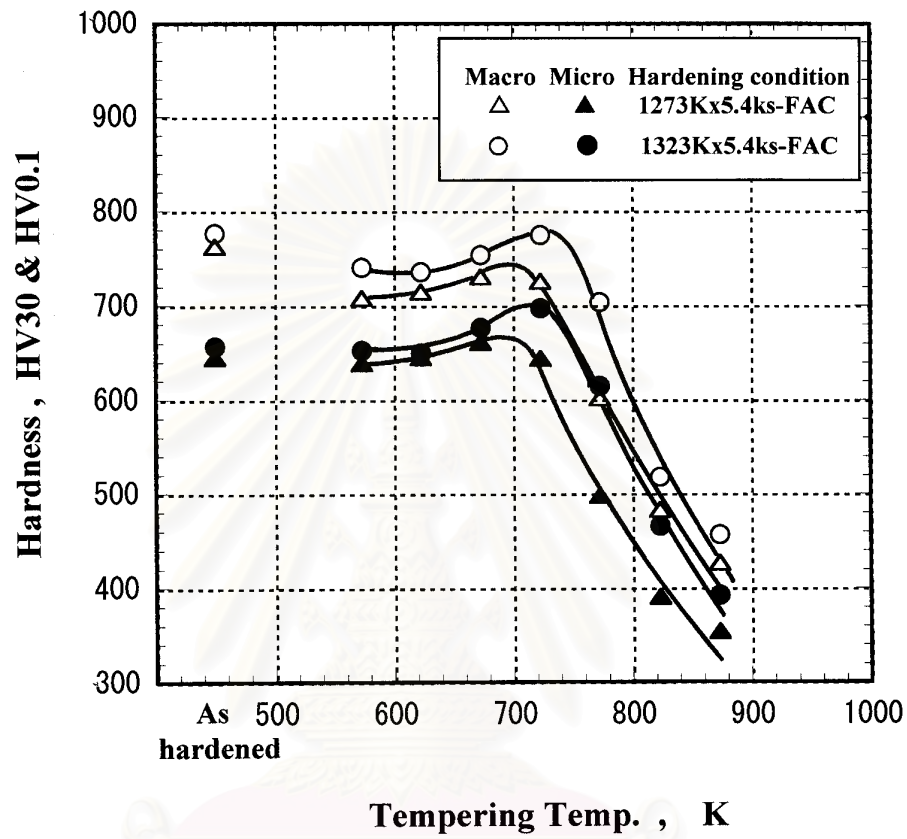


Fig.4-12 Comparison of micro-hardness of matrix with macro-hardness.  
(Specimen No. 5)

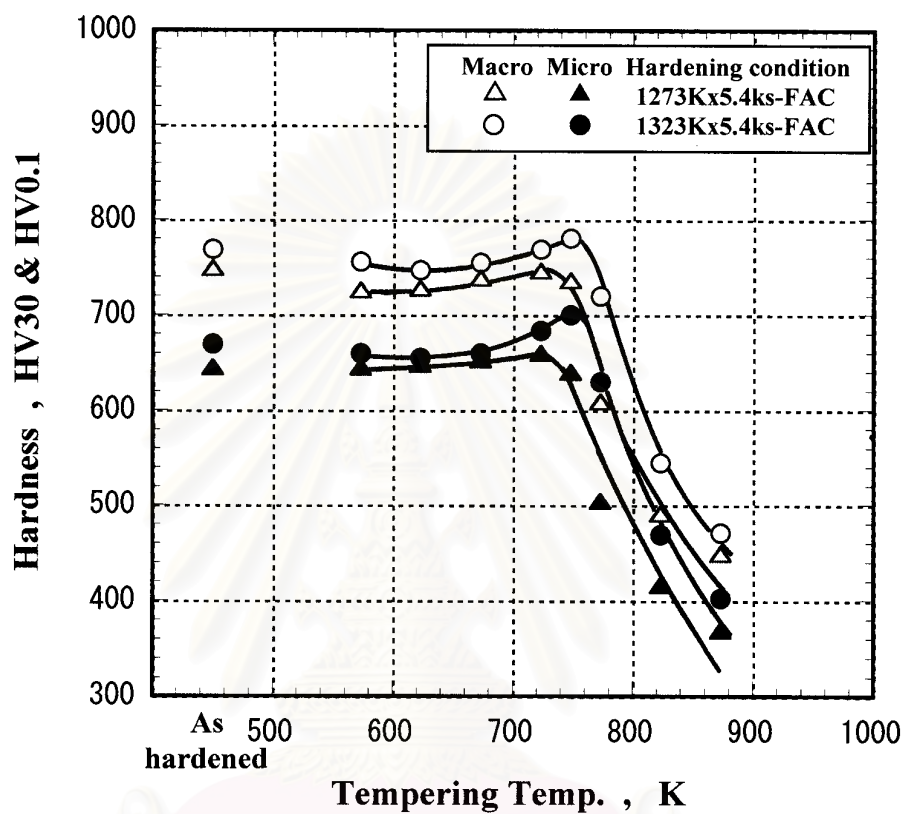


Fig.4-13 Comparison of micro-hardness of matrix with macro-hardness.

(Specimen No. 6)

จุฬาลงกรณ์มหาวิทยาลัย

## Chapter 5

### Discussions

#### 5.1 Relationship between $V_\gamma$ and Cr/C value

It is known that the amount of martensite transformation depends on how much percentage of temperature of the specimen is cooled down between  $M_s$  and  $M_f$  temperatures. In high chromium cast iron, the  $M_s$  temperature is changed by chromium and carbon contents. Carbon has a much more influence on  $M_s$  temperature of the cast iron than other alloying element, the more the carbon content, the lower the  $M_s$  temperature. When austenitizing temperature increases, chromium and carbon dissolve more in austenite matrix and therefore the  $M_s$  temperature reduces. As a result, the large volume fraction of austenite retains in the matrix. According to the literatures [14,18], a parameter, Cr/C value is introduced to understand the simultaneous effect of carbon and chromium on transformation behavior of alloyed white cast irons. The  $M_s$  temperature increases in proportion to a parameter of Cr/C value that implies both chromium and carbon contents. The  $V_\gamma$  values of all the as-hardened specimens were arranged in accordance with their Cr/C values and the relationship is shown in Fig.5-1. In the case of 1273 K austenitization, for example, the  $V_\gamma$  decreases gradually from 29% to 19% in 16%Cr cast irons as the Cr/C value increases from 4.2 to 6.1. The  $V_\gamma$  in 26% Cr irons change little within 3% to 4% even if Cr/C value varies from 8.4 to 11.

In the case of hardening from 1323 K, the relation of  $V_\gamma$  and Cr/C value shows a similar behavior as that in the case of 1273 K austenitization. That is, the  $V_\gamma$  decreases synthetically as the Cr/C value increases. However, the  $V_\gamma$  at the same Cr/C value is greater in compare with those austenitized at 1273 K. It is because more retained austenite formed in the matrix by the increasing dissolution of chromium and carbon in austenite. Even if the as-hardened matrix is considered to be in

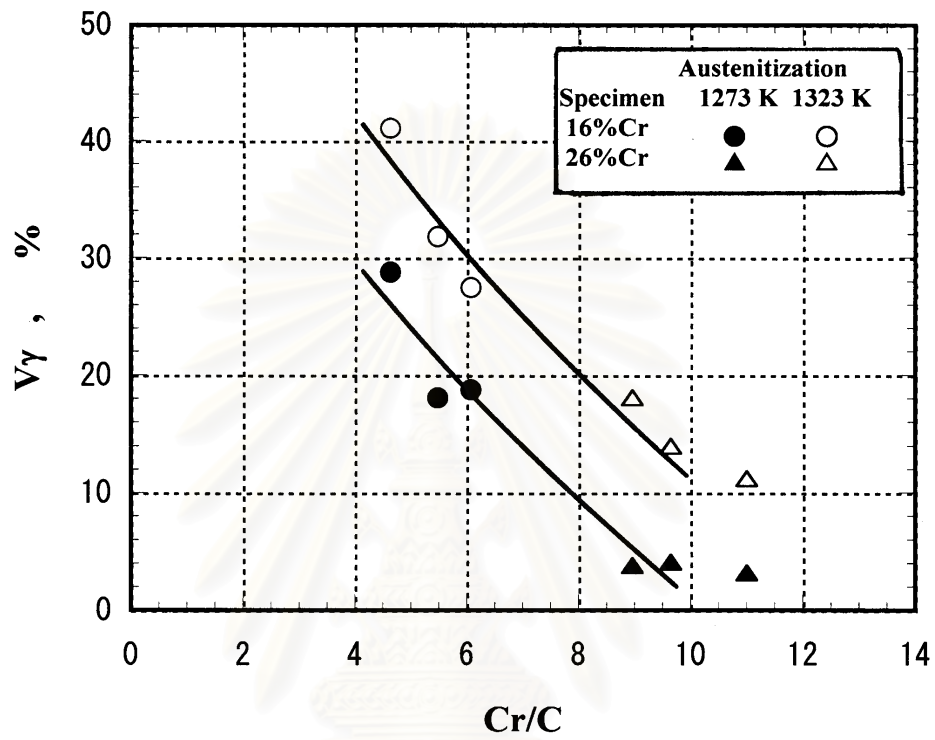


Fig.5-1 Relationship between volume fraction of retained austenite( $V\gamma$ ) and Cr/C value of as-hardened specimens.

สถาบันวิทยบริการ  
จุฬาลงกรณ์มหาวิทยาลัย



non-equilibrium, it can be said that the  $V_\gamma$  reduces roughly in proportion to the Cr/C value. From above reasons, the  $V_\gamma$  value is overall larger when the specimens are austenitized at higher temperature.

## **5.2 Relationship between Macro-hardness and Cr/C value in As-hardened State**

Macro- and micro-hardness in as-hardened state are closely related to the retained austenite. As shown Table 4-2, the macro-hardness are higher in the specimens austenitized at higher temperature. It may be due to the enrichment of carbon in martensite and the hardness of martensite itself is increased. Maratray and Poulalion[18] reported that the hardness of high chromium white cast irons in as-hardened state increased as the austenitizing temperature rose to 1323 K and then reduced. The maximum hardness was obtained when some retained austenite existed. Another reason why the hardness goes up when the austenitizing or hardening temperature rises is that an increase in the austenitizing temperature delays pearlite and bainite transformations and that improves the hardenability. The effect of carbon and chromium on the hardness of the cast iron must be explained by the parameter of Cr/C value. The relationship between hardness and Cr/C value is shown in Fig.5-2. Regardless of austenitizing temperature, the hardness rises in the range of Cr/C from 4.5 to 6 and reduces in the range from 9 to 11 as the Cr/C value increases. The hardness in the case of 1323 K austenitization seem slightly high. However, the change in the hardness corresponding to the change of the Cr/C value is only 50 HV30. By estimating the peak of hardness in the diagram, it could be obtained near a Cr/C value of 8. The influence of  $V_\gamma$  on macro-hardness is shown in Fig.5-3. As the  $V_\gamma$  increases, the hardness rises first and then decreases. The peak or the highest hardness lies near 20 %  $V_\gamma$ . This value is in good accordance with the result of high chromium cast iron with molybdenum [14]. In the range of high carbon content which is sufficient to depress the martensite transformation near or

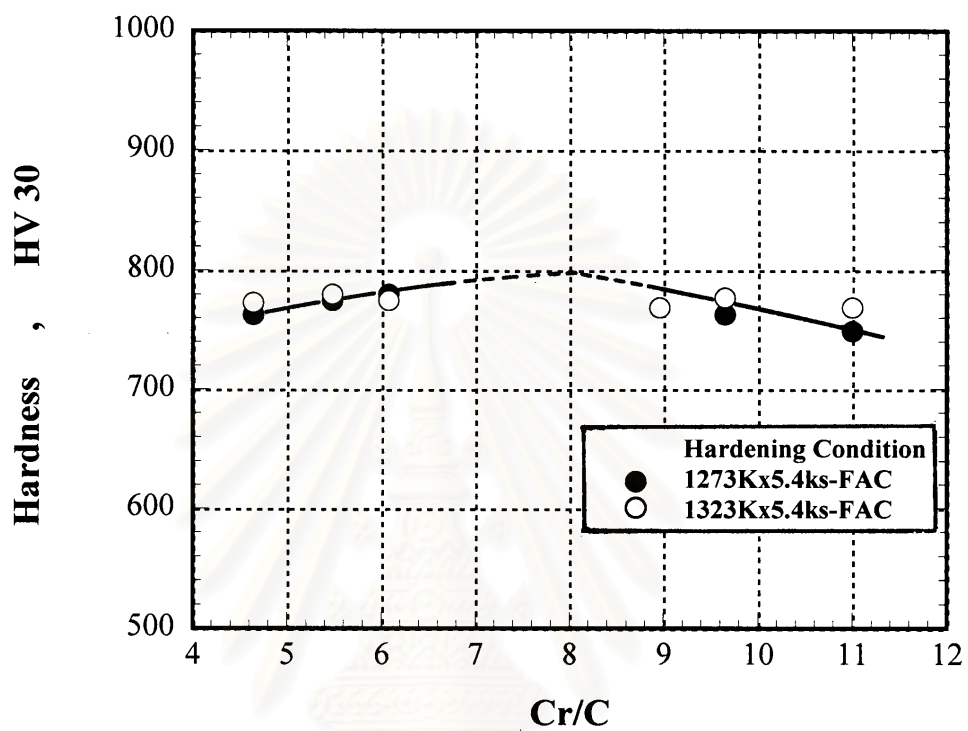


Fig.5-2 Relationship between macro-hardness and Cr/C value of as-hardened specimens.

สถาบันวิทยบริการ  
จุฬาลงกรณ์มหาวิทยาลัย

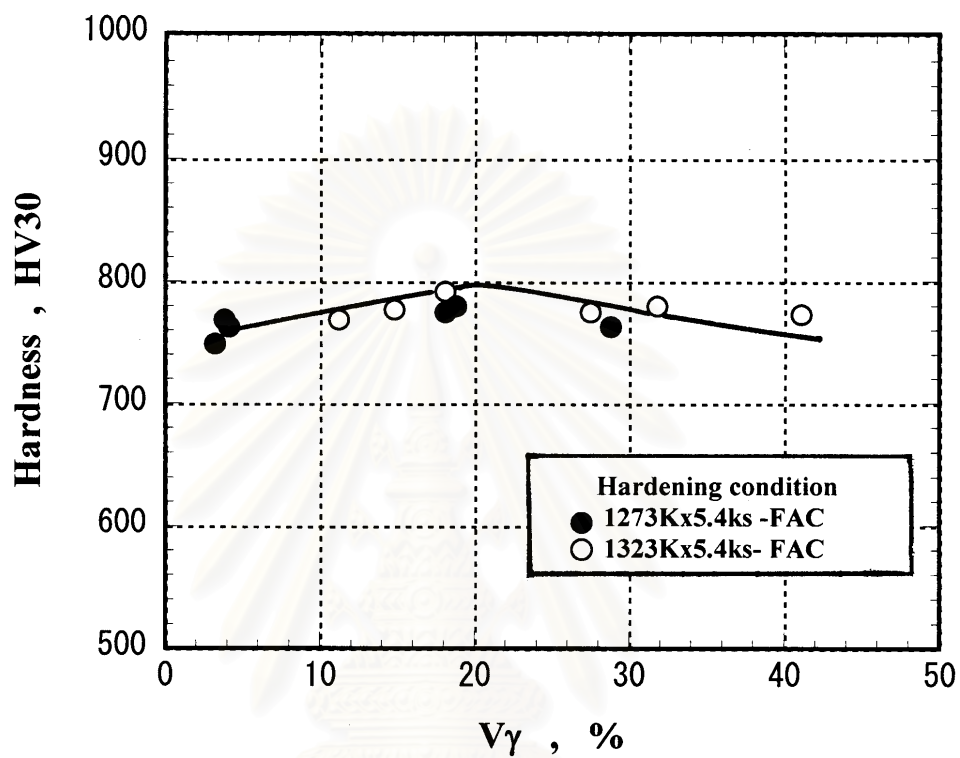


Fig.5-3 Influence of volume fraction of retained austenite( $V_\gamma$ ) on macro-hardness in as-hardened state.

สถาบันวิทยบริการ  
จุฬาลงกรณ์มหาวิทยาลัย

below the room temperature, the  $V_\gamma$  increases as carbon content rises, and resultantly in the range of high  $V_\gamma$  the hardness continue to decrease with an increase in the  $V_\gamma$ . From above experimental results, it can be summarized that the hardness in as-hardened state is determined by the hardness of martensite which controlled by the dissolved carbon content and the quantity of  $V_\gamma$ .

### **5.3.1 Relationship between Macro-hardness and Volume Fraction of Retained Austenite in Tempered State**

Macro-hardness of specimens is sum of the hardness of eutectic carbides and matrix, and therefore the  $V_\gamma$  in the tempered matrix can also affect the macro-hardness. In steels, it is known that subcritical heat treatment or tempering varies the hardness and reduces the quantity of retained austenite in matrix, and that the hardness in tempered state increases in the case of alloyed steel because of precipitation of the fine hard carbides during carbide reaction. The relation of macro-hardness and  $V_\gamma$  is obtained for all tempered specimens, and it is shown in Fig.5-4 for the specimens austenitized at 1273 K and Fig.5-5 for those austenitized at 1323 K.

In the case of 1273 K austenitization, the hardness of specimens with 0%  $V_\gamma$  distribute widely from 460 to 765 HV30 in 16%Cr and 420 to 735 HV30 in 26%Cr cast irons. It is considered that the wide distribution of hardness is due to the microstructural constituents in the matrix. In 16%Cr cast irons, the hardness do not change much in the range of  $V_\gamma$  up to 20%, but the maximum hardness is around 7 - 8%  $V_\gamma$  in 16%Cr and about 3%  $V_\gamma$  in 26%Cr cast irons. The 26%Cr cast iron has a tendency that the hardness decreases from 760 to 710 HV30 corresponding to the change in  $V_\gamma$  from 1% to 4%.

In the case of specimens austenitized at 1373 K, the  $V_\gamma$  scatters much more than the specimens austenitized at 1273 K, because an increase in austenitizing temperature makes carbon and chromium

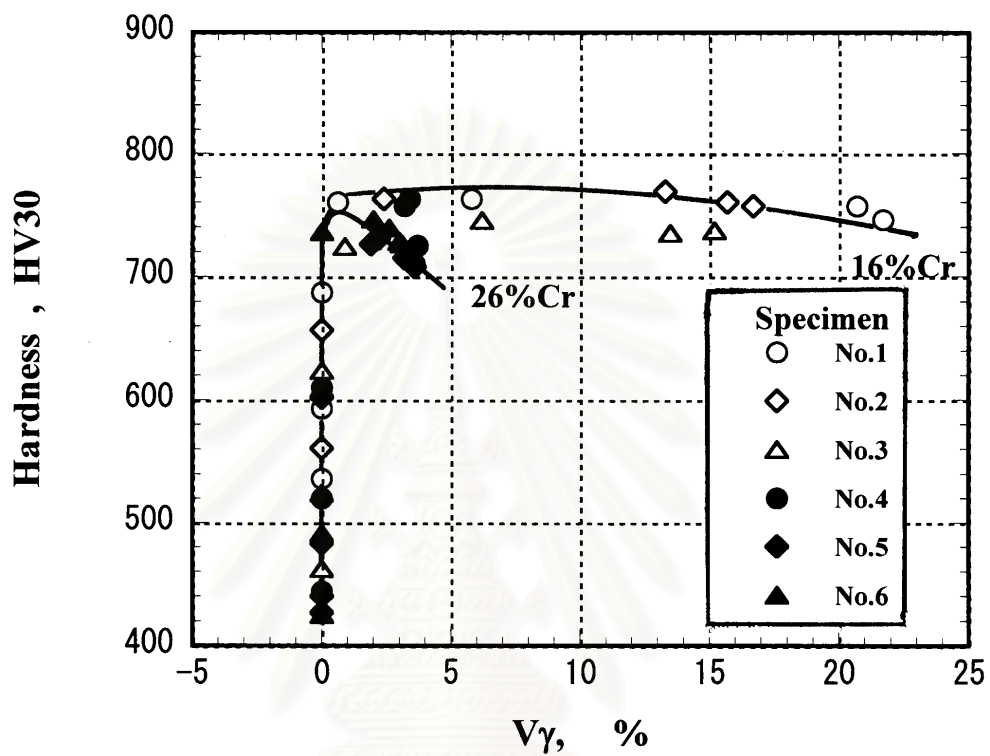


Fig.5-4 Relationship between macro-hardness and volume fraction of retained austenite( $V\gamma$ ) of tempered specimens.(Austenitized at 1273 K)

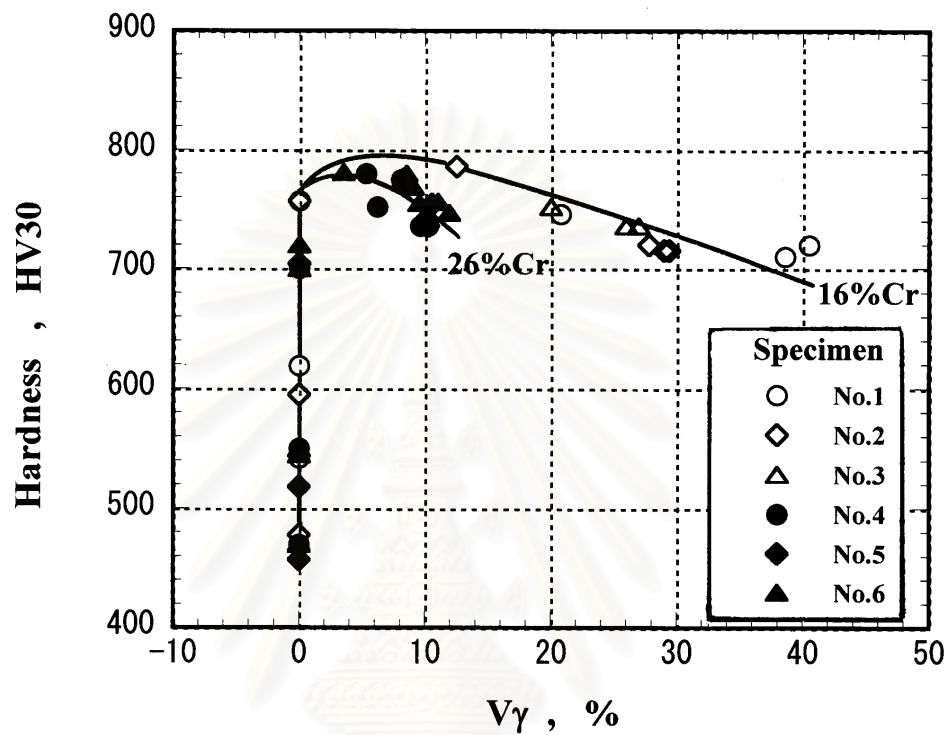


Fig.5-5 Relationship between macro-hardness and volume fraction of retained austenite( $V_\gamma$ ) of tempered specimens. (Austenitized at 1323 K)

จุฬาลงกรณ์มหาวิทยาลัย

dissolve more in austenite and then  $M_s$  temperature falls down. The hardness at 0%  $V_\gamma$  range from 470 to 760 HV30 in 16%Cr and 460 to 720 HV30 in 26%Cr cast irons in the same manner as in the case of 1273 K austenitization. However, it is clear in this case that the hardness reaches the maximum value at a certain  $V_\gamma$  and decreases gradually as the  $V_\gamma$  increases. The maximum hardness are approximate 800 HV30 at 6 - 8%  $V_\gamma$  in 16%Cr irons and 780 HV30 at 5%  $V_\gamma$  in 26%Cr cast irons. It is noted that in higher austenitization like 1323 K, relatively large amount of austenite retains in the specimens tempered at low temperature and then the hardness is low.

From the relationship between tempered macro-hardness and  $V_\gamma$  shown by Fig.5-4 and Fig.5-5, it is found that the hardness in tempered state is related to the chemical composition of cast iron, particularly chromium content because the hardness behave in a family of same chromium content against the  $V_\gamma$  in as-hardened state, the more the  $V_\gamma$  in as-hardened state, the wider the tempered hardness changes.

#### **5.4 Relationship between Maximum Tempered Hardness ( $H_{Tmax}$ ) and Cr/C Value**

Under a certain wear condition, it is done for superior wear performance to make the macro-hardness increase by hardening the matrix. Therefore, the maximum hardness ( $H_{Tmax}$ ) obtained by tempering should be clarified for a series of high chromium cast iron. It is already found that the  $H_{Tmax}$  is related to austenitizing temperature, chemical composition and tempering temperature. The  $H_{Tmax}$  which is obtained from the tempered hardness curve of each specimen is connected to the Cr/C value of specimen, and it is shown in Fig.5-6.  $H_{Tmax}$  are a little high in the specimens hardened from higher austenitizing temperature at the same level of the Cr/C value. The  $H_{Tmax}$  are almost same in the low Cr/C range of 4.5 - 6.1. In the region of high Cr/C values like 9 to 11, the  $H_{Tmax}$  changes little in the specimens hardened from 1323 K, while it decreases

in the specimens hardened from 1273 K as the Cr/C value increases. This can explain that an increase in Cr/C value rises Ms temperature and at the same time shifts the pearlite and bainite transformations to the short time side, and therefore the  $V_\gamma$  in as-hardened state, which works to increase the tempered hardness, is reduced. The  $H_{T_{max}}$  are ranged from 740 to 780 HV30 in the specimens hardened from 1273 K and 780 to 805 HV30 in those hardened from 1323 K. In the case of 1273 K, the  $H_{T_{max}}$  of 16% Cr cast irons, that is, low Cr/C region are a little higher than those of 26%Cr cast irons, that is, greater Cr/C region because the large volume fraction of retained austenite contributes to increase the precipitation of carbides and more carbon dissolved in martensite contribute to rise the hardness of martensite itself.

### **5.5 Relationship between Maximum Tempered Hardness ( $H_{T_{max}}$ ) and $V_\gamma$**

Since the  $V_\gamma$  value in as-hardened state is directly related to the  $H_{T_{max}}$  under the same tempering condition, the  $H_{T_{max}}$  are connected to the  $V_\gamma$  and the relation is shown in Fig.5-7. Irrespective of the austenitizing temperature, the  $H_{T_{max}}$  is found to vary on one line or in a same family against the  $V_\gamma$ . The  $H_{T_{max}}$  rises as  $V_\gamma$  increases and gets to 800 HV30 of the maximum value at approximately 30%  $V_\gamma$ . Over 30%  $V_\gamma$ , however, the  $H_{T_{max}}$  is kept constant at 800 HV30. It is evident that the cast iron so as to remain the  $V_\gamma$  more than 30% can provide the highest hardness after tempering.

In practical uses of high chromium cast iron, the hardness of 16%Cr cast iron used for hot working mill roll is 560 to 700 HV and that of 26%Cr cast iron for the mineral pulverizing mill roll and table is 650-750 HV. All the  $H_{T_{max}}$  are over the hardness required for each kind of roll. Therefore, if the high chromium cast irons are used for the practical rolls, much lower hardness than  $H_{T_{max}}$  should be applied to the casting by increasing the tempering temperature, and it is needless to say that this



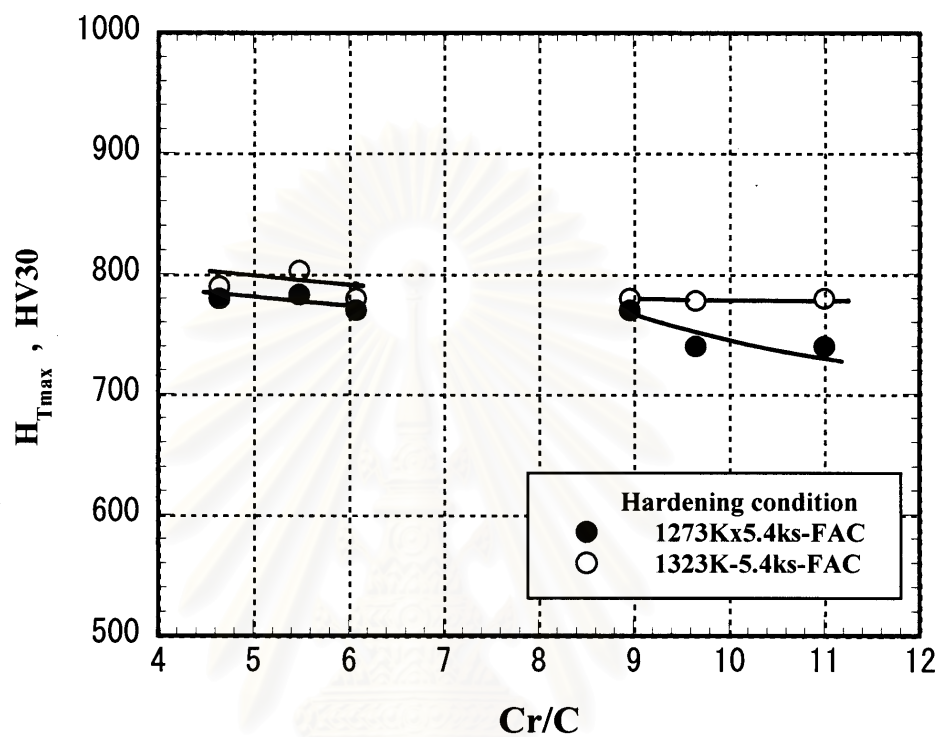


Fig.5-6 Relationship between maximum tempered macro-hardness ( $H_{Tmax}$ ) and Cr/C value.

สถาบันวิทยบริการ  
จุฬาลงกรณ์มหาวิทยาลัย

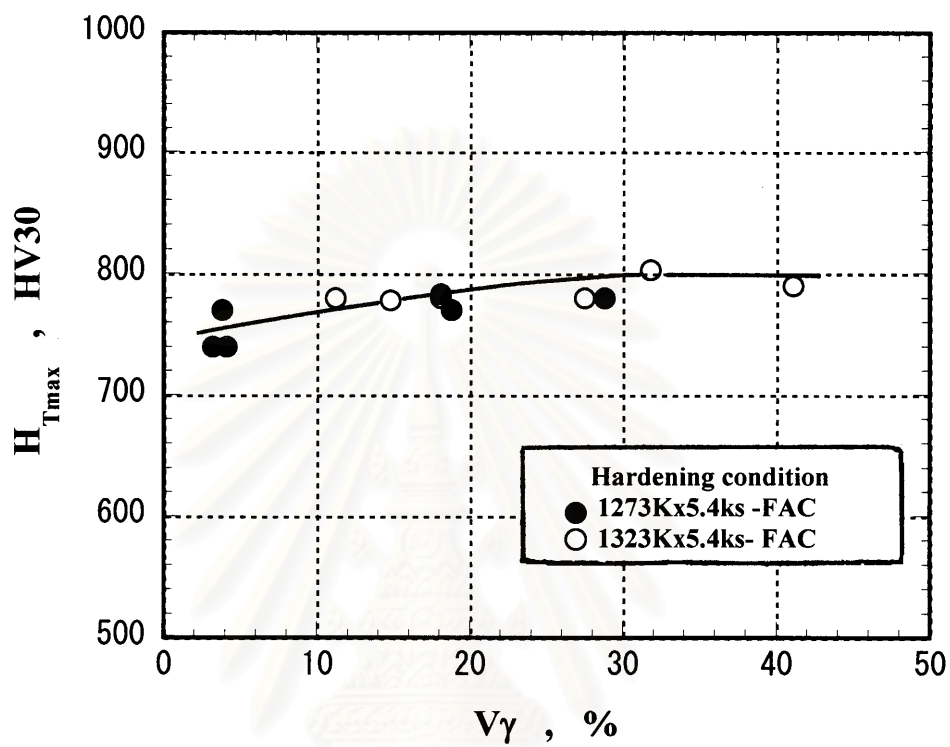


Fig.5-7 Influence of volume fraction of retained austenite( $V\gamma$ ) in as-hardness state on maximum tempered hardness( $H_{Tmax}$ ).

heat treatment improve the toughness of the casting. In general, the high chromium cast iron with heavy section contains other alloying elements such as Ni, Cu, Mo and V of which purpose is to improve the hardenability and simultaneously to form the special carbides with high hardness than chromium carbides during tempering. More investigation to clarify the heat treatment behavior of high chromium cast iron with such alloying elements should be needed in near future date.

## 5.6 Observation of Transformed Matrix by SEM

Transformation behavior of matrix in high chromium cast iron is closely related to the change in hardness, consequently to the mechanical properties. Then, SEM observation is employed to clarify the transformed microstructure of matrix.

SEM microphotographs of 16%Cr hypo-eutectic cast iron (Specimen No.2), which are hardened from 1323 K austenitization and tempered at 673 K, 723 K, 773 K and 823 K, are shown in Fig. 5-8. At 2500 magnifications, the matrix structure can be revealed in detail. In the matrix of as-hardened specimen, many carbides exist mixing with martensite and retained austenite. Large particles of carbides could be indissoluble carbides already existed in annealed state. It is found that the appearance of secondary carbides changes depending on the tempering temperature. At 673 K tempering, the austenite still remains but morphology of secondary carbides is similar to that in as-hardened matrix. When the tempering temperature is increased to 723 K, however, more secondary carbides exist in the matrix but among them very fine carbides are seen in the specimen tempered at 673 K. The carbides in the matrices of specimens tempered over 723 K decrease in number and increase in size as the tempering temperature rises. In this point, either martensite or retained austenite can not always be distinguished. This tempering condition that the coarsening of carbides is taking place can be called as “over tempering”. The matrix structure tempered at 723 K corresponds to

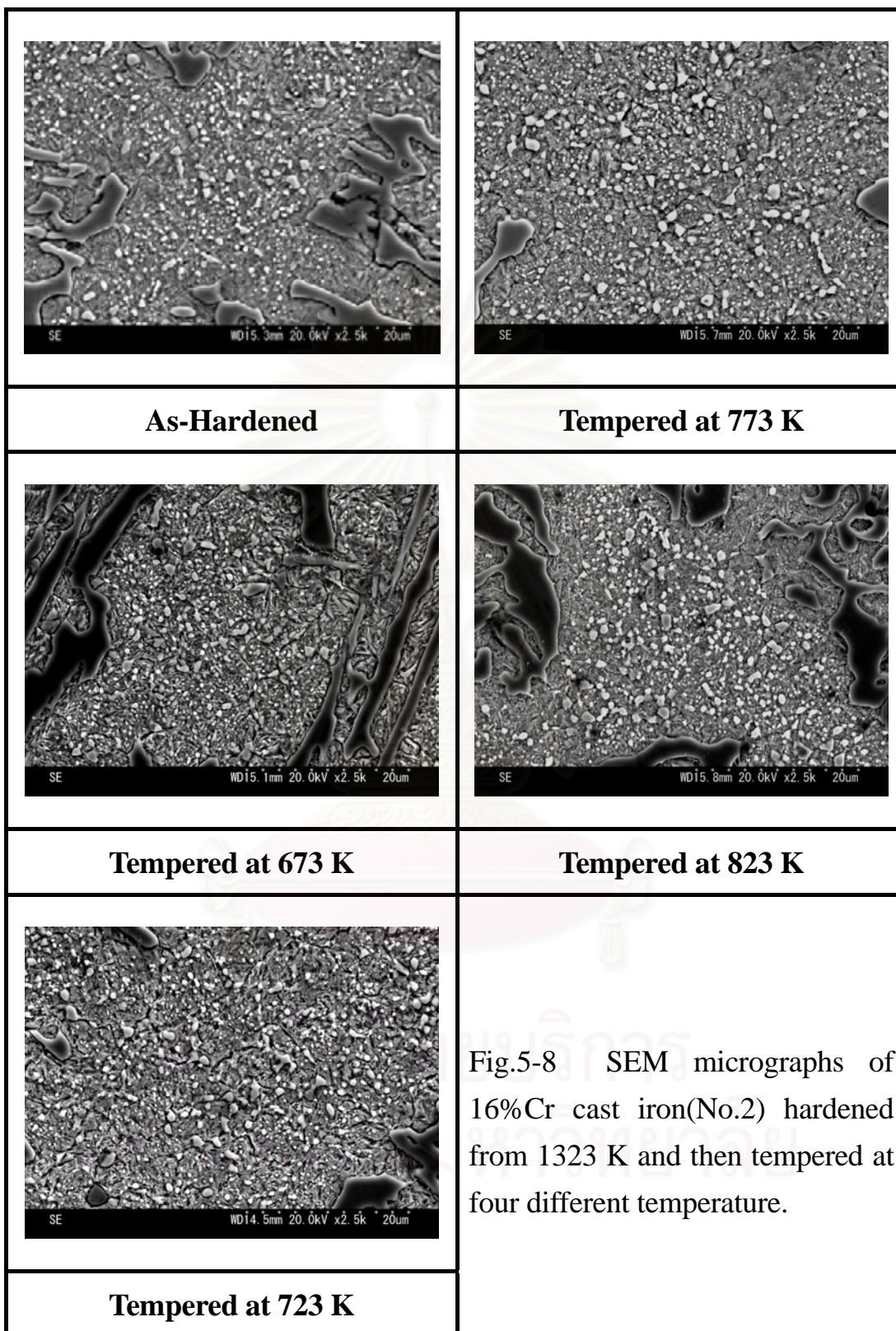
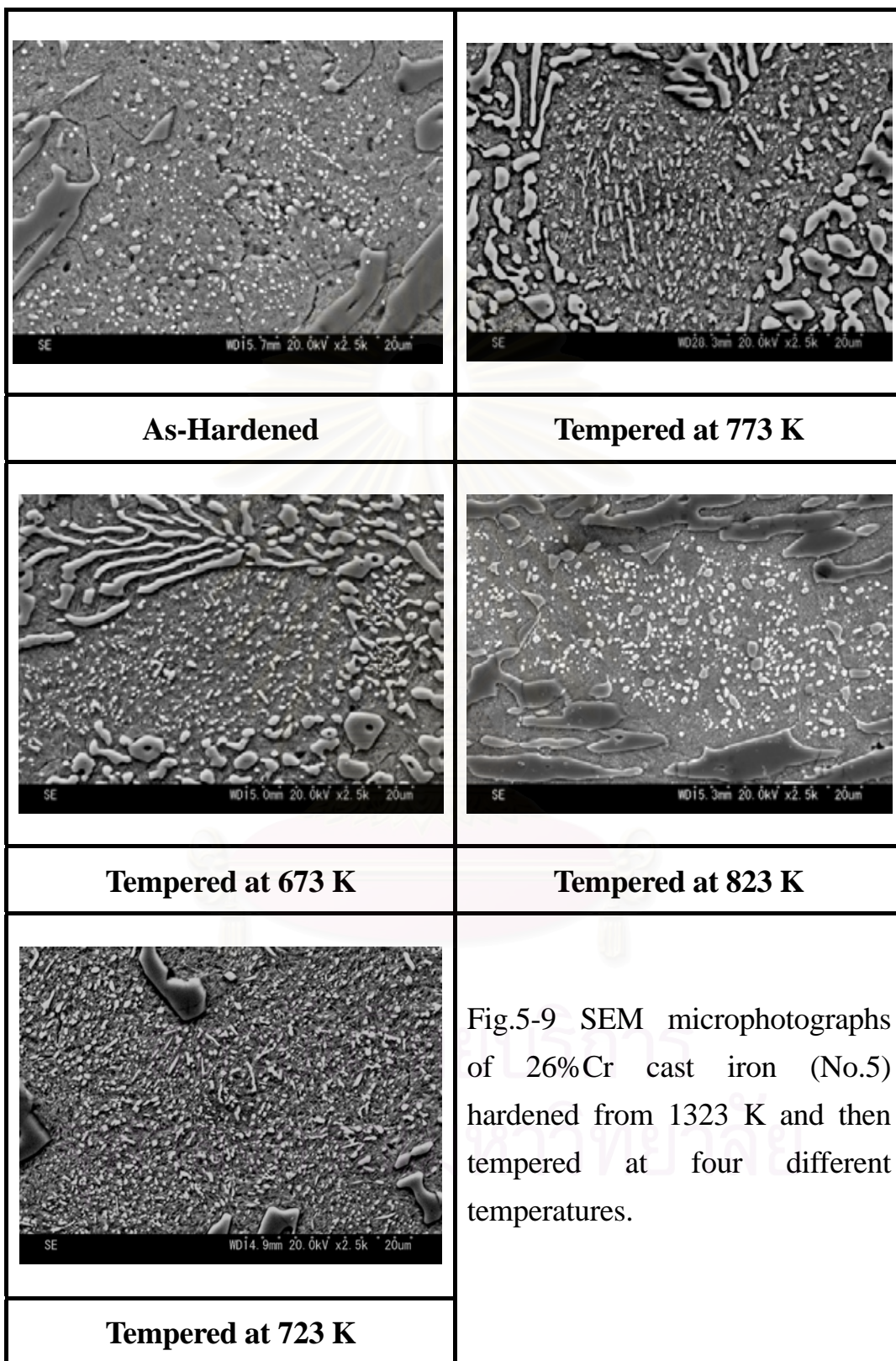


Fig.5-8 SEM micrographs of 16%Cr cast iron(No.2) hardened from 1323 K and then tempered at four different temperature.

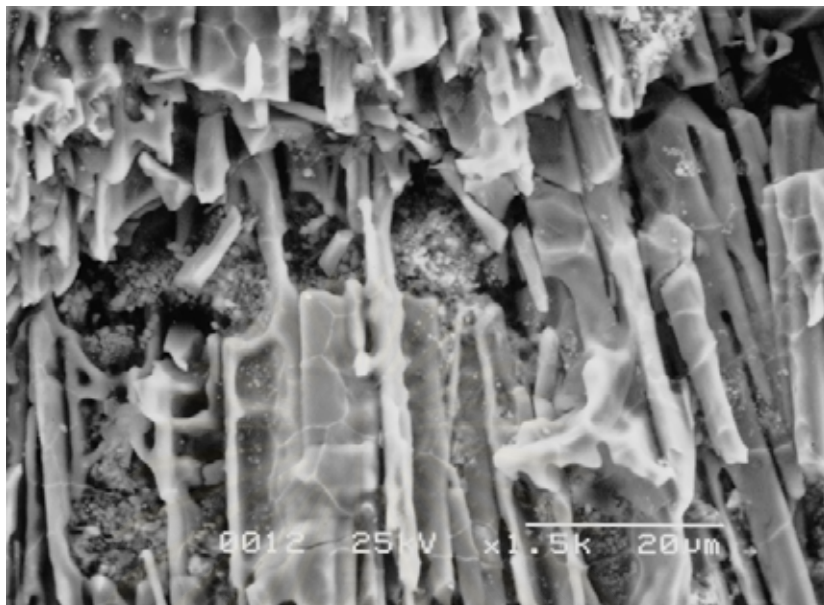
that of a specimen with  $H_{T_{max}}$ , and the hardness of the other three specimens are all low. The difference in hardness among them must be due to the matrix itself filling up the spaces among carbide particles. Though it is not so clear, fine matrices which could be the tempered martensite and transformed martensite from retained austenite can be observed. These matrix structures could contribute to the highest hardness in the tempered state.

SEM microphotographs in the case of 26%Cr cast iron (Specimen No.5) hardened from 1323 K austenitization and tempered at different temperatures are shown in Fig.5-9. The variation of matrix structure such as martensite and retained austenite can be seen little from these microphotographs with 2500 magnifications. However, the behavior of secondary carbides is evident, and the transition of carbide structure associated with tempering temperature is quite similar to that of 16%Cr cast iron. The amount of carbide is increased by tempering and the carbides are most and finest in the specimen tempered at 723 K. It is clear that these carbides are coarsened and decrease in number as the tempering temperature rises over 723 K. It can be understood from the change of carbide structure that the specimen with most and finest secondary carbides, which tempered at 723 K, shows  $H_{T_{max}}$ .

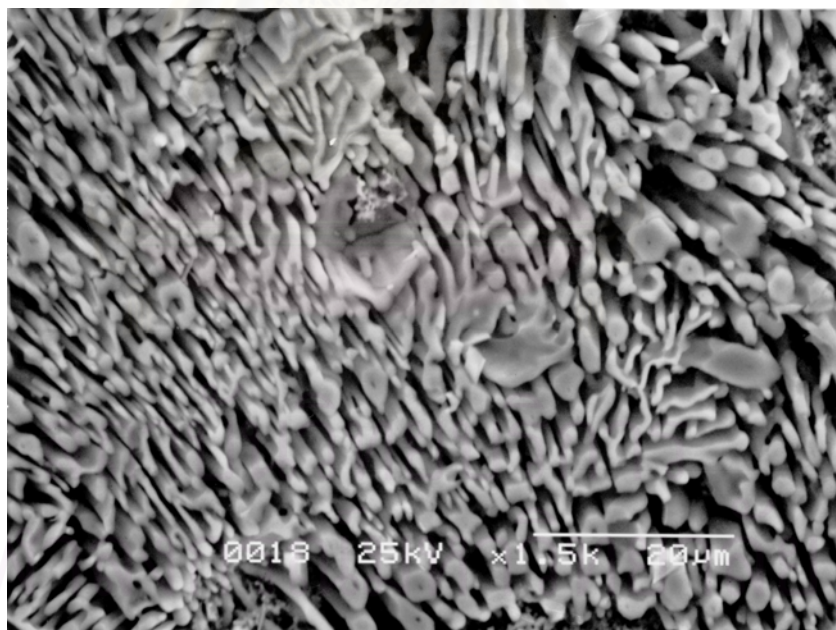
Here, one question is left, why is the  $H_{T_{max}}$  value of 16%Cr cast iron higher than that of 26%Cr cast iron?, whereas more secondary chromium carbides with higher hardness[26] precipitate in the matrix of 26%Cr cast iron. According to the relationship between micro-hardness of matrix and tempering temperature shown in Fig.4-10 (16%Cr cast irons) and in Fig.4-12 (26%Cr cast irons), the  $H_{T_{max}}$  values of micro-hardness of both specimens are close each other. This means that the difference in macro-hardness between 16%Cr and 26%Cr cast irons arises from the difference in the hardness of eutectic carbides between both irons. In the case of irons with eutectic composition (Specimen No.1 and No.4), for example, the volume fractions of eutectic carbide calculated from the equation 2.3 [14] are 36.2% in 16%Cr and 36.4% in 26%Cr irons,



respectively. In the irons with hypoeutectic composition, therefore, the volume fractions of eutectic carbide should be approximately same if the irons have similar eutectic ratio. Resultantly, the influence of the amount of eutectic carbide on the macro-hardness is considered to be less. From above discussions, it is concluded that the higher macro-hardness in 16%Cr cast iron is due to the difference in morphology of eutectic chromium carbide; the carbide morphology of 16%Cr cast iron is thicker and more interconnected in comparison with that of 26%Cr cast iron which is thin or fine and more discontinuous[6]. In order to prove this consideration, the three dimensional microstructures of eutectic chromium carbide are investigated by SEM using deep-etched specimen. As an example, the SEM microphotographs of eutectic chromium carbides are shown in Fig.5-10 (a) for 16%Cr and (b) for 26%Cr cast irons. By dissolving matrix of the specimen using deep etching method, the three dimensional of eutectic carbides are revealed. It is observed that eutectic carbides in 16%Cr cast iron are more connected or more discontinuous. It is no exaggeration to say that such a difference in morphology of eutectic chromium carbide may produce the difference in hardness of cast irons with 16% and 26%Cr.



(a)



(b)

Fig.5-10 SEM microphotographs of eutectic chromium carbides.  
(a) 16%Cr and (b) 26%Cr cast irons.



## Chapter 6

### Conclusions

The heat treatment behavior of high chromium cast irons containing 16%Cr for main materials of hot finishing work rolls and 26%Cr for materials of abrasive wear resistant parts for pulverizing mills were investigated. After annealing, the alloys were hardened and tempered, and the effects of heat treatment condition and chemical composition on the hardness and volume fraction of retained austenite were clarified. The following conclusions have been drawn from the experimental results and discussions.

#### **In as-hardened state**

- (1) The macro-hardness and volume fraction of retained austenite ( $V_{\gamma}$ ) changes widely depending on the combination of carbon and chromium content in the cast iron.
- (2) In a family of the cast iron with same chromium contents, however, the macro-hardness does not change much even when the carbon content varies within the range of chemical composition of this experiment, and the clear relationship between macro-hardness and carbon content is not discovered.
- (3) The  $V_{\gamma}$  is always more at the same carbon level when the austenitizing temperature is higher.
- (4) The  $V_{\gamma}$  decreases roughly in proportion to the Cr/C value. At the same Cr/C value, the higher the austenitizing temperature, the more the  $V_{\gamma}$ .

### In tempered state

- (1) Hardness of tempered specimens varies depending on the chemical composition and the tempering temperature under the same holding time.
- (2) Tempered macro-hardness curve shows a secondary hardening due to the precipitation of fine chromium carbides in matrix and the reduction of  $V_\gamma$ .
- (3) By increasing the austenitizing temperature, the peak of the hardness which is expressed as  $H_{T_{max}}$  (the maximum of tempered hardness) shifts to the high temperature side, and the  $H_{T_{max}}$  is obtained mostly when the cast iron is tempered at 723 K to 730 K.
- (4) The  $H_{T_{max}}$  rises to the highest value of about 800 HV30 as the  $V_\gamma$  in as-hardened state increases up to 30% and over 30%  $V_\gamma$  it settles at the same hardness.
- (5) Micro-hardness of tempered matrix changing very similar manner as the change of tempered macro-hardness.
- (6) The cast irons with  $V_\gamma$  values more than 30% in as-hardened state provide the maximum hardness ( $H_{T_{max}}$ ) after tempering.
- (7) The tempering temperature to obtain the  $H_{T_{max}}$  is higher in 1323 K than that in 1273 K austenitization in the family of cast irons with same chromium level.
- (8) The  $H_{T_{max}}$  of specimens hardened from 1323K is higher than those hardened from 1273 K at the same Cr/C value.

- (9) From SEM observations, it is found that the specimens of which matrix contains large amount of finer carbides provide the maximum tempered hardness.
- (10) The reason why the macro-hardness of 16%Cr irons are higher than that of 26%Cr cast iron under the same matrix hardness is considered due to the difference in the morphology of eutectic chromium carbides, say, their more interconnectivity and larger cross-section.



สถาบันวิทยบริการ  
จุฬาลงกรณ์มหาวิทยาลัย

## References

1. Powell, G.L.F, Morphology of Eutectic  $M_3C$  and  $M_7C_3$  in White Iron Castings, Metals Forum, Vol.3 (1980) : 37-46.
2. Matsubara, Y., K. Ogi and K Matsuda, Eutectic Solidification of High Chromium Cast Iron-Eutectic Structures and Their Quantitative Analysis, AFS Transaction, Vol. 89 (1981) : 183-196.
3. Yu, S.K., N. Sasaguri and Y. Matsubara, Effect of retained austenite on abrasion wear resistance and hardness of hypoeutectic high Cr white cast iron, Int. J. Cast Metals Res., Vol. 11 (1999) : 561-566.
4. Sare, I.R., and B.K. Arnold, The Effect of Heat Treatment on Gouging Abrasion Resistance of Alloy White Cast Iron, Metallurgical Transactions A, vol. 26A (1995) : 359-370
5. Matsubara, Y., et al., BASIC STUDIES ON MULTI-COMPONENT WHITE CAST IRON AND ITS PRACTICAL USE FOR ROLLING AND PULVERIZING MILLS, Proc. of the International Conference on the SCIENCE OF CASTING AND SOLIDIFICATION, Romania, (2001) : 377-386.
6. Matsubara, Y., K. Ogi and K Matsuda, Eutectic Structures of High Chromium Cast Iron, J. JFS, Vol.48 (1976) : 706-711.
7. Ogi, K., Y. Matsubara and K. Matsuda, Eutectic Solidification of High Chromium Cast Iron – Mechanism of Eutectic Growth, AFS Transactions, Vol. 89 (1981) : 197-204.
8. Ogi, K., K. Nagasawa, Y. Matsubara and K. Matsuda, REDISTRIBUTION OF ALLOYING ELEMENT DURING EUTECTIC GROWTH OF HIGH CHROMIUM CAST IRON, International Colloquium on Wear Resistance Materials-Frame, Vol. 18 (1983) : 1-12.
9. Liang, G.Y. and J.Y. Su, The Effect of Rare Earth Elements on the Growth of Eutectic Carbides in White Cast Irons Containing Chromium, Cast Metals, Vol. 4 (1991) : 83-88.
10. Dogan, O.N., J.A. Hawk and G. Laird II, Solidification Structure and Abrasive Resistance of High Chromium White Irons, Metallurgical Transactions A, Vol. 28A (1997) : 1315-1328.
11. Kuwano, M., et al., Influence of Destabilization Heat Treatment on Martensitic Transformation of High Chromium Cast Iron, J. JFS, Vol. 54 (1982) : 586-592.
12. Trope, W.R., Chicco, B., The Fe-Rich Corner of the Metastable C-Cr-Fe Liquidus surface, Metallurgical Transactions A, Vol. 16A (1981) : 11-19.

13. Thong, C.P., Suzuki, T., Umeda, T., Eutectic solidification of High-Chromium Cast Irons, Physical Metallurgy of Cast Iron IV, G.Ohira, T. Kusakawa, E. Niyama, Editors, Materials Research Society, Pittsburgh, PA, (1989): 403-410.
14. Maratray, F., Usseglio-Nanot, R., Factors Affecting the structure of Chromium and Chromium-Molybdenum White Irons, Climax Molybdenum S.A., Paris, France, (1971) : 32.
15. Laird II, G., Microstructure of Ni-hard I, Ni-hard IV and High-Cr White cast irons, AFS Transactions, Vol. 99 (1991) : 339-357.
16. Rickard, J., Some Experiments Concerning the As-cast Grain Size in 30% Chromium Cast Irons, BCIRA Journal, Vol. 8 (1960) : 200-216
17. Matsubara, Y., K. Ogi and K. Matsuda, Influence of Alloying Elements on the eutectic Structures of high Chromium Cast Iron, J. JFS(IMONO), Vol. 51 (1979) :545-550.
18. Maratray, F., Poulalion, A., Austenite Retention in High-Chromium White Iron, AFS Transactions Vol. 90 (1982) :795-804. Andrew, K.W., Empirical Formulae for the Calculation of Some transformation Temperatures, JISI, Vol. 203 (1988) : 678-685.
19. Andrew, K.W., Empirical Formulae for the Calculation of Some transformation Temperatures, JISI, Vol. 203 (1988) : 678-685.
20. Biss, V., unpublished research, Climax Molybdenum Co. (1981).
21. Sare, I.R. and B.K. Arnold, The Influence of Heat Treatment on the High-Stress Abrasion Resistance and Fracture Toughness of Alloy White Cast Irons, Metallurgical Transactions A, Vol. 26A (1995) : 1785-1793.
22. Matsubara, Y., unpublished report, Kurume National College of Technology, (1988).
23. Khanitnantharak, W., N. Sasaguri, K. Nanjo, P. Sricharoenchai and Y.Matsubara, Heat Treatment Behavior of Low Carbon Multi-component Cast Alloy, Proceeding of the 7 th Asian Foundry Congress-Taipei, (2000) : 63-72.
24. Kim, C., X-Ray Method of Measuring Retained Austenite in Heat Treat White Cast Irons, J. Heat treating ASM, Vol. 1(1979) : 43-51.
25. Matsubara, Y., Y. Yokomizo, N. Sasaguri and M. Hashimoto, Effect of Carbon Content and Heat-treating Condition on Retained Austenite and Hardness of Multi-component White Cast Iron, J. JFS, Vol.74 (2000) : 471-477.
26. Matsubara, Y., and N. Sasaguri, Improvement of Toughness of Alloyed White Cast Iron for Wear Resistance by Hot Rolling, J. JFS, Vol. 68 (1996) : 1099-1105.



**Appendix**

สถาบันวิทยบริการ  
จุฬาลงกรณ์มหาวิทยาลัย

All digital data of Fig.4-3 to Fig.4-13 are tabulated in the appendix.  
Volume fraction of retained austenite ( $V\gamma$ ), macro-hardness and micro-hardness at austenitizing temperature of 1273 K.

No	Tempering temperature(K)	$V\gamma$ , %	Macro-hardness (HV30)	Micro-hardness (HV0.1)
1	As-hardened	28.8	763	720
	573	20.7	757	697
	623	21.7	746	698
	673	5.8	763	710
	723	0.0	760	690
	773	0.0	687	551
	823	0.0	593	492
	873	0.0	536	441
2	As-hardened	18.1	775	673
	573	15.7	760	670
	623	16.7	757	673
	673	13.3	769	685
	723	2.4	763	678
	773	0.0	657	573
	823	0.0	561	435
	873	0.0	440	405

สถาบันวิทยบริการ  
จุฬาลงกรณ์มหาวิทยาลัย

All digital data of Fig.4-3 to Fig.4-13 are tabulated in the appendix.  
 Volume fraction of retained austenite ( $V\gamma$ ), macro-hardness and  
 micro-hardness at austenitizing temperature of 1273 K.

No	Tempering temperature(K)	$V\gamma$ , %	Macro-hardness (HV30)	Micro-hardness (HV0.1)
3	As-hardened	18.8	780	660
	573	15.2	737	664
	623	13.5	735	668
	673	6.2	745	682
	723	0.9	727	627
	773	0.0	624	503
	823	0.0	524	441
	873	0.0	462	410
4	As-hardened	3.8	769	-
	573	3.6	710	-
	623	3.7	725	-
	673	3.4	763	-
	723	3.2	757	-
	773	0.0	610	-
	823	0.0	520	-
	873	0.0	444	-

สถาบันวิทยบริการ  
 จุฬาลงกรณ์มหาวิทยาลัย



All digital data of Fig.4-3 to Fig.4-13 are tabulated in the appendix.  
Volume fraction of retained austenite ( $V_{\gamma}$ ), macro-hardness and micro-hardness at austenitizing temperature of 1273 K.

No	Tempering temperature(K)	$V_{\gamma}$ , %	Macro-hardness (HV30)	Micro-hardness (HV0.1)
5	As-hardened	4.1	763	657
	573	3.6	708	653
	623	3.2	715	650
	673	2.2	731	677
	723	1.9	726	698
	773	0	602	615
	823	0	483	466
	873	0	427	393
6	As-hardened	3.2	749	670
	573	3.1	726	660
	623	3.0	728	655
	673	2.6	739	660
	723	2.0	746	684
	748	0	736	700
	773	0	609	579
	823	0	491	469
	873	0	425	403

สถาบันวิทยบริการ  
จุฬาลงกรณ์มหาวิทยาลัย

All digital data of Fig.4-3 to Fig.4-13 are tabulated in the appendix. Volume fraction of retained austenite ( $V\gamma$ ), macro-hardness and micro-hardness at austenitizing temperature of 1323 K.

No	Tempering temperature(K)	$V\gamma$ , %	Macro-hardness (HV30)	Micro-hardness (HV0.1)
1	As-hardened	41.0	773	743
	573	40.5	738	682
	623	38.6	730	671
	673	20.8	746	695
	723	8.1	775	720
	773	0.0	757	644
	823	0.0	619	520
	873	0.0	542	646
2	As-hardened	31.8	780	685
	573	29.0	715	655
	623	29.4	715	649
	673	27.8	720	660
	723	12.5	786	696
	773	0.0	757	641
	823	0.0	595	468
	873	0.0	478	429

สถาบันวิทยบริการ  
จุฬาลงกรณ์มหาวิทยาลัย

All digital data of Fig.4-3 to Fig.4-13 are tabulated in the appendix. Volume fraction of retained austenite ( $V\gamma$ ), macro-hardness and micro-hardness at austenitizing temperature of 1323 K.

No	Tempering temperature(K)	$V\gamma$ , %	Macro-hardness (HV30)	Micro-hardness (HV0.1)
3	As-hardened	27.5	775	670
	573	27.0	710	664
	623	26.0	705	655
	673	20.0	709	657
	723	8.5	782	705
	773	0.0	705	597
	823	0.0	548	470
	873	0.0	484	430
4	As-hardened	18.1	792	-
	573	10.2	736	-
	623	9.6	736	-
	673	6.2	752	-
	723	5.3	780	-
	773	0.0	700	-
	823	0.0	550	-
	873	0.0	470	-

สถาบันวิทยบริการ  
จุฬาลงกรณ์มหาวิทยาลัย

All digital data of Fig.4-3 to Fig.4-13 are tabulated in the appendix. Volume fraction of retained austenite ( $V\gamma$ ), macro-hardness and micro-hardness at austenitizing temperature of 1323 K.

No	Tempering temperature(K)	$V\gamma$ , %	Macro-hardness (HV30)	Micro-hardness (HV0.1)
5	As-hardened	14.8	777	657
	573	10.0	741	653
	623	10.2	736	650
	673	10.5	754	677
	723	8.2	775	698
	773	0.0	704	615
	823	0.0	518	466
	873	0.0	457	393
6	As-hardened	11.8	769	670
	573	11.0	756	660
	623	11.9	747	655
	673	9.5	755	660
	723	9.0	769	684
	748	3.5	781	700
	773	0	720	579
	823	0	545	469
873	0	471	403	

## Biography

My name is Mr. Sudsakorn Inthidech. I was born on December 25, 1976 in Srisaket. I graduated with a degree of Bachelor degree of Engineering (Metallurgical Engineering) from Chulalongkorn University in 1998. I have been studying for the degree of Master of Engineering in Metallurgical Engineering since 2000. In November 2001, I have carried out to work on this thesis as a research student at Department of Materials Science and Metallurgical Engineering, Kurume National Collage of Technology, Japan.



สถาบันวิทยบริการ  
จุฬาลงกรณ์มหาวิทยาลัย